



## **Diploma Thesis**

### **Supervisory and Control System for Havana Radio Astronomical Station**

**Alexander Karl  
Matr. Nr. 171488**

**Supervisors:**

**Prof. Dr.-Eng. W. Ley**

**Prof. Dr. Eng. Ramón E. Rodríguez**

**Prof. Dr. Eng. Luis M. Fernández**

**Ciudad de La Habana  
May 2004**

<b><u>Contents</u></b>	<b><u>Page</u></b>
<b>Abstract</b>	<b>4</b>
<b>1. Introduction</b>	<b>5</b>
<b>2. Radio Astronomy</b>	<b>6</b>
<b>2.1 Introduction</b>	<b>6</b>
<b>2.2 Fundamentals of Radio Astronomy</b>	<b>6</b>
<b>2.2.1 Electromagnetic Radiation</b>	<b>6</b>
<b>2.2.2 Absorption of Electromagnetic Radiation</b>	<b>10</b>
<b>2.2.3 Thermal Radiation</b>	<b>11</b>
<b>2.2.4 Non-Thermal Radiation</b>	<b>12</b>
<b>2.2.5 Types of Radio Emission Mechanisms</b>	<b>12</b>
<b>2.3 Instruments</b>	<b>13</b>
<b>2.3.1 Aerials</b>	<b>13</b>
<b>2.3.1.1 Dipole</b>	<b>13</b>
<b>2.3.1.2 Parabolic Dish</b>	<b>15</b>
<b>2.3.1.3 Interferometer</b>	<b>17</b>
<b>2.3.2 Receivers</b>	<b>18</b>
<b>2.4 Radio Astronomical Objects</b>	<b>19</b>
<b>2.4.1 The Planets</b>	<b>20</b>
<b>2.4.2 The Milky Way</b>	<b>20</b>
<b>2.4.3 Discrete Radio Sources</b>	<b>20</b>
<b>2.4.3.1 Stars</b>	<b>21</b>
<b>2.4.3.2 Pulsars</b>	<b>22</b>
<b>2.4.3.3 Galactic Objects</b>	<b>22</b>
<b>2.4.3.4 Quasars and Lobe Radio Sources</b>	<b>23</b>
<b>3. Solar Radio Astronomy</b>	<b>24</b>
<b>3.1 Radio Emission of the Sun</b>	<b>25</b>
<b>3.1.1 Radiation of the Quiet Sun</b>	<b>25</b>
<b>3.1.2 Slowly Variable Spot Components</b>	<b>28</b>
<b>3.1.3 Noise Storms in the Meter-Wave Region</b>	<b>29</b>
<b>3.1.4 Solar Activity</b>	<b>29</b>
<b>3.1.4.1 Flares</b>	<b>29</b>
<b>3.1.4.2 Radiation Outbursts</b>	<b>30</b>
<b>3.2 Space Weather</b>	<b>32</b>
<b>3.3 Solar Radio Experiments</b>	<b>32</b>

<b>4. Havana Radio Astronomical Station</b>	<b>34</b>
<b>4.1 The Importance of the ERH</b>	<b>34</b>
<b>4.2 The Radio Telescopes of the ERH</b>	<b>35</b>
<b>4.3 The Process of the Solar Observation</b>	<b>39</b>
<b>4.4 Post Processing of the Measurements</b>	<b>41</b>
<b>4.5 Important Data for the Automation</b>	<b>42</b>
<b>5. Astrodata</b>	<b>46</b>
<b>5.1 Hardware Components</b>	<b>46</b>
<b>5.2 Software Components</b>	<b>50</b>
<b>5.3 Structures and Functions of the Astrodata Software</b>	<b>51</b>
<b>5.4 The Theory of the Process Control in Astrodata</b>	<b>58</b>
<b>5.5 The Results</b>	<b>62</b>
<b>6. Selection of the Solution</b>	<b>66</b>
<b>6.1 The Low Frequency Blocks</b>	<b>66</b>
<b>6.2 The Signals</b>	<b>67</b>
<b>6.3 Digital Signal Processing (DSP)</b>	<b>70</b>
<b>6.4 Technical and Scientific Requirements</b>	<b>72</b>
<b>6.5 Shopping</b>	<b>73</b>
<b>7. Implementation of the Solution</b>	<b>76</b>
<b>8. High Tech Sensors &amp; ERH, IGA, ICIMAF</b>	<b>77</b>
<b>9. Summary</b>	<b>78</b>
<b>References</b>	<b>79</b>
<b>List of Figures</b>	<b>80</b>
<b>List of Tables</b>	<b>81</b>
<b>Appendix 1 – The TERN A-Engine-86</b>	<b>82</b>
<b>Appendix 2 – Oscilloscope Measurements of the Signals</b>	<b>84</b>
<b>Appendix 3 – Price Comparison List</b>	<b>85</b>
<b>Appendix 4 – Space Missions Database (Fragment)</b>	<b>86</b>
<b>Appendix 5 – Data Sheets</b>	<b>87</b>
<b>Appendix 6 – Module Blueprints and List of Components</b>	<b>88</b>

## **Abstract**

The radio astronomical observations of the Sun are increasing in importance in regard to the effects that space weather has on Earth and on objects in Earth orbit. The Havana Radio Astronomical Station (ERH) has three telescopes with which the radio emissions from the Sun are being observed. With its observations the ERH is contributing to the growing knowledge of solar physics and monitoring the state of solar activity. To keep the observational standard up to date, a constant development of the station is needed. Work begun on an affordable supervisory and control system called Astrodata in a cooperation between the Institute of Geophysics and Astronomy (IGA) and the Institute of Cybernetics, Mathematics and Physics (ICIMAF). This thesis presents the study carried out to complete the process of installing the supervisory and control system by the removal of the analog working low frequency blocks with a digital solution.

Key Words: solar radio astronomy, radio telescopes, supervisory and control system, analog-to-digital conversion, digital signal processing, high-tech sensors

## **Übersicht**

Die radioastronomischen Beobachtungen der Sonne werden im Bezug auf die Auswirkungen, die das Weltraumwetter auf die Erde und Objekte im Erdorbit hat, immer wichtiger. Die radioastronomische Station von Havanna (ERH) besteht aus drei Teleskopen, mit denen die Radioemissionen der Sonne beobachtet werden. Mit diesen Observationen trägt die ERH zum wachsenden Wissen über Solarphysik bei und überwacht den Status der Sonnenaktivität. Um den Beobachtungsstandard auf dem neuesten Stand zu halten, ist eine konstante Weiterentwicklung der Station erforderlich. In Kooperation zwischen dem Institut für Geophysik und Astronomie (IGA) und dem Institut für Kybernetik, Mathematik und Physik (ICIMAF) begann die Arbeit an einem preiswertem Überwachungs- und Kontrollsystem mit dem Namen Astrodata. Diese Diplomarbeit spiegelt die Studie wieder, die durchgeführt wurde, um die Installation des Überwachungs- und Kontrollsystems abzuschließen, indem die analog arbeitenden Tieffrequenzblöcke mit einer digitalen Lösung ersetzt werden.

Stichwörter: solare Radioastronomie, Radioteleskope, Überwachungs- und Kontrollsystem, Analog-Digital Wandlung, digitale Signalverarbeitung, High-Tech Sensoren

## **1. Introduction**

The radio astronomical observation of the Sun is increasing in importance. The effects of Coronal Mass Ejections (CMEs) on Earth and on objects in Earth orbits are increasing in relation to the amount of affectable technology used. In the foreseeable future this situation will even increase. In regard to manned space missions outside Earth's protecting magnetosphere a good understanding or even the possibility to predict the space weather is of great importance.

The Havana Radio Astronomical Station (ERH) has three radio telescopes with which five frequencies of radio emissions from the Sun are being observed. These radio emissions are linked to different phenomena of solar activity. With its observations the ERH is contributing to the growing knowledge of solar physics and monitoring the state of solar activity.

To keep the observational standard up to date, a constant development of the station is needed. Due to the economic situation in Cuba the last update was made nearly 25 years ago with the help of soviet technology.

Work begun on an affordable supervisory and control system called Astrodata in a cooperation between the Institute of Geophysics and Astronomy (IGA) and the Institute of Cybernetics, Mathematics and Physics (ICIMAF). They implemented technology to resolve among other things, the tracking of the Sun by the antennas and the elimination of the paper registry.

This thesis presents the study carried out to complete the process of installing the supervisory and control system by the removal of the analog working low frequency blocks with a digital solution.

## 2. Radio Astronomy

### 2.1 Introduction

Radio astronomy, which is concerned with the analysis of high-frequency radiation arriving on the Earth from distant parts of the Universe, is still a very young branch among the astronomical sciences. Although originally discovered by Karl G. Jansky in 1930, the importance of this extraterrestrial radio radiation became apparent only in the years 1940-1944, when a completely new way was opened up for the exploration of astronomical objects [4]. Compared with the intensity in broadcasting and television, the radiation from cosmic radio sources is very weak; furthermore, special arrangements are necessary to achieve a sufficient resolution in direction. This requires in many cases very large receiving aerials and very powerful receiving instruments. Special precautions are required to achieve interference-free operation of the instruments. Practical work in radio astronomy therefore demands a large and complex instrumental outfit, and thus great financial means, quite apart from a detailed knowledge of the technique of high-frequency work.

### 2.2 Fundamentals of Radio Astronomy

#### 2.2.1 Electromagnetic Radiation

Figure 2-1 shows the useful part of the electromagnetic spectrum. Obviously, it covers many decades in frequency  $\nu$  (or wavelength  $\lambda$ ). In the International System (IS) the unit of the frequency is 1 Hertz (Hz) = 1 wave per second.

The lowest frequencies (longest wavelengths) constitute the radio spectrum. Above the radio frequency spectrum lays the infrared spectrum, followed by the visible range, which is quite narrow. Above the visible spectrum lies the ultraviolet spectrum and, overlapping it, the X-ray spectrum. Finally, at the highest frequencies are the gamma rays.

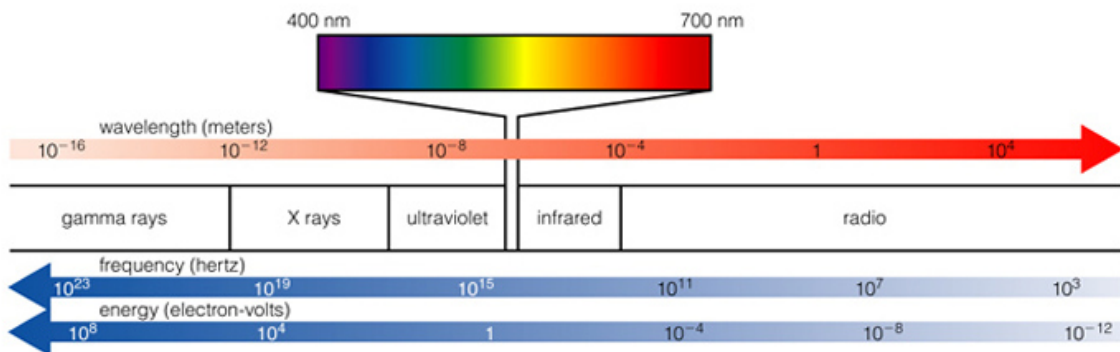


Figure 2-1: The electromagnetic spectrum

An electromagnetic (EM) wave is radiated into space from an arbitrary source (antenna system, star, galaxy, etc.). Such a radiated wave consists of electric and magnetic fields,

which are in time phase although the two sets of flux lines are 90° apart in space. Consequently, if an EM wave contains electric flux lines that are vertical, the corresponding magnetic flux lines will be horizontal. Both of these sets of flux lines are also at right angles to the direction in which the electromagnetic energy is traveling. In other words, the electric and magnetic fields are transverse to the direction of propagation. Such a wave is of the transverse electric, transverse magnetic (TEM) type, which occurs only in free space and on a conventional transmission line (not in a waveguide).

Mathematically, the electric field (E [V/m]), the magnetic field (H [A/m]), and the transfer of EM energy in a particular direction represent a right-handed system of vectors. This transfer of EM energy is measured by the Poynting vector S, which represents the amount of radiated energy passing through a unit area (1 m<sup>2</sup>) in unit time (1 s). E, H, and S (in that order) form a right-handed system with S as the vector product of E and H; in terms of units,

$$[\text{V/m}] (E) \times [\text{A/m}] (H) = [\text{V}] \times [\text{A/m}^2] = [\text{W/m}^2] = [\text{J/m}^2\text{s}] (S).$$

If the instantaneous E direction is rotated through 90° to lie along the instantaneous H direction, the direction of S is the same as the movement of a right-handed screw that is subjected to the same rotation.

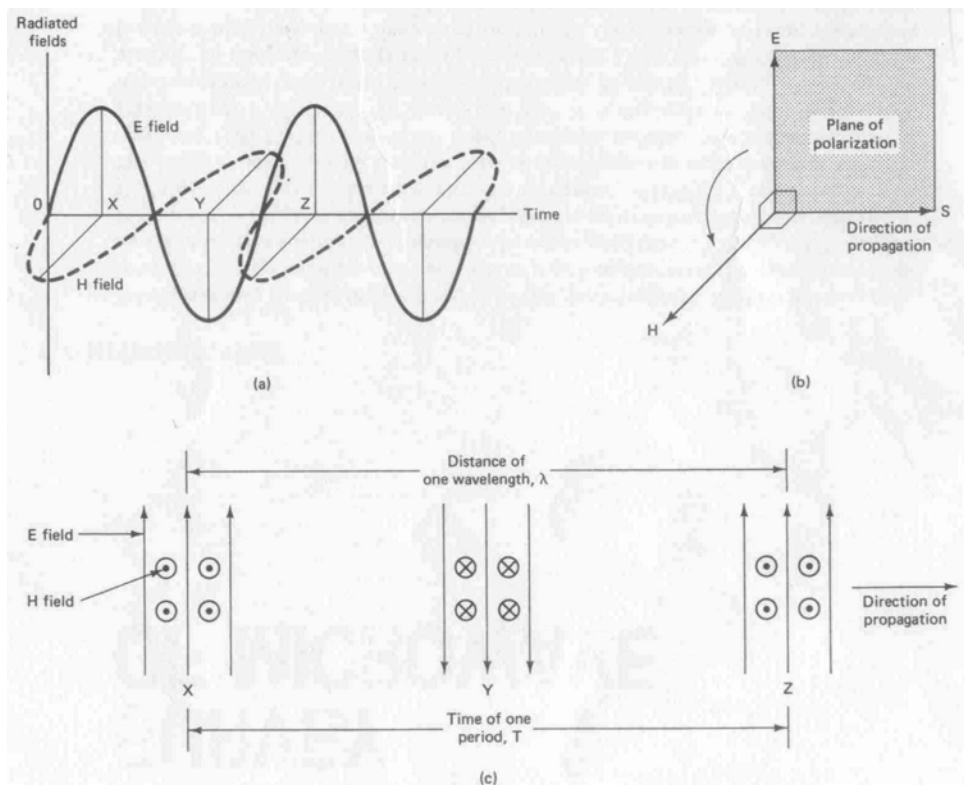


**Figure 2-2: (a) Peak condition for the electric and magnetic fields of a vertically polarized TEM wave, (b) vector diagram of a vertically polarized wave, (c) electric and magnetic fields in the TEM wave**

Figure 2-2 illustrates the various features of a TEM wave. The peak conditions of E and H fields in the path of the wave are shown in figure 2-2a. Positions X and Z represent adjacent identical conditions and are therefore separated by a distance of one wavelength. For the instantaneous fields at position X to travel to position Z would require a time equal to one period (Figure 2-2c). It follows that the wave travels a distance of one wavelength  $\lambda$  in a time equal to one period T. Since velocity = distance / time, the velocity of the electromagnetic wave in free space,

$$c = \lambda / T = \lambda \cdot 1/T = \lambda v.$$

In the IS of units, the permeability of free space in  $\mu_0 = 4\pi \times 10^{-7}$  H/m, and the permittivity is  $\epsilon_0 = 8.85 \times 10^{-12}$  F/m. In 1865, Clerk Maxwell predicted that the velocity of all electromagnetic waves in free space would be given by

$$c = 1 / \sqrt{\mu_0 \epsilon_0} \approx 3 \cdot 10^8 \text{ m/s.}$$

The value c is equal to light velocity, which is another example of an electromagnetic wave. If the wave is traveling through a medium whose relative permittivity is  $\epsilon_r$ , the velocity is reduced and equal to  $c / \sqrt{\epsilon_r}$ .

For a similar medium, the velocity of all electromagnetic waves is a constant. Then this velocity is equal to the product of frequency and wavelength. Either a wavelength or a frequency scale may be used to distinguish one signal from another. The energy, which is linked with the electromagnetic radiation, is directly proportional to the frequency by  $E = hv$ , where h is the Planck's elementary quantum. The energy is quantified in units of that value, called photon.

### Radio Frequency Bands

At the Atlantic City Conference of 1947 [2], the following radio frequency bands were adopted:

Very low frequency (VLF)	3-30 kHz
Low frequency (LF)	30-300 kHz
Medium frequency (MF)	300 kHz -3 MHz
High frequency (HF)	3-30 MHz
Very high frequency (VHF)	30-300 MHz
Ultra high frequency (UHF)	300 MHz-3 GHz
Super high frequency (SHF)	3-30 GHz
Extremely high frequency (EHF)	30-300 GHz

Beyond these frequencies lies the infrared region (heat and black light), which extends approximately from 1 to 375 THz. At these frequencies more convenient smaller units are introduced to measure the wavelength. They are the micron or micrometer ( $\mu\text{m}$ ), which is



one millionth of a meter, and the Angstrom unit ( $\text{\AA}$ ), where  $1 \text{ \AA} = 10^{-8} \text{ cm} = 10^{-10} \text{ m} = 10^{-4} \text{ \mu m}$ .

### Plane of Polarization

Summarizing, a radiated EM wave consists of electric and magnetic fields that are in time phase. The two sets of flux lines are  $90^\circ$  apart in space and each set is at right angles to the direction of propagation. That means they lay in the wave planes in which arbitrary orientation is possible. The plane of polarization is defined by the directions of the E field and the Poynting vector S. For example, a vertical antenna system radiates a vertically polarized EM wave in which the electric field is vertical and the magnetic field is horizontal.

In natural light (thermal radiation) the directions of the fields are statistically distributed. This kind of radiation is called unpolarized. Lies the field in one direction, like Synchrotron radiation, then the radiation is linearly polarized. By superposition of light with different directions of polarizations, elliptical or circular polarized light is created. The degree of polarization indicates the amount of polarized radiation within a mix with natural light. By preferred absorption of light in a determined direction of polarization, natural light can be partially polarized.

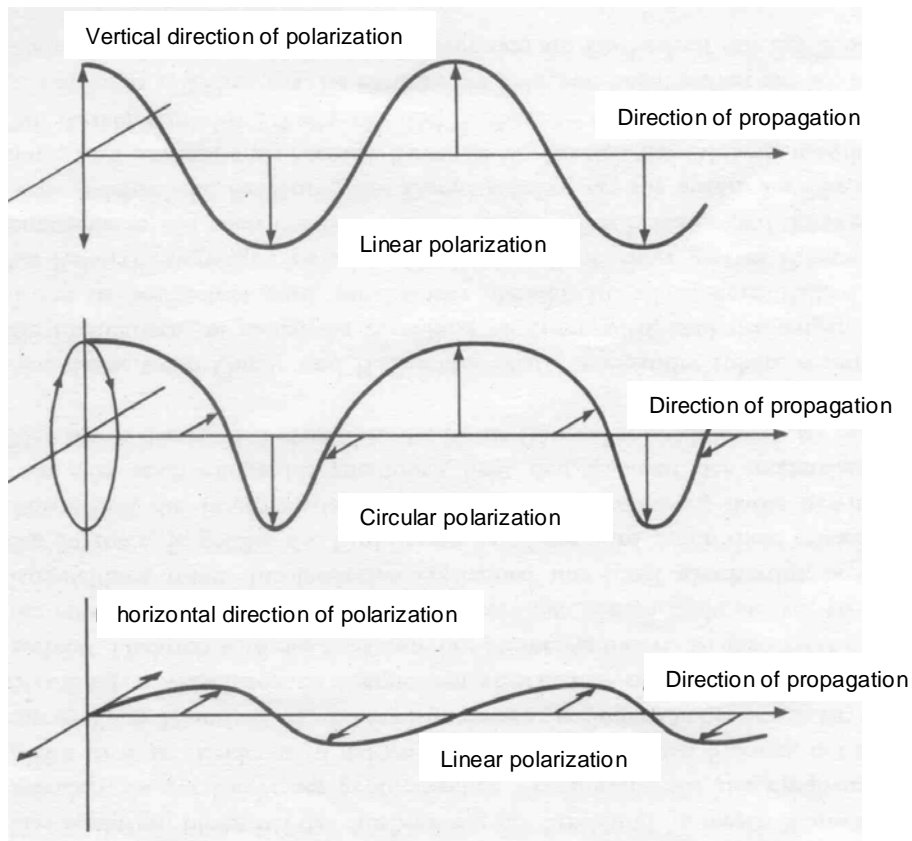


**Figure 2-3: Polarized light**

### **2.2.2 Absorption of the Electromagnetic Radiation**

The absorption in the Earth's atmosphere is the reason why it is impossible to utilize the whole range of wavelengths, as long as the observation is done from the Earth's surface. The various atmospheric gases absorb in very different parts of the spectrum. The superposition of all these effects makes the atmosphere opaque for most rays; it is transparent only in two relatively narrow regions. The classic range lies between about 3000 and 10000 Å. [ $1 \text{ Å} = 10^{-10} \text{ m}$ ] These limits, particularly the upper one, are not well defined; bright objects like the Sun can still be observed between the spectral bands of water vapor until up to about 100000 Å.

The shortwave limit is due to the content of ozone in the air; in the far ultraviolet, the Rayleigh scattering is dominant, which increases inversely to the fourth power of the wavelength. In the infrared, the absorption is due mainly on water vapor and reaches far into the millimeter-wavelength range. Radio astronomy has only become possible because there exists a second transparency range in the atmosphere, namely, between about  $\lambda = 1 \text{ cm}$  and  $\lambda = 30 \text{ m}$ . Its upper limit is determined by the conditions in the ionosphere. This particular layer has no uniform structure, but rather consists of different layers (D, E, F<sub>1</sub> and F<sub>2</sub>-layer) of appreciable ionization, the lowest of which is the D-layer at a height of about 90 km, but reaches up to 500 km and higher (F<sub>2</sub>-layer). Within these layers, the atmospheric gases (N<sub>2</sub>, O, and N) are ionized by the ultraviolet and high-energy particles radiated from the Sun; the degree of ionization therefore varies with the intensity of this excitation. It shows daily and annual variations apart from considerable fluctuations that are correlated with solar activity, and thus also displays an 11-year cycle.

The action of the ionosphere on the high-frequency radiation can be described as a reflection effect due to the ionized layers. This effect reaches into shorter wavelengths the stronger the ionization. This is why the region of transparency in the meter range becomes narrower when solar activity is greater. This radio-astronomical "window" is restricted toward the centimeter waves by the increasing amount of water vapor in the air. These restrictions would be removed for an extraterrestrial observatory, and this is a reason for aiming at satellite and lunar observatories.

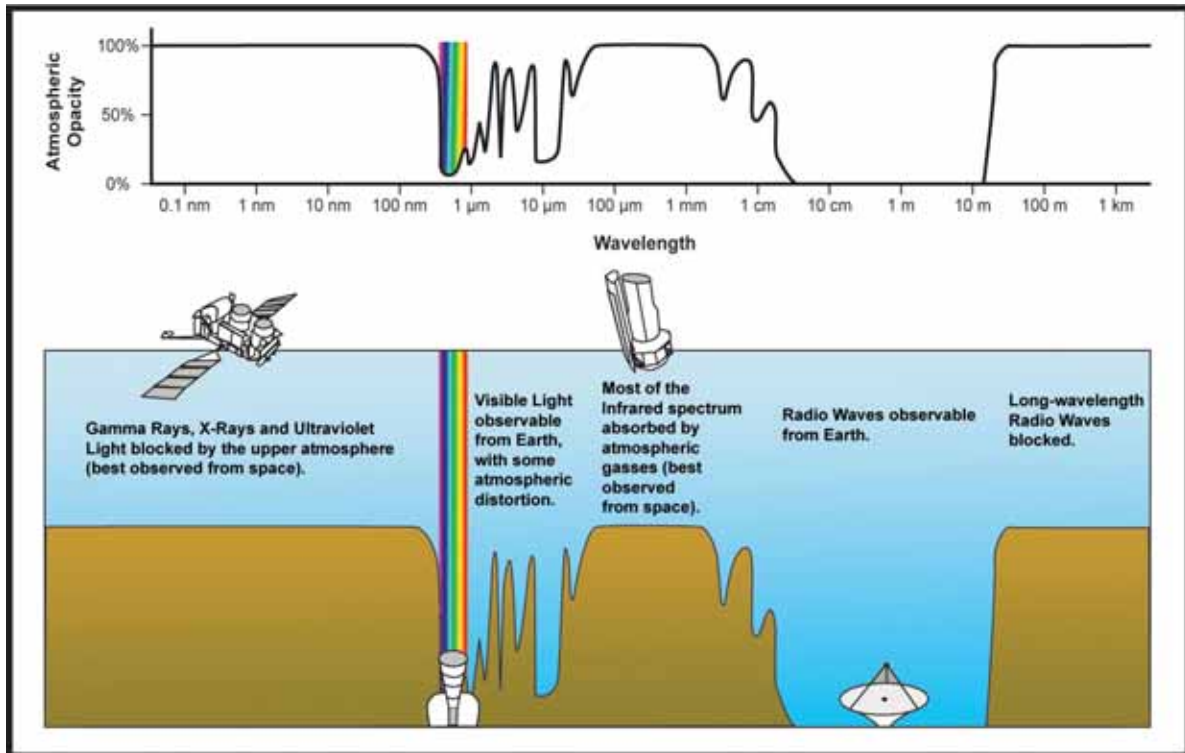


Figure 2-4: Absorption in the atmosphere

### 2.2.3 Thermal Radiation

The surface brightness (intensity) of a radiating body can, under certain assumptions, be represented by Planck's radiation law as a function of the wavelength  $\lambda$  and the temperature  $T$ . The assumption is that the radiator is a so-called "black body" i.e., that it completely absorbs all incident radiation. Many astronomical objects, in particular the photospheres of the stars, fulfill this condition relatively well, and thus Planck's law can be used as a good approximation. The radiation  $I(\nu)$  is given by

$$I(\nu) = (2h\nu^3) / (c^2 \cdot e^{h\nu/kT} - 1)$$

Where  $\nu = c/\lambda$  is the frequency,  $\lambda$  is the wavelength,  $h$  is the Planck's elementary quantum,  $k$  is Boltzmann's constant, and  $c$  is the velocity of light.

Due to the very low frequencies dealt with in radio astronomy, this expression can be replaced in very good approximation by the much simpler one

$$I(\nu) = 2kT/\lambda^2 = 2.77 \cdot 10^{-23} T/\lambda^2 \text{ W/m}^2 \text{ Hz rad } (\lambda \text{ in m})$$

This is the case of the "thermal radiation." As does every other radiation, it originates in quantum-mechanical emission processes involving atoms and ions, and these processes depend on the characteristics of these particles and on their present conditions. Since

Planck's equation does not contain any such factors, it follows that it represents a statistical law, which already contains averages made up of many individual processes.

#### **2.2.4 Nonthermal Radiation**

Frequently, however, the conditions for the validity of Planck's equation are not fulfilled. This applies particularly to very diffuse gases that are too transparent to absorb the radiation completely and can therefore not be considered as black bodies. Here the calculation of the radiation must take into account the individual radiation processes.

An important example of such a non-thermal process is the emission of synchrotron radiation. It is demonstrated theoretically and experimentally by the electrodynamics that the free electrons radiate energy as soon as they are accelerated, that is, as soon as their motion is not any longer uniform and on a straight line. An electron that moves in a circular orbit will thus radiate electromagnetic radiation. This situation occurs when the electron moves perpendicularly to a magnetic field. The moving electron may then be considered as an electric current, which is subject to a force due to the magnetic fields in accordance with the fundamental laws of electrodynamics. This process produces circular orbits that are perpendicular to the magnetic field or spirals that are a combination of such a circular motion and of a uniform displacement in the direction of the lines of force. In the large electron synchrotrons, the electrons traverse a magnetic field on circular orbits; the resulting radiation has been found experimentally and has been named accordingly. Since many cosmic objects contain both fast electrons as well as sufficiently strong magnetic fields, it is often possible to trace the non-thermal radiation of both the optical and the radio range to synchrotron radiation.

There also exist other non-thermal radiation processes that are particularly active in the range of the radio frequencies. They depend on very complicated phenomena in plasmas (highly ionized gases). If a gas contains many ions and free electrons, that is, many free electrically charged particles, then one observes, apart from the normal forces (like gas pressure and inner friction), additional electromagnetic forces, since the moving charge carriers produce electric fields in accordance with the laws of induction. Additionally, vibrations can develop within the plasma, which in the limiting case can produce oscillations and thus radio radiation. The special scientific branch that deals with this interplay of mechanical and electrodynamic forces and their action on the motion and the condition of a plasma is called magneto hydrodynamics.

#### **2.2.5 Types of Radio Emission Mechanisms**

Summarizing, a list of radio emission mechanisms is given.

- Atomic transitions
- Molecular transitions
- Free particle emission
  - Cerenkov emission
  - Bremsstrahlung (Coulomb collisions)

- Magneto-Bremsstrahlung (gyro emission)
- Transition radiation
- Coherent free-particle emission (wave-particle interactions)
  - Plasma emission
  - Electron-cyclotron emission
- Wave emission (wave-wave interactions)

## **2.3 Instruments**

### **2.3.1 Aerials**

The design of a device that is able to record cosmic radio radiation and the direction from where it comes shall now be considered. An instrument of this kind in optics is called a telescope, and the radio astronomical counterparts are therefore briefly named “radio telescopes”. If the measuring process is to be emphasized, one also speaks of radiometers. If the instrument does not work in fixed wavelength regions and if  $\lambda$  can be changed continuously, one speaks, in analogy to optical spectrographs, of radio spectrometers.

A radio telescope consists of two parts, the aerial system and the receiver. Since the work is carried out in the range between centimeter and meter waves one should expect to use the same type of instrument as in the normal shortwave and ultra shortwave broadcasting. Indeed, such receivers have been the starting point for the development of special aerials and amplifiers.

#### **2.3.1.1 Dipole**

The basic form of the aerial is an ordinary dipole (see Fig. 2-5a). It consists in its simplest form (as half-wave dipole) of a rod of the length  $\lambda/2$ , which is divided in the middle, with its inner ends connected to the receiver. The electric field strength of an incident high-frequency radiation produces within the rod periodic motions of the electrons, that is, a high-frequency alternating current, which is then applied to the receiver. Since one is here concerned with transverse oscillations, the effect will depend on the direction of the oscillation and on the direction of propagation of the emission; it is strongest when the radiation oscillates in the direction of the rod, i.e., when it arrives perpendicularly to the rod; it is zero when the wave proceeds in the direction of the rod. The dipole is therefore most effective and most sensitive perpendicularly to its direction. If one plots the sensitivity (which equally applies to reception as to emission) as a function of the direction of the beam (e.g., as power expressed in an arbitrary unit), the so-called aerial polar diagram is obtained. One can immediately see its essential point, if it is wished to find the direction to a radiating object: the polar directivity diagram must be of such a kind that the sensitivity remains mainly restricted to an angular region that must be kept as small as possible. The simple dipole is still far off from this ideal case (see Fig. 2-5a).

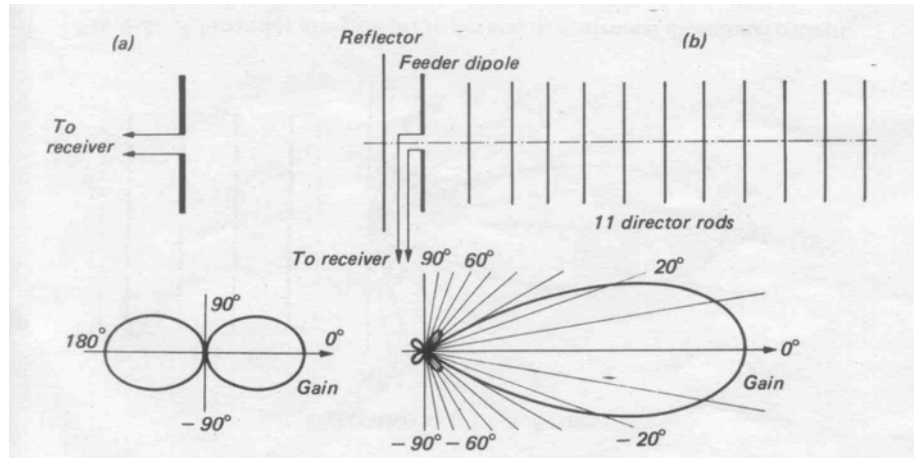


Figure 2-5: (a) Half-wave dipole aerial, and (b) 13-element Yagi aerial with its directional polar diagram.

The requirements of terrestrial broadcasting have already led to the construction of aerials with directional characteristics, the aim being to single out certain transmitters from the general radiation field. This led to the development of the well-known television aerials, and in particular to the Yagi aerials (see Fig. 2-5b): a second rod is fixed parallel to the dipole (on the opposite side of the transmitter) in such a way that it reflects the incident waves and thus improves the reception on the desired side while it disturbs it for the other one. In addition, one can also attach – again parallel to the dipole on the transmitter side – a sequence of (up to 20) additional rods, the so-called directors. They bundle the incident radiation provided they are fixed at the exactly calculated or tested distances, giving more gain the larger their number. They are most effective in the plane perpendicular to the dipole (see Fig. 2-5b) and are less effective within their own plane. The dimensions are an optimum only for a given wavelength region, but the more directors used, the wider the band covered by the aerial. Frequently, to suppress branches of the polar diagram, which points backward or sideways, additional reflectors are added.

These directional diagrams can be characterized by a few data. Thus the gain  $G$  is the ratio of the maximum sensitivity to the sensitivity of an undirected aerial of the same total energy input. The angle between the direction of maximum sensitivity and the direction in which the sensitivity of the receiver is reduced by one-half is then doubled and called the half-width  $\beta$  of the aerial diagram. The half-width is a particularly important quantity since it is a measure of the direction-resolving power of the aerial. Two emitters must be apart by at least this angle  $\beta$  for the aerial to register them as separate objects.

Also other methods have been used to increase the performance of the receiver at the same time, i.e., that they arrive “in equal phase”. In the case of radiation that arrives perpendicularly to the plane of the dipole, the contributions of both part-aerials will add up in the receiver. The wave fronts of obliquely incident radiation reach the two dipoles at different times and excite them with different phases. If the phase difference of the excitation is just a half-wave, aerial currents are obtained that are opposed and cancel each other in the receiver. The angle between the directions where this happens contains

the main sensitivity region of the aerial system, and its polar diagram demonstrates a corresponding half-width. Similar considerations can be applied to a larger number of dipoles, which are regularly placed side by side. The achieved resolving power  $\beta$  depends on the wavelength  $\lambda$  and on the length  $D$  of the series, and is in a plane perpendicular to the dipoles:

$$\beta \sim 50 \lambda/D \quad (\text{in degrees}).$$

If now several such dipole series are placed above each other, that is, if a kind of “aerial wall” is build (see Fig. 2-6), the resolving power also perpendicularly to the series is increased. The gain due to wall consisting of  $m$  rows, of  $n$  elements in each, is:

$$G = 3.28 nm.$$

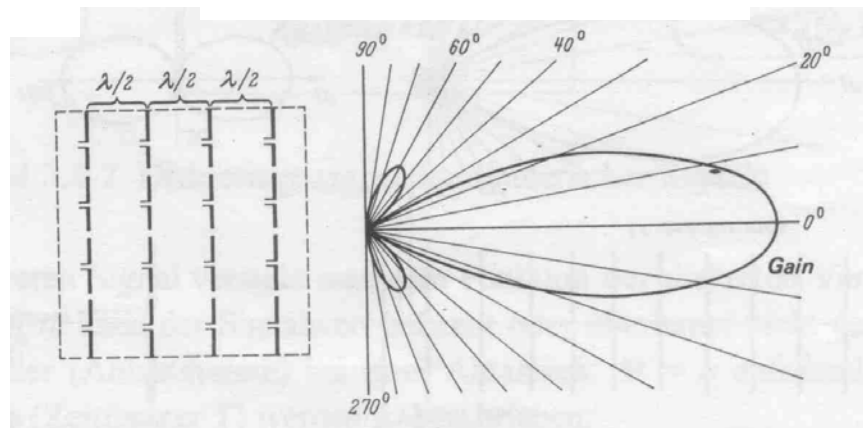


**Figure 2-6: A broadside array of 16 dipoles and its horizontal directional pattern.**

The performance of such an arrangement is improved if the simple dipoles are replaced by Yagi aerials, or if a reflecting sheet one quarter of a wavelength is placed behind the aerial. This can consist of a metal sheet, but usually a net of wire mesh will be sufficient, provided that the openings of the meshes are considerably smaller than the wavelengths to be received.

### **2.3.1.2 Parabolic Dish**

The reflector (mirror) has the task to focus the incoming radiation from a determined direction. To be able to observe radiation from different directions, the reflecting surface must be movable. If a parabolic reflector aerial is designed, which is approximately ten times larger than the wavelength, the reflected energy will be collected approximately within a single focus (see Fig. 2-7). A dipole with an underlying reflector plate is often used as feed or for more focused illumination, a little horn antenna in form of a stretched horn or funnel. Here the radiation is detected and forwarded to the amplifier.



**Figure 2-7: Green Bank Telescope (GBT): The largest fully steerable single dish in the world, 100 x 110 m. Located in Green Bank, Virginia, USA (c) National Radio Astronomy Observatory / Associated Universities, Inc. / National Science Foundation**

The most used type is the round parabolic mirror; the same laws apply here as for optical reflectors. Rays, which come in parallel to the axis, are focused in one point. The installed feed here must have such a directive effect that it only receives the radiation from the reflecting surface but not the direct radiation of the sky or the surface of the Earth. The term illumination of the antenna area by the feed is used in analogy to transmitting in receiving as well.

The resolving power then becomes (assuming optimum properties of the dipole) the same as the corresponding optical reflecting telescope:

$$\beta \sim 59 \lambda/D \quad (\text{in degrees}),$$

where  $\lambda$  is the wavelength and  $D$  the diameter of the reflector.

At full illumination of the reflector area by the feed there would be weak side beams surrounding the main beam circularly, but that can be reduced if the illumination decreases towards the edge of the area.

The main advantage of a parabolic mirror is its easy principle of focusing and its usefulness for every arbitrary wavelength (above an accuracy border) and bandwidth. Radiation of every wavelength is automatically in phase. The disadvantage is the high price. To move a big paraboloid freely in every direction, without that one of its parts is sagging or moving more than  $\lambda/10$  in the wind, there is a high constructive effort to be made.



The great difficulties encountered by radio astronomy can now be easily recognized. Since the resolving power must always be proportional to the wavelength, its value for radio astronomy will be poorer than in optics (for the same given dimensions) by a factor of about one million. To compensate for this disadvantage as much as possible, radio telescopes must have extremely large dimensions. At the moment the record is about 110 m diameter for a moveable telescope (Green Bank, West Virginia) and 305 m for a fixed paraboloid (Arecibo, Puerto Rico).

### **2.3.1.3 Interferometer**

Nevertheless it is possible to increase the resolving power still further if the well-known principle of the interferometer is applied from optics to radio astronomy. Here, the basic considerations are just the same as discussed for the dipole pair, only that now two or more complete radio telescopes are joined that are very far apart, perhaps hundreds of meters and in some cases hundreds of kilometers (Fig.2-8). Special methods guarantee that the theoretical resolving power can be applied. The correct phase combination of such systems offers problems that can be solved only with great technical effort, but resolving powers of much less than a minute of arc have been achieved in this way.



**Figure 2-8: Aerial view of VLA in its most compact configuration. Located near Socorro, New Mexico, USA. (c) National Radio Astronomy Observatory / Associated Universities, Inc. / National Science Foundation**

Another concept that is essential for the assessment of the performance of an aerial system is the reception area  $A$ . If the aerial extracts  $N$  W/Hz from the radiation flux  $S'$  W/m<sup>2</sup> Hz of a radio source and applies it to the receiver, then  $A$  is defined by

$$A = N/S'$$

This reception area is related to the gain  $G$  by the equation

$$A = G \lambda^2/4\pi.$$

Accordingly, the effective material surface can be calculated for any aerial whose  $G$  is known. For a parabolic reflector, or for an aerial wall with a not too large distance of the single elements, a value of  $A$  is obtained that is nearly equal to the geometrical surface. For a Yagi aerial the effective receiving surface is given by an effective cross-section for the radiation. For a system of 9 directors, for instance, one obtains:

$$A = 2.54 \lambda^2.$$

If  $A$  is known, as well as the minimum performance  $N$  to which the receiver still responds it is possible to state the “brightness” of the radio sources that will be still observable with the instrument. Since the aerial always receive radiation in only one plane of polarization they only make use of half the energy flux, that is,  $S' = S/2$ . Furthermore, the instrument responds only to a certain bandwidth. If the bandwidth is called  $B$ , then is

$$P = \int N dv = \int AS' dv \approx ASB/2 \text{ W/m}^2$$

the power gained by the aerial.

### **2.3.2 Receivers**

It should be possible to connect the receiver with an amplifier of practically unlimited amplification and thus to achieve any amount of sensitivity. This, however, would be of little purpose since the receiver output is not only the received signal, but also comprises, equally amplified, all disturbances in the receiving system, the so-called “background noise”. What actually matters is therefore not the absolute sensitivity, but the “signal to noise” ratio.

This noise level of the receiver has different causes. One of its important components is the resistance noise, i.e., the irregular fluctuations of a current consisting of a finite number of electrons. It depends on the absolute temperature of the aerial and receiver and is, in principle, unavoidable. A resistance transfers the noise,

$$P_R = kTB,$$

to another resistance of the same size. Additional noise contributions are due to the statistical fluctuations of the processes in the valves and transistors. The noise temperature is in the most favorable case given by the temperature of the receiver (i.e., about 290K). The imperfections of the instrument increase this value (assuming that the noise that originates in the receiver can be represented by the noise rate input end of a noise-free instrument of the same output amplification). One can therefore write

$$P_R = kT_R B, \quad T_R = F \cdot 290 \text{ K}.$$

The quantity  $F$  is a measure of the additional noise contributions.

Receivers must be as noise-free as possible. For this reason new valves were developed, masers used, certain components specially cooled, and special circuits invented (e.g., the so-called “parametric amplifier”). The optimum-noise figure,  $F$ , can reach about 0.1; the normal receiver has  $F$ -values between 3 and 10.

It shall now be discussed how the reception can be made visible. One can use an indicator with a pointer or a continuous recording device. The reaction time of the instrument, its so-called “time constant”, must be of such a size that noise fluctuations are smoothed out without affecting the existing time variation of the desired signals. These time constants usually lie between 1 and 0.5 min. Irregular fluctuations in a recording can afterwards be eliminated by forming mean values. Ingenious circuits can be designed that correct for changes in the receiver sensitivity. If such methods are used and the bandwidths of the reception and the time constant of the recording are chosen in a suitable way, it is possible to detect the existence of signals of 1/1000 of the receiver’s noise level.

## **2.4 Radio Astronomical Objects**

An important reason to explore astronomical objects in radio wavelengths is that the emission properties provide quantitative physical information about conditions in the source. Radio emission is produced in a large number of ways (see 2.2.5). The low-energy radio photons are relatively easy to produce, which makes radio emission sensitive to a great number of parameters. However, the number of mechanisms is itself a problem. Before one can use the emission to give information, one must first determine which radio emission mechanism is responsible for the emission. In practice, the most accurate way to determine the emission mechanism is to have spectral information, since different emission mechanisms have different characteristic spectral properties. In addition to helping to determine the emission mechanism, quantifying spectral properties such as peak brightness, peak frequency, spectral slopes, etc., also provides quantitative diagnostic parameters.

The fundamental radio sources are: the Sun, Jupiter, interstellar hydrogen and ionized gas, pulsars, quasars and the cosmic microwave background radiation. The accessible frequencies cover the wide range from 10 MHz to 300 GHz. There are some frequency bands that are internationally protected against interference with man-made emitters, like the natural frequency of the atomic hydrogen at 1,421 MHz (wavelength 21 cm).

The radio telescopes are used as single element instruments with diameters of up to 100 m or in arrays as radio interferometer. Single element instruments have limited spatial resolution, so that they are used primarily for scientific objectives, which do not need high spatial resolution like the analysis of pulsar signals over time or the investigation of the spacious distribution of gases or the cosmic background radiation. For high spatial resolution, i.e. the investigation of the structure of radio galaxies and quasars, interferometers are used. Since the development of radio telescopes in the 1940’s astronomers made a number of fundamental discoveries. Among these are pulsars, quasars, the cosmic background radiation and the 21-cm-line of the atomic hydrogen.

The Sun will be discussed in detail in chapter 3.

### **2.4.2 The Planets**

Planets and other solar system objects are in general only thermal emitters (producing radio emission only due to black body radiation from their surfaces). Since they are generally cold (700 K for Mercury down to 30 K or so for Pluto), they are weak emitters. This weak radiation is measured in the centimeter and millimeter region. For the temperature of 700 K a value of  $S = 1 \cdot 10^{-24} \text{ W/m}^2 \text{ Hz}$  at  $\lambda = 1 \text{ cm}$  is obtained, taking the distance from the Earth equal to one astronomical unit.

Jupiter is the main exception, since it has a very large magnetosphere that traps high-energy electrons which afterwards emit synchrotron radiation. The produced radiation bursts have been found for wavelengths between 3 and 60 cm; and at  $\lambda = 60 \text{ cm}$  they can reach  $S \sim 10^{-25} \text{ W/m}^2 \text{ Hz}$ .

It is also possible to bounce radar signals off the nearby planets (Mercury and Mars) and image the echoes.

### **2.4.3 The Milky Way**

The H I (atomic hydrogen) regions of the Milky Way show emissions due to the hydrogen line at 21 cm. These observations are of fundamental importance for the analysis of the structure of the Milky Way. These lines are of relatively small bandwidth (below 1 MHz) and of small intensity.

The Galaxy as a whole has a radiation that is nonthermal and corresponds at  $\lambda = 1.5 \text{ m}$  in the direction to the galactic center to an equivalent temperature of  $T_E = 1300 \text{ K}$ , whereas it decreases at the galactic equator by a few hundred degrees; at the galactic poles it is hardly 100 K. At longer wavelengths, its intensity increases, and at  $\lambda = 3.7 \text{ m}$  a temperature of about 15.000 K is measured at the center, and of about 2000 K in the opposite direction, while 800 K is the minimum value near the poles.

### **2.4.4 Discrete Radio Sources**

A large number of radio sources of a very small angular diameter are known, the so-called radio stars. Some can be identified with unusual galactic objects, for instance with nebulae, which are also anomalous in the optical wavelength region; others are extragalactic.

The radio emission of most of the more intense radio stars is approximately proportional to the wavelength and can therefore not be of thermal origin.

### 2.4.4.1 Stars

A good place to start with stellar radio emission is to look at an H-R diagram.

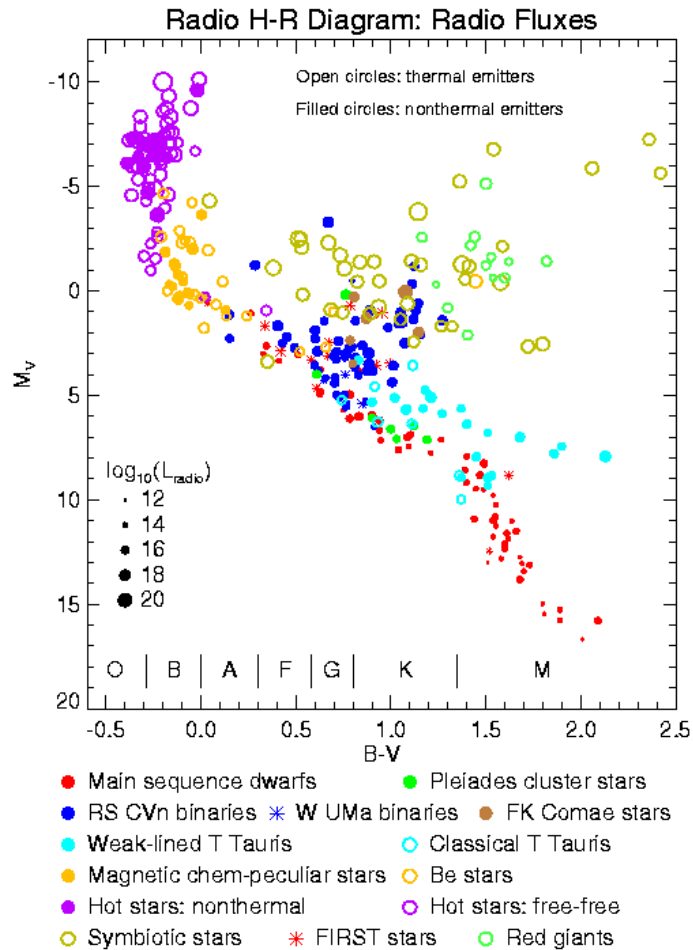


**Figure 2-9: Radio H-R diagram**

This diagram is from Stephen White, at University of Maryland. The placement of the symbols is according to the star's classical visual magnitude vs. color (B-V), but the symbols themselves encode the information about the radio emission. Most of the main sequence and subgiant objects are nonthermal emitters (filled circles), while most of the giants and many of the O-B stars are thermal emitters (simply because they are big). The blue circles near the center of the diagram are RS CVn binaries. These have a late-type subgiant "revved up" by tidal interactions with its close binary companion. The open circles just above the RS CVn ones are symbiotic stars, which again are binaries, but now with a compact companion (perhaps a black hole).

It can be noted that the G, K and M dwarfs (red dots) are weak emitters. These objects are also flare stars, meaning that occasionally they have strong radio outbursts. Flare stars have both optical and radio flares that are giant in comparison to solar flares. There is good evidence that such stars have a large fraction of their surfaces covered with "sunspots." This is probably because they have a fast rotation coupled with a fully

convective interior, so that dynamo generation of magnetic fields is much larger than for the Sun. A few stars have so much activity that they can be said to have detectable "quiescent" radio emission all of the time (e.g. the star UV Cet).

#### **2.4.4.2 Pulsars**

When a star's mass at the end of its life is  $M > 1.4 M_{\text{Sun}}$ , electron degeneracy is no longer enough to keep gravity at bay, and matter is crushed to force inverse  $\beta$  decay



so the protons and electrons are combined to form neutrons--a neutron star. The state of matter is a neutron degenerate gas. Degenerate objects have the peculiar property that with greater M they have smaller radii, up to  $\sim 3 M_{\text{Sun}}$ . Radii are typically 10-30 km.

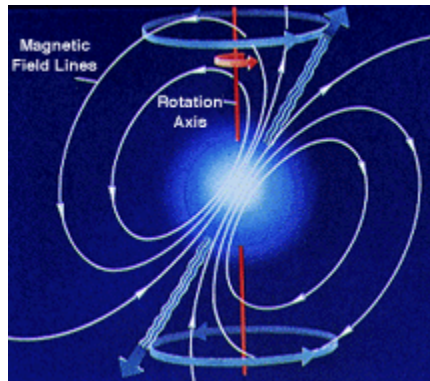


**Figure 2-10: Schematic of a pulsar**

Pulsars are rapidly rotating neutron stars that have a very high magnetic field (concentrated during the collapse of the core of a star into a neutron star) whose poles happens to be offset from the direction of the spin axis. If the spinning happens to bring the poles around to point at Earth, these bright poles will briefly be seen as an intense radio emitting source. The emission is due to synchrotron emission of electrons in the high magnetic fields. The pulses, of course, are repeated on each spin. Pulsars spin at periods ranging from 4 s to 1.6 ms.

#### **2.4.4.3 Galactic Objects**

Cassiopeia A is a supernova remnant that has been studied with detailed maps over a couple of decades, now. One can actually see the expansion by watching the detailed images as a movie. What can be seen is the outer envelope of an exploded star that is moving outward into the interstellar medium with high velocity, surrounded by a shock wave that is still heating material to emit X-rays.

SiO maser emission from stellar atmospheres, and water maser emission from H II and star formation regions, so the surprising variety of radio emission mechanisms. The SiO molecules surrounding some stars with extended, cool atmospheres is preferentially in the  $J = 1$  spin state, and as radio emission at the right frequency (43 GHz) stimulates the

transition from  $J = 1$  to  $0$ , they emit another photon. This photon, along with the original one, proceed into the cloud of molecules and stimulates more transitions, giving rise to a very bright line emission in small regions. The direction of the magnetic field can be deduced from the direction of linear polarization of the emission. Likewise for the water ( $H_2O$ ) maser, operating at 22 GHz.

The Crab Nebula (Taurus A) deserves particular mention; it probably originated as a consequence of a supernova explosion, and it emits in the optical part of its spectrum nearly completely polarized light. This and other facts make it highly probable that the emission is due to synchrotron radiation.

#### **2.4.4.4 Quasars and Lobe Radio Sources**

Quasars are Active Galactic Nuclei (AGN), i.e. the centers of extremely active galaxies. For a time they were mysterious objects because they appear only like a faint star optically (the term quasar is short for quasi-stellar object), but recent observations show that they do have faint "nebulousity" around them, which is actually the light from the rest of the galaxy in which they are embedded. It is now known that these are powered by super massive black holes. They have extremely well collimated jets, seen both optically and in the radio (as below). The jets culminate in giant radio lobes (sometimes on only one side), which are many, many times the size of the parent galaxy.

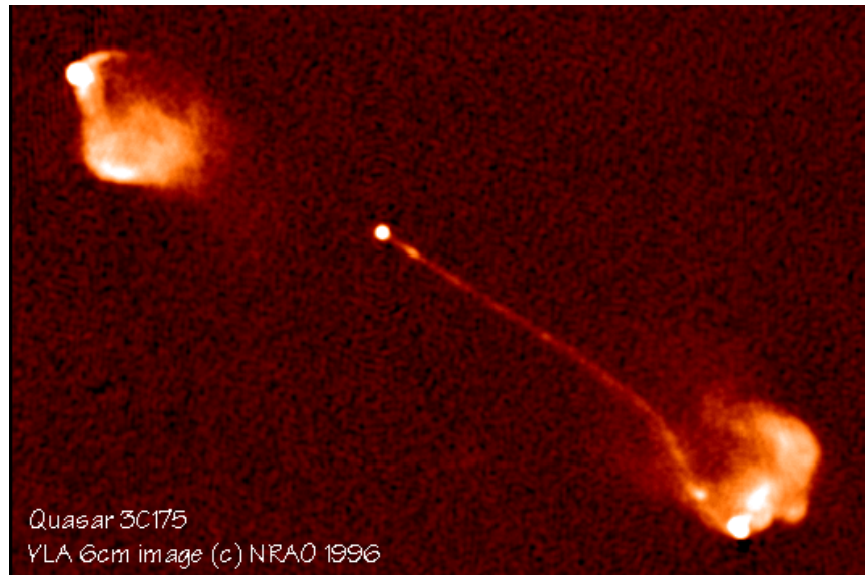


**Figure 2-11: Quasar 3C175, Image courtesy of NRAO/AUI**



### **3. Solar Radio Astronomy**

The Sun is the strongest discrete radio source that can be detected from Earth. The radio noise covers nearly the complete radio region. Due to particular circumstances the radio noise can increase by a factor of 100,000, while the optical intensity changes only by about 1%.

The principal goal of the radio astronomical observations of the Sun is to measure these emissions in various frequencies and to obtain the emission spectrum to receive information about the mechanisms and dynamics of the processes which take place. These processes can inflict its possible action on the interplanetary medium and in particular on Earth.

Before launching into the radio science itself, it will be helpful to look briefly at the structure of the Sun. The Sun is a normal star of spectral type G2V, which means that it is burning hydrogen in its core, as it has been doing for the last 5 billion years, and as it will continue to do for about 5 billion years more.

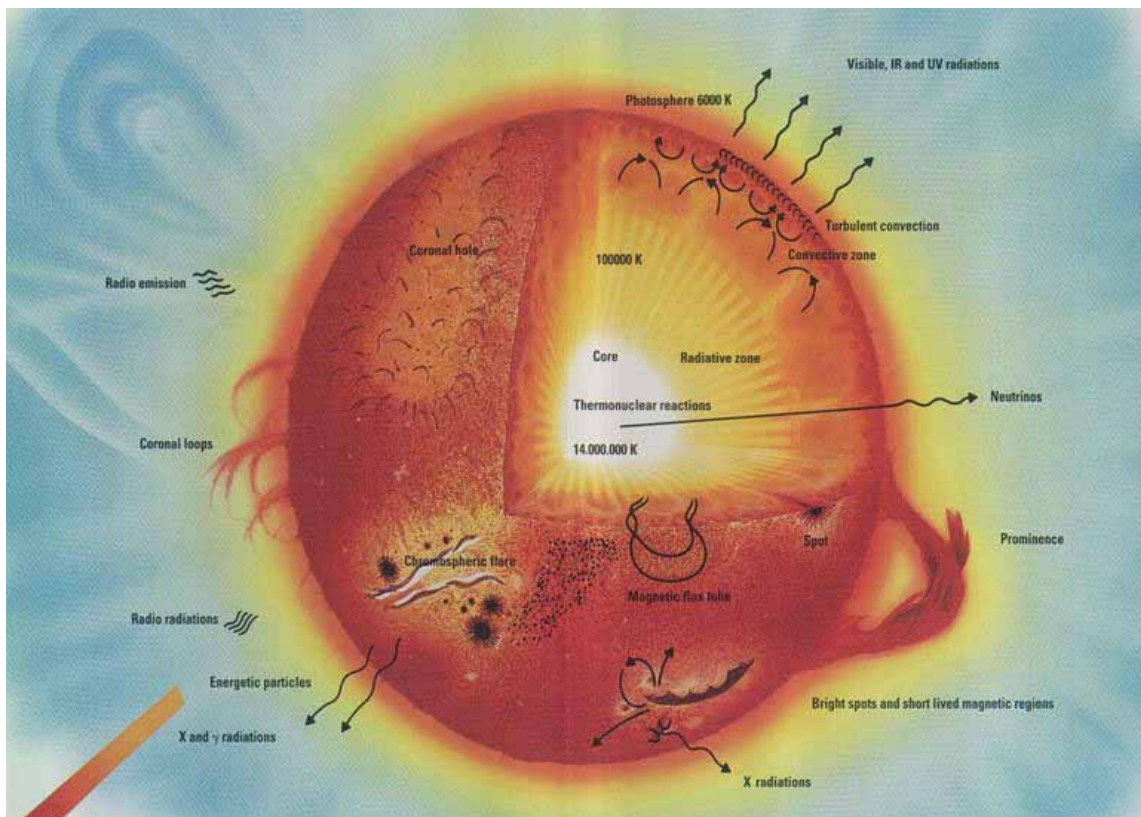


**Figure 3-1: A schematic view of solar structure**

The core temperature is about 14 million K, and the temperature falls off with distance from the core, eventually reaching the surface temperature of 5800 K. The photons generated in the core take about 1 million years to reach the surface, since they propagate outward in a random walk with a very short mean free path. Their point of last scattering is in the photosphere, after which they are finally free to stream out into space. Because



they are in thermal equilibrium with the photosphere, they have a pure blackbody spectrum corresponding to the 5800 K temperature, but en route to space they encounter the more tenuous gas of the other layers of the solar atmosphere--the temperature minimum region, the chromosphere and the corona--so the solar spectrum shows many spectral lines. The fact that these lines are mostly absorption lines indicates that the temperature falls to yet lower values above the photosphere, to about 4500 K in the temperature minimum region. This is fully expected, but what is surprising is that above this height the temperature rises again, and in fact rises very steeply at about 2000 km above the photosphere to form a very hot (several million K), very tenuous plasma that is called the corona.

### **3.1 Radio Emission of the Sun**

The radio emission of the Sun has different causes. The fundamental components involved in the Sun's noise are:

- the radiation of the quiet Sun
- slowly variable spot components
- noise storms in the meter-wave region
- outbursts

In general the radiation intensity depends on the electron densities and temperature in the different layers of the Sun's atmosphere. Due to the high temperatures that dominate in the Sun, it can be assumed that the gas in the Sun's atmosphere is almost completely ionized.

Furthermore, it can be said that longer waves from the Sun's interior cannot pass through the lower layer of the Sun's atmosphere. Only wavelengths smaller than a few millimeters can pass through the lower chromosphere. In the upper chromosphere wavelengths that are smaller or equal to 10 centimeters can do this. The corona is finally passable as well for meter waves. This means that most radiation of a determined frequency range originates in a region where the atmosphere is almost opaque for the observed wavelength:

- millimeter wave radiation → lower chromosphere (10.000 K)
- 10cm-radiation → upper chromosphere (75.000 K)
- meter waves → corona (1.000.000 K)

Following the causes and effects of the components of the Sun noise will be presented in some more detail.

#### **3.1.1 Radiation of the Quiet Sun**

During periods of quiet Sun (no sunspot activity etc.) a constant amount of radio emission is observed. It has its origin in the corona and the photosphere. The corona is optically dense at frequencies below 200 MHz; therefore its radiation temperature of one

million Kelvin is seen. Towards higher frequencies the corona gets thinner, until above 10 GHz only the photosphere shines through. Above 10 GHz and below 150 MHz the Sun has the characteristics of a black radiator.

The appearance of the "quiet time" solar atmosphere at radio wavelengths is governed by the plasma parameters (temperature, density, and magnetic field strength) and the radiation mechanisms that generate the radio emission. These signals are not constant, as even the radiation of the "Quiet Sun", that is of a Sun free of spots and centers of activity, varies within an 11-year cycle. The radiation of the quiet Sun is mostly of thermal nature.

The quiet Sun flux can be estimated by assuming a brightness temperature of  $10^6$  K over a radius of 1 to 2  $R_{\text{Sun}}$ , depending on frequency, leading to roughly  $20000 (f/100 \text{ MHz})^2$  Jy (Jansky - spectral flux density,  $1 \text{ Jy} = 10^{-26} \text{ Wm}^{-2}\text{Hz}^{-1}$ ). The quiet Sun flux does however vary considerably with the solar cycle; it has been reported to be as low as 2000 Jy at 50 MHz during solar minimum, which is much fainter than sources such as Cas A and Cygnus A. Furthermore, the solar flux can vary dramatically at low frequencies: an example was observed on June 2, 2002, where the quiet Sun flux was just 19 sfu (1 solar flux unit = 1 sfu =  $10^4$  Jy), but the peak flux during flares raised to 300 times this level, when (at  $\sim 10^8$  Jy) the Sun will be easily the brightest object in the sky.

### **The Chromosphere**

Because of the huge increase in electron density at the chromosphere, radio emission becomes optically thick due to free-free emission at heights higher than the solar minimum region, even at the highest frequencies. Therefore, radio observations pertain only to the upper chromosphere and higher. One can start at the chromosphere and move outward in the solar atmosphere. This is also equivalent to starting at the highest frequencies and moving to lower frequencies.

The chromosphere is dominated by the super granular structure – large-scale convective cells of the order of 30" (200,000 km) in size. The gas rises in the center of the cells, moves to the edges, and descends. As a result, it tends to sweep relatively weak magnetic fields to the edges, where it collects to form the chromospheric network structure. Radio images (at 8.5 GHz) show a good correspondence of the radio sources with the magnetic elements, as shown in Figure 3-2. Quantitative results are frustrated by the fact that such images from the VLA require an all-day (8 - 12 hours) synthesis, and so time-variability cannot be easily followed.

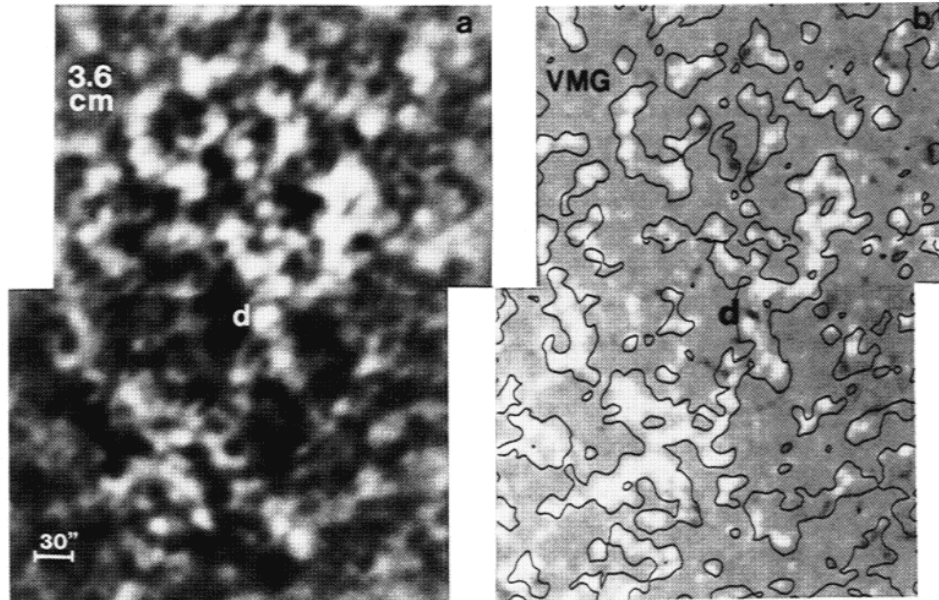


**Figure 3-2: Radio images of the chromospheric network structure and sources of magnetic elements.**  
The panel on the left shows the radio image at 8.5 GHz (3.6 cm wavelength), showing the network structure. The corresponding magnetogram on the right shows a high degree of agreement, with each source overlaying a magnetic element of the chromospheric network. The feature marked with a "d" is the only one representing a magnetic dipole.

In addition to the ability of radio emission to give the temperature of the chromosphere, it can also be used to learn something about the magnetic field strength, derived from the magnetic field dependence of the polarization.

The degree of polarization is directly proportional to longitudinal (line-of-sight) component of magnetic field strength,  $B_l = B \cos \theta$ . This gives a means to measure relatively weak magnetic fields in the chromosphere. Depending on the sign of  $B$ , a given mode (i.e. x-mode), can correspond to either R or L polarization, which are the two senses of circular polarization. Now, however, the polarization is due to the mode-dependence of the brightness temperature due to the temperature gradient, therefore a method to get the otherwise unknown temperature gradient is needed. Luckily, if one measures the brightness temperature at many frequencies one can use the slope of the radio spectrum, which itself is related to the temperature gradient.

### Active Region Corona

As we go higher in the solar atmosphere, the temperature rises steeply to millions of K, while the electron density falls greatly. This hot, tenuous plasma was first discovered through radio observations, was quite unexpected, and still remains unexplained. There have been many theories to try to explain it, but none of these theories seem to work.

The corona is everywhere hot, but certainly is hottest in active regions, which are regions associated with sunspots. Here we see that micro flares and larger flaring events tend to concentrate, and it shows that flares are closely related to magnetic fields, that get stressed due to motions and new flux emergence to provide energy for the sudden

releases that are called a flare. However, many aspects of this release of energy are still unknown.

### **3.1.2 Slowly Variable Spot Components**

The slowly varying component that is strongly correlated with the sunspot number, which is also called the spot component, adds to the basic noise of the quiet Sun. It can surpass the total noise of the quiet Sun by a factor of five.

The frequency region is between 150 MHz and 10 GHz, with the maximum being observed at 2 GHz.

The cause of the radio emission of the slowly variable spot component is as well thermic.

This radiation is superimposed by rapid emissions from the centers of activity, for instance, by “radiation bursts”. The main phenomenon, which lasts about 5 to 10 min, is usually followed by a slow fading, which can extend over several hours. The most intense radiation bursts in the centimeter and meter region reached intensities of  $S = 10^{-18} \text{ W/m}^2 \text{ Hz}$  or more, lying generally between  $S = 10^{-21}$  and  $10^{-20}$  (in the centimeter region). The mean frequency of such a phenomenon somewhat increases with time (“frequency drift”).

Furthermore, for wavelengths  $\lambda > 1 \text{ m}$  the “radio storms” (“noise storms”) can be observed, which consist of a large number of radiation bursts, each lasting for a few seconds only; they can remain observable for several hours or many days. The S-values for the radiation bursts can exceed  $2 \cdot 10^{-20} \text{ W/m}^2 \text{ Hz}$ . Isolated bursts that occur in the shortwave range up to a few centimeters are usually considerably weaker; like the other bursts, they are restricted to narrow frequency regions ( $\Delta\nu \sim 100 \text{ MHz}$ ). This shows that these emissions have no thermal origin.

### **3.1.3 Noise Storms in the Meter-Wave Region**

Many individual radiation shocks with durations of a few seconds and bandwidths of several MHz form the so-called noise storms in the meter-wave region. The total duration of a storm is confined to several hours or a few days and covers the frequency band below 100 MHz. The centers of the noise storms are being observed exclusively near the Sun’s meridian. Obviously the radiation is being bundled in perpendicularly direction to the Sun’s surface. Although noise storms occur in connection with sunspot regions, it cannot be concluded that strong sunspot activity causes noise storms. Nevertheless there are noise storms more than 10% of the time during a sunspot maximum.

The observed temperatures are above  $10^7 \text{ K}$ , which in connection with the strong polarization indicates nonthermal causes.

### **3.1.4 Solar Activity**

In addition to the structure of the non-flaring Sun, radio emission is exquisitely sensitive to flaring emission. One can define such emission to be any brightening with time variability on scales shorter than a few hours. Of course, the Sun is continuously variable on all timescales, so this division is somewhat arbitrary, but it will suffice for the purpose. The brightening can take on a fantastic range of forms, from a slight increase due to heating (thermal emission) to 1000-fold increases in seconds or less. All of solar activity arises due to the solar magnetic field.

The solar flare starts with a period of energy storage, called flare build-up, that can occur over a period of days, but often results from the eruption of new magnetic flux from below the photosphere, which can take only hours. The stored energy takes the form of a non-potential magnetic field distribution. During this time, the changes take place in conditions of ideal magneto hydrodynamics (MHD), meaning that there is a balance of magnetic and gas pressures and the field lines are "frozen in." If the conditions in the corona are right, the magnetic field can release its energy, sometimes in seconds, through a process called magnetic reconnection. In this process, the field lines are cut (something normally impossible in ideal MHD) and reconnected to a lower-energy configuration that is closer to potential. The difference in energy between the original non-potential configuration and the resulting, more potential configuration is available for mass motions, acceleration of charged particles, and generation of waves.

What is called the flare can represent the immediate release of energy, the initial heating and acceleration of the charged particles, and all phenomena associated with the resulting mass motions and subsequent thermalization of the particles. One associated phenomenon is the Coronal Mass Ejection (CME), which is a magnetic bubble that becomes unstable and buoyant, leaving the Sun and propagating out into interplanetary space.

#### **3.1.4.1 Flares**

The figure below shows a schematic view of the relationships between the different components of a flare, somewhat late in its development. The point marked "acceleration site" is relatively high in the corona, and is the point where reconnection is taking place. Loops labeled MW and SXR are the locations of the microwave and soft X-ray sources, respectively. These are recently reconnected loops, with overlying loops being most recently formed. The part of the diagram at right shows a schematic of what actual radio observations show -- type III bursts going upward, RS (reverse slope) bursts going downward, and DCIM (decimetric pulsations) at higher frequencies. One can see that the region sampled by the decimetric range of frequencies (300 MHz to 3 GHz) is a very interesting one, since it covers the typical range of heights corresponding to the reconnection region. As a reminder, the microwave frequency band is about 1 – 300 GHz.

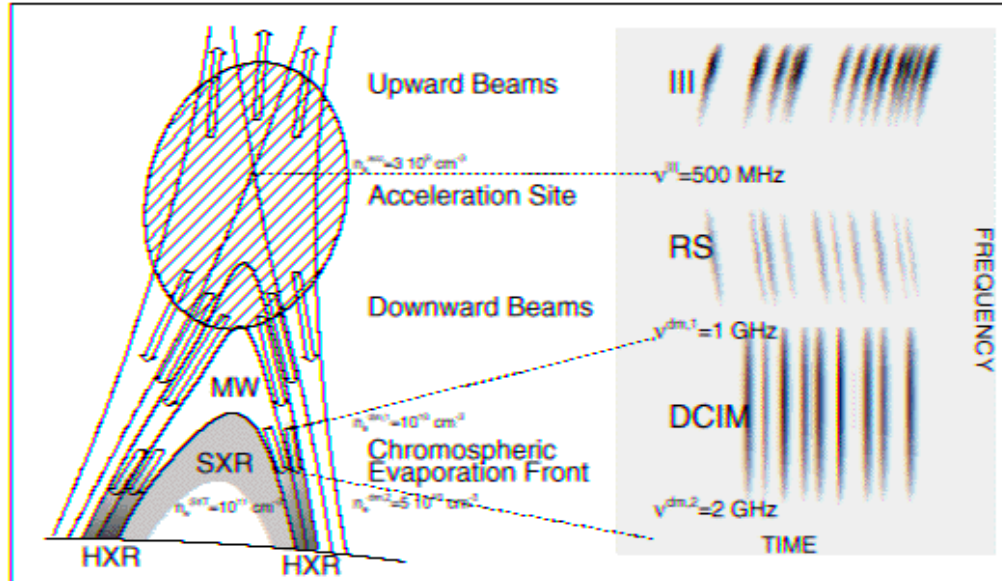


Figure3-3: A schematic view of a solar flare

At still higher frequencies, electrons trapped on closed loops (the loops labeled MW) cause the gyro synchrotron emission. There are several useful diagnostics that can be deduced from gyro synchrotron emission. The emission is broadband emission, with optically thick emission at low frequencies (typically 2-5 GHz), optically thin emission at high frequencies (>10 GHz), and a peak around 5-10 GHz. The peak frequency is related to the magnetic field strength and number density, the optically thin spectral index is related to the electron powerlaw index, and the polarization tells indicates the direction of the magnetic field. The sensitivity of microwave emission to these parameters makes it a useful complement to other measures of the accelerated electrons, i.e. hard X-rays.

This means that microwaves are far more sensitive to high-energy electrons than are hard X-rays. Thus, they are well suited for those studies.

### **3.1.4.2 Radiation Outbursts**

Radiation outbursts of the Sun can be observed in the whole radio region. They normally coincide with visible eruptions (flares or sub flares). The radiation flux of centimeter-waves can increase in comparison with thermal radiation including the spot components by a factor of 20, of meter-waves even by a factor of 1000. The duration of an outburst can last between a few seconds and several hours.

At still lower frequencies (<300 MHz), the metric burst types are seen. These types were discovered in the 1950's, through the use of spectrographs, and each type has a unique signature in frequency and time.

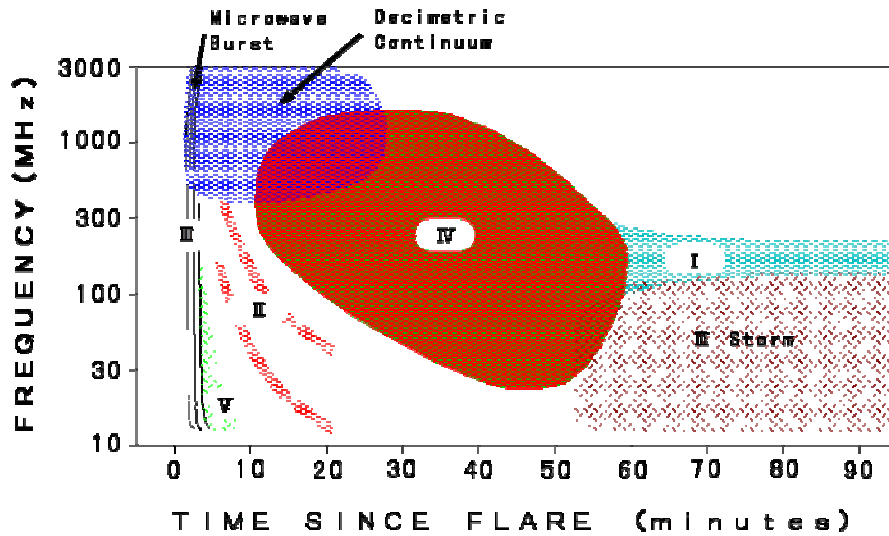


Figure 3-4: Schematic diagram of metric bursts types

The types are:

- **Type I**
  - *type I bursts* or chains, narrowband, non-drifting bursts of short duration
    - cause is unknown, but emission appears to be plasma emission
  - *type I storm* -- a continuum emission with many type I bursts embedded, duration days
    - cause is unknown, but related to continuous reconnection above active region
- **Type II**
  - *type II burst*, slowly drifting, often with fundamental/2nd harmonic structure, due to plasma emission
    - cause is a shock wave, propagating at 500-2000 km/s outward into the corona into interplanetary space (*also seen down to kilometric wavelengths*).
- **Type III**
  - *type III burst*, rapidly drifting, often with fundamental / 2nd harmonic structure, due to plasma emission. The fundamental is highly o-mode polarized, and the 2nd harmonic is weakly (15%) x-mode polarized.
    - cause is a stream, or beam, of electrons moving at speed  $\sim c/3$ , propagating from low corona into interplanetary space (*also seen down to kilometric wavelengths*).
  - *type III storm* -- a long lasting (up to a day or more) series of type III bursts, RS (reverse slope) bursts, reverse-drift pairs, and continuum.
- **Type IV**
  - *stationary type IV* -- broadband continuum emission, sometimes highly polarized, due to either plasma emission (o-mode polarized) or gyro synchrotron emission (x-mode polarized).
    - cause is a plasmoid or high, filled loops of non-thermal particles

- *moving type IV* -- a similar cause, but entrained in a CME or expanding arch.
- **Type V**
  - *type V burst*, continuum emission following a type III burst, x-mode polarized (opposite sense to the associated type III)
    - cause is slower type III-like electrons in widely diverging magnetic fields, with both forward and counterstreaming Langmuir waves, perhaps generated by previous passage of type III electrons.

The radiation temperature rises during outbursts up to  $10^{11}$  K, which clearly indicates to nonthermic radiation processes.

One can observe type III bursts propagating all the way to Earth and beyond.

### **3.2 Space Weather**

The field of Space Weather has taken on increasing importance in recent years, as the realization of just how damaging space influences on the terrestrial environment can be. Geomagnetic fluctuations caused by currents in the Earth's magnetosphere can overwhelm long-distance power grids and cause huge economic disruption, and threaten life if it causes power loss in communities that depend on electrical heating to survive the polar winters. Energetic particles accelerated close to the Sun can damage solid-state electronics on satellites, and there are numerous examples of satellite loss attributed to this cause; further, solar-induced heating of the ionosphere can cause it to expand upwards into the altitudes occupied by low-Earth-orbit satellites, increasing the drag on them and causing them to drop out of orbit and burn up in the Earth's atmosphere. Energetic particles also pose a health risk to astronauts and to high-altitude flyers such as commercial and military pilots, while ionospheric disturbances cause disruption to long-range radio communications.

As can be seen from this list, the sources of Space Weather are diverse. Coronal mass ejections play a major role in causing geomagnetic storms and disrupting the auroral particle belts, and any means of studying CMEs is of potential importance. Other aspects of Space Weather may also prove to be best addressed through low-frequency observations. The energetic protons and  $\alpha$  particles that bombard the Earth following some solar events are an important feature of Space Weather and there are efforts to correlate their occurrence with phenomena in the solar corona.

### **3.3 Solar Radar Experiments**

In addition to the passive detection of radio emission from CMEs in the solar corona, active detection of CMEs using radar techniques has great potential for Space Weather research. Solar radar with a suitably equipped transmitting facility and using for example the planned Low Frequency Array (LOFAR) as the detecting and imaging element may



provide a unique technique for detecting and tracking CMEs, opening up an entirely new and exciting field of solar research.

The interest in this proposal is generated by the results of a unique experiment carried out in the 1960's with the El Campo radar, built by the Lincoln Laboratory (MIT), which detected 38 MHz radar echoes from the Sun for a period of 9 years. Huge, rapidly-moving targets were occasionally observed but this was before the space-borne coronagraph discovery of coronal mass ejections (CMEs), and the physical nature of these "targets" was a mystery. It is now thought that CMEs were being observed. Subsequent radar experiments have been unsuccessful, but none have had the combination of transmitting power and receiving area possessed by El Campo.

Radar experiments transmit a very narrow band signal and detect any frequency shifts in the reflections (or echoes). The Doppler shift introduced by different parts of an outward-moving CME will result in a characteristic frequency- and time-dependent signature in the reflected signal. The rich information inherent in this measurement could open an entirely new window on CME studies, yielding their angular distribution, ranges, and line-of-sight velocities. Combining the radial velocity obtained from the Doppler shift with the transverse velocity obtained from imaging would yield the CME total velocity vector. This may allow for accurate predictions of CME Earth-arrival times. Aside from the macroscopic physics of direct interest to the space weather program, there is great potential in unraveling the microscopic physics of the solar radar scattering mechanism. An understanding of this mechanism is key to solving the puzzles of the spectral shape, the large Doppler spread, the Doppler shift, and the variation in solar radar cross section observed by James. Various mechanisms have been suggested, including turbulence in the local medium, fluctuations in the altitude of the plasma resonance level due to electron density fluctuations in the solar wind, ion acoustic waves, and coherent lower hybrid waves. If the radar technique is successful, it will also provide a sensitive probe of turbulence in the solar corona.

Two transmitters for solar radar applications are being discussed at present. A monostatic 26 MHz solar radar system has been proposed for Arecibo. The stand-alone version of this system will be powerful enough to confirm James' results using modern technology, with the advantage of the availability of the extensive monitoring of the upper solar atmosphere and CMEs at other wavelengths that James did not have at his disposal. This system would provide a steppingstone to a more powerful system that would use Arecibo as the transmitter and LOFAR as a receiving element to provide two-dimensional information. In addition, there is a Swedish proposal to construct a phased-array transmitting antenna ("LOIS"). The elements of the transmitter will be distributed over a large area so that the power from each element will be low enough to avoid creating plasma irregularities in the ionosphere, with the signals being phased to merge at the target location in the interplanetary medium. LOFAR would provide much greater collecting area, and hence sensitivity, than LOIS itself would achieve as the receiving element. If they are successful, these solar radar techniques could revolutionize the way in which coronal mass ejections are studied.

## **4. Havana Radio Astronomical Station**

The Havana radio astronomical station (ERH) is located at the Institute of Geophysics and Astronomy (IGA) and was founded in September 1969 under a collaboration agreement of the Cuban Science Academy and the Council for Radio astronomy of the Science Academy of the Soviet Union. This agreement, like many others in matters of collaboration between socialist countries that expressed the interest in investigations of global character, were supported financially by the USSR, who provided the necessary materials. Whereas in Cuba, particularly in this case, the ERH was planned as an observation point among the other stations forming the so-called “Sun service” net. Now Solar Patrol Service Net (World Data Center B).

These stations, which not only contribute to the search of new appearances, regularities and periodicity of solar phenomena (investigations of basic character), keep a continuous look at the state of solar activity, the interplanetary medium and the near-Earth environment. These states are reported by established methods to the space flight centers and to the communication centers.

### **4.1 The Importance of the ERH**

The importance of the observational activity is determined by the fact that until now there is no total protection system for the crews of space vehicles against the effects of high-energy particles. These are ejected by the Sun into the interplanetary medium and propagate for great distances through the solar system.

At the moment of the foundation of the station, it had a privileged position in the western hemisphere because it could keep up the observation of the Sun while the other stations linked to the system of the Science Academy of the Socialist Countries could not because they were all located in the eastern hemisphere. The observations of solar explosions of high intensity were reported immediately to the Cosmic Research Institute of the Soviet Union, so that they could take appropriate measures. In fact, this activity is even more important today, with plans for long duration manned space flights without the protecting magnetosphere of the Earth, like missions to Mars, the Moon or an asteroid.

The ERH fulfills also a function of national interest. The state of Earth’s ionosphere depends highly on the state of the interplanetary environment in the vicinity of the Earth. The ionosphere is a region of the upper atmosphere (~ 90–500 km) with a high degree of ionization that allows long distance communication by radio waves. It seems that in the era of satellite communication, this way might be obsolete, but in reality the ionosphere has two characteristics of great importance. First, it cannot be blocked or destroyed like satellites, and secondly, but not less important, provides a simple and cheap way of communication. These observations permit the prediction of the state of the ionosphere and therefore the optimal frequencies to establish the long distance communication circuits and the transmissions of the radio stations, commercials or not.

Furthermore the ERH formed the core of the formation of personnel specialized in astrophysics and related techniques that are used in the different branches of astronomy. Thus giving the nation the capacity to respond to questions related to space and its use in the integral formation of its citizens, the spread and the popularization of science (like the Cuban participation with various experiments on Interkosmos with the first flight of a Latin-American cosmonaut, Arnaldo Tamayo).

## **4.2 The Radio Telescopes of the ERH**

The element commonly used to define a radio telescope is the antenna. This is because it is the most stable of the three that define the instrument (antenna, receiver and recorder). In the majority of the cases, an antenna supports various receivers that work alternating or simultaneously depending on the scientific objective at the moment. The ERH consists of three radio telescopes:

- The RT2, which holds a receiver of 9.5 GHz
- The RT3 in which receivers of 15 GHz and 6.7 GHz are installed
- The RTM with receivers of 230 and 280 MHz.

The radio telescope of 9.5 GHz employs a receiver above a parabolic antenna that measures the total radio emission of both polarizations. (see figures 4-1a and 4-2).

Depending on the antenna type, the radio telescopes can receive different types of radiation. The parabolic antennas permit to receive circularly polarized waves; therefore they are called radio polarimeters. Of the three radio telescopes that are used by the ERH at the moment, the one observing the frequencies of 15 GHz and 6.7 GHz (RT3) belongs to this category (see figures 4-1b and 4-3).



**Figure 4-1: Radio telescopes of the ERH: The RT2 (a), the RT3 (b) and the RTM (c)**

The radio telescope of 230 and 280 MHz (see figure 4-1c) is a so-called “switch interferometer”, which is a type of radio telescope in which the antenna (in this case a 32 element Ude-Yagi array, see also 2.3.1.1) is divided into two sections that are connected alternately in phase and contra phase (see figure 4-4). Because its branches are constituted by Ude-Yagi antenna arrays it can only register one type of linear polarization.

Figures 4-2, 4-3 and 4-4 are block diagrams for each radio telescope.

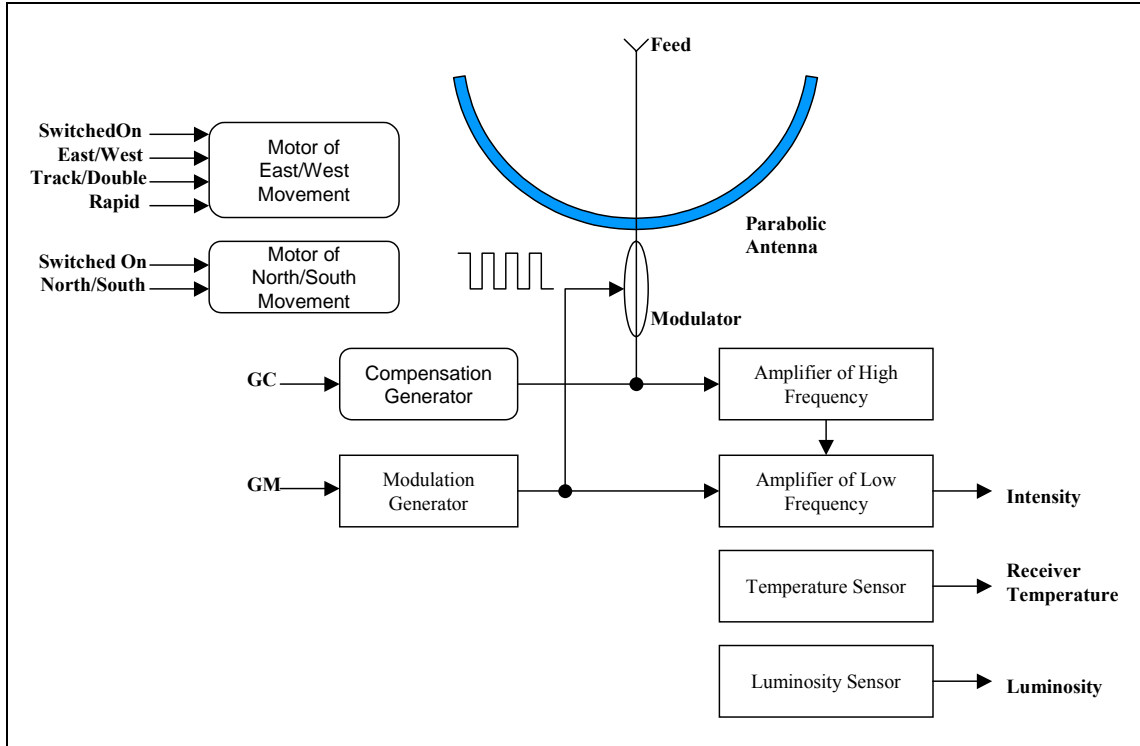


Figure 4-2: Block diagram of RT2

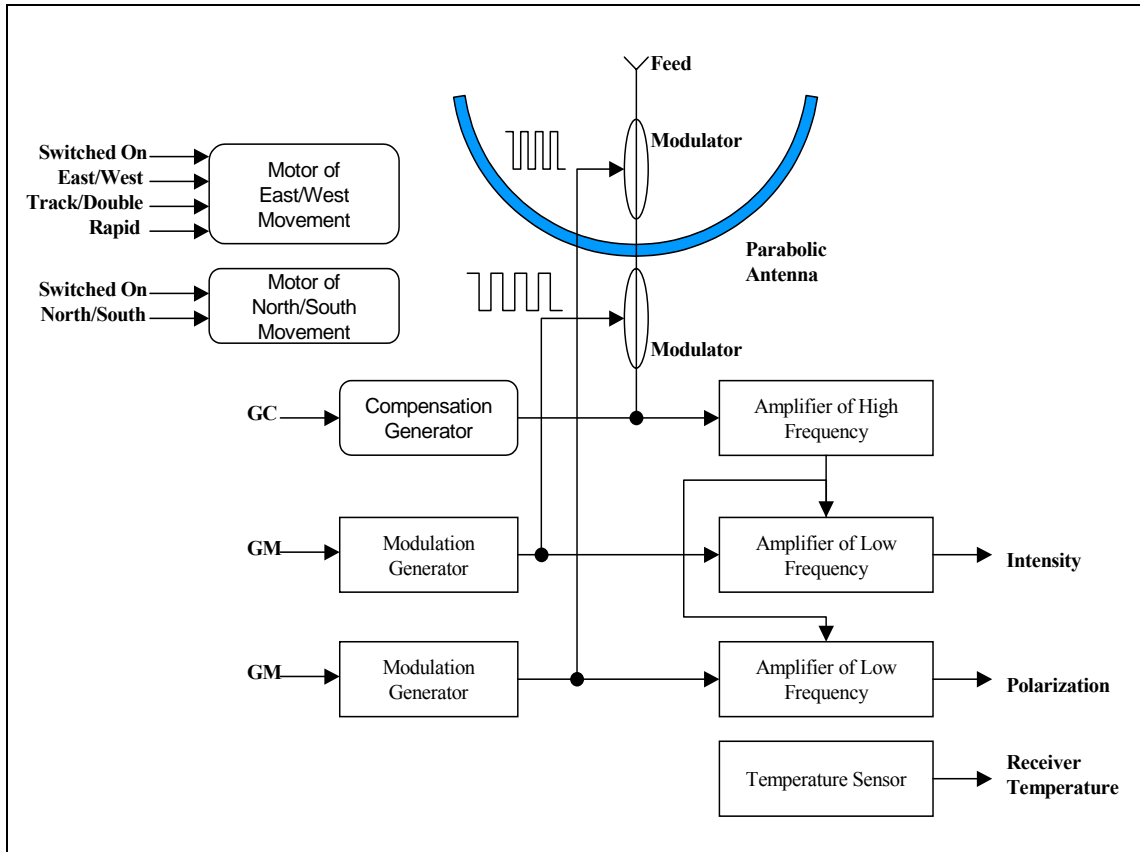


Figure 4-3: Block diagram of RT3

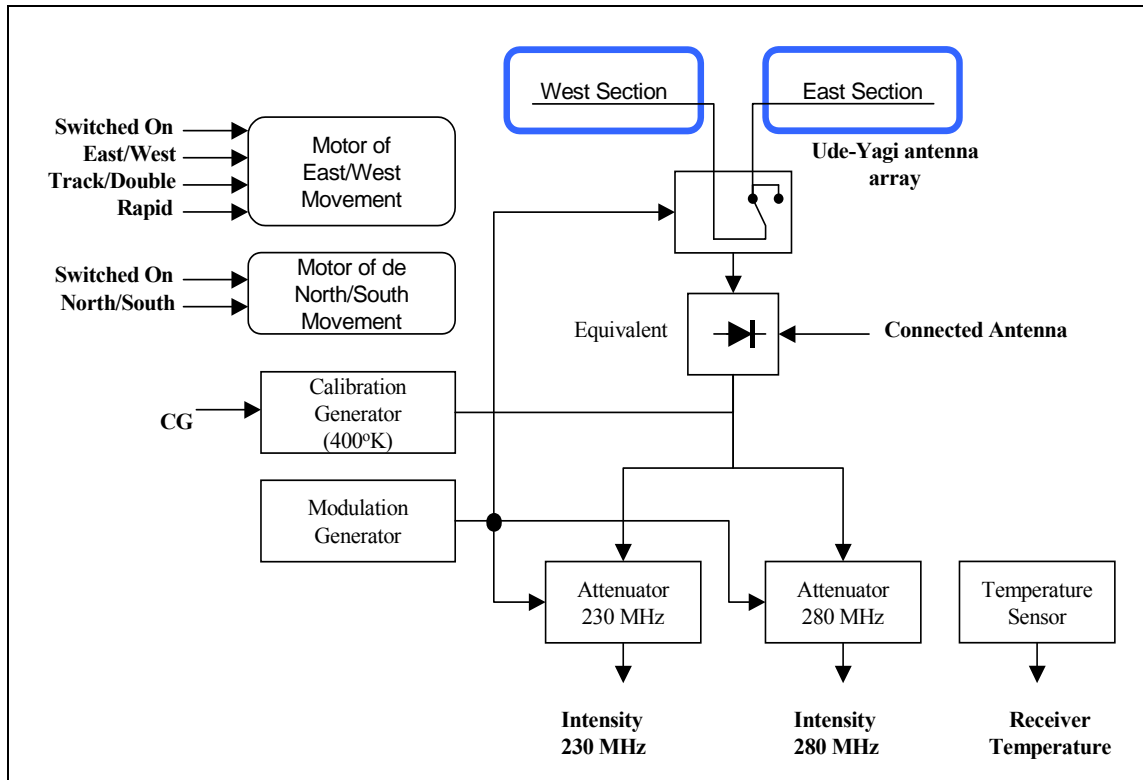


Figure 4-4: Block diagram of RTM

In solar observations the unit of measurement used for the radiation is the Solar Flux Unit (SFU), expressed in units of energy over time unit over area unit over bandwidth unit,  $10^{-22} \text{ W m}^{-2} \text{ Hz}^{-1}$ . To give an idea of the magnitude of the measured signals one can say that during normal solar activity, which is without any events, the intensity measurement reports values like the ones shown in table 4-1.

Table 4-1 Values of the intensity in different frequencies and during a period of normal solar activity (without events).

Frequency	Intensity
15 GHz	500 SFU
9.5 GHz	300 SFU
6.7 GHz	150 SFU
280 MHz	10 SFU
230 MHz	10 SFU

As mentioned earlier in chapter 3, it is important to point out that during a solar event the intensity can grow several times with respect to its value in normal state. This natural amplification varies based on the observed frequency, and can be 2 times or more at 15 GHz, and up to 16 times at 280 and 230 MHz. These maximum values have been surpassed in very few occasions since the creation of the ERH.

### 4.3 The Process of the Solar Observation

The observation is carried out by pointing the antenna towards the Sun and compare the received emission with that of a known emission source. In the case of the radio telescopes of 15, 9.5, 6.7 GHz the known emission source is a load that is coupled to the waveguides emitting the receiver temperature, which is kept at a fixed temperature with the help of a thermo-regulation system.

In practice this coupled load is injected in contra phase with the signal coming from the antenna. Since the two temperatures cancel each other, the sky appears “cold” in these frequencies. The approximate radiation level that will be observed can be seen when directing the antenna towards the zenith (and away from the Sun). Easier said, when the intensities of both signals (the object and the load) are compared, the relative value of the signal coming from the region where the antenna is pointed can be measured. That is, when the radiometer is linear within the intensity interval. The so-called “zero level” is taken as reference level when the receiver practically perceives only its own noise.

However, the amplification of the receivers can vary with time. In the case of solar observations, the total intensity of the object can be relatively great, therefore the variations of the amplification can induce variations in the signal, comparable with the own variations of the Sun’s emission.

To calibrate this situation Dicke-receivers have been developed. In these receivers, an instrument injects a signal through the channel where the charged load is situated, so that it annulates the signal coming from the object in question (the Sun). This way, nulling the signal that arrives at the receiver, it is not important if the amplification varies or not, because the value will stay zero. Only variations of the object’s emission will then be registered, while the background emission is calculated beginning from the emission of the “compensation” instrument, which is normally a noise generator diode or a tube of gaseous discharge.

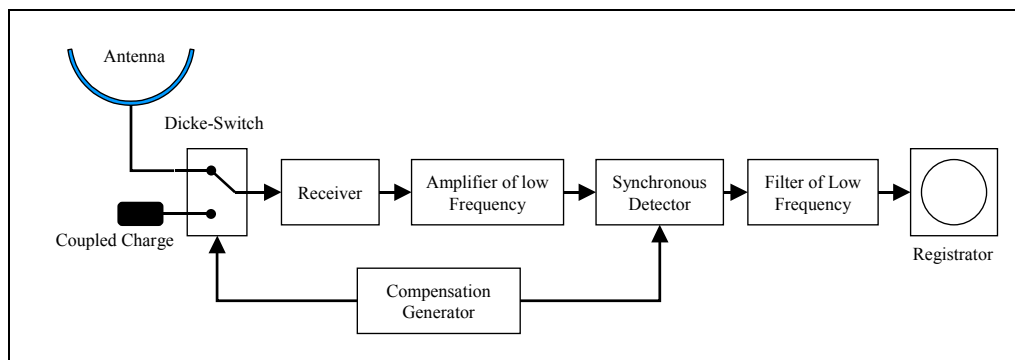


Figure 4-5: Block diagram of a Dicke-Receiver

In this type of receiver, besides the previously mentioned zero level, two other reference values need to be known: the values of the compensation generator and the sky level. The level of the compensation generator is obtained by disconnecting the modulation generator so the signal of the solar radiation will be zero. The sky level is being measured

by orientating the antenna to an area far away from the Sun, which in the morning as well as in the evening has to be the meridian.

In the case that the instrument is a radio polarimeter, the antenna must have a generator of polarized waves located at the entrance. A generator of polarized waves is a round waveguide with a plate inside that blocks part of the incoming polarization so that it allows the calibration of the instruments with the help of the polarization coming through. Only the levels of zero and the sky will be measured, since there is no compensation generator. From now on these three values will only be called reference levels.

Following the previous general alignments, the observation process in the frequencies of 6.7, 9.5 and 15 GHz at the ERH, is being conducted following these steps:

***Initial daily calibration***

- (only for the radio polarimeter) with the help of the polarized waves generator located at the entrance of the antenna signal, positioning of the antenna at the meridian
- (only for the radio polarimeter) determining the reference level in the polarization channel and removing the polarized waves generator
- positioning of the antenna at the meridian
- determination of the reference levels in the intensity channel

***Observation***

- positioning of the antenna at the Sun and begin of the tracking
- adjusting of the tracking
- measurement of the Sun's emission

***Final daily calibration***

- positioning of the antenna at the meridian
- determination of the reference levels in the intensity channel
- (only/just for the radio polarimeter) placing the polarized waves generator and positioning the antenna at the meridian
- (only for the radio polarimeter) determination of the reference levels in the polarization channel, the polarized waves generator is left for the calibration on the following day

The processes of adjusting the focus of the antenna at the Sun and the measurement of the Sun's emission are repeated every hour. The adjustment of the focus is nothing else than positioning the antenna with the maximum signal value possible. The measurement of the Sun's emission is the determination of the zero reference level and of the levels which are obtained with the antenna focused at the Sun and with the compensation generator switched on and off.



#### **4.4 Post Processing of the Measurements**

The obtained measurements are registered in millimeter paper and require a post processing for their application.

This is done manually, first measuring the different emission levels referring to the zero level in millimeters and obtaining the so-called Sun antenna temperature. This antenna temperature of the Sun is the temperature that should have a cavity of a black body, so that it produces the really registered intensity of the signal at the exit of the radio telescope, when the antenna is introduced into the cavity.

The construction of the spectra requires absolute values since in the majority of the cases the measurements are made by different instruments. For that reason each radio telescope has its own value conversion factor from antenna temperatures to absolute values. This coefficient is calculated by special observations of known emission sources. At the ERH a calibration method was developed based on the observation of the moon, which is used as reference source for the determination of this factor in the RT2 and RT3 radio telescopes. For the RTM this type of calibration is achieved using the reference radio source Cassiopeia A.

The World Data Center has established a guide to determine the emission levels and parameters of phenomena of explosive character which can be impulsive or gradual. This guide is used as well during the observations at the ERH.

It must be pointed out here that the results of these measurements are being used in different programs that perform the calculations. These are inserted in folders that form the database of the ERH.

The precision of the calculations is determined by two factors: the system noise and the way in which the measurements are conducted. The system noise is a factor that depends on the technology and is always present independent of the measurement method. In the case of the ERH, in the instruments that are being analyzed this factor is in the order of 6 K or less of the antenna temperature. The amplification factor of the paper registers, which is due to the measurement method, causes that they have values of 25 K per millimeter. Because of that, the registration method on paper is above the intrinsic precision of the instrument. In addition to this the appreciation factor of the observer is introduced in all processes, e.g. when determining the reference levels by means of leveling straight lines. Thus, always differences exist between one criteria and another.

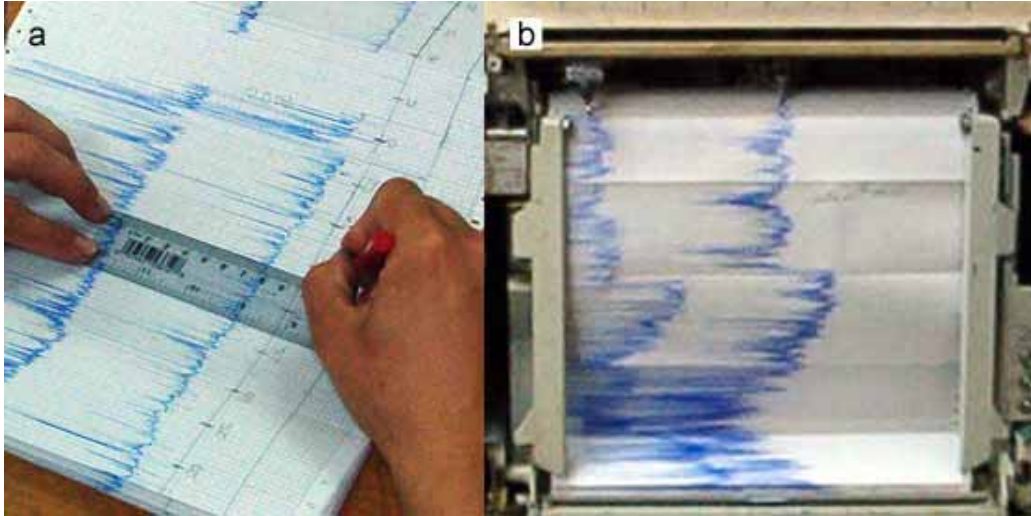


**Figure 4-6: Post processing of the measurements of a day of observation (a). Data recorder (b).**

It is obvious that the used methods are old, below the precision of the instrument and are great consumers of time, human resources and material; especially registry paper. All this without considering that the investigation task - actually appropriate for the instruments of low angular resolution (which they are) - is based in great part on the possibility of doing observations of medium or high temporal resolution with them.

This being the situation at the ERH and with the necessity to modify the measurement system, an automation study was initialized with the objective to execute such a project afterwards.

#### **4.5 Important Data for the Automation**

The study for the automation of the ERH produced a large amount of information that had to be verified and corrected during the execution of the Astrodata project. Among the most significant analyzed aspects were the operation requirements and the characteristics of every one of the inputs and outputs, associated with the radio telescopes of the ERH.

The most significant operation requirements were:

- that all variables are actualized, registered and saved with a sample rate equal to 1s.
- that the instant values of every variable are shown, accompanied by a graphical presentation and an elementary online statistical analysis.
- that it is possible to save the value of the signals on disk with a compatible format of different analysis tools.
- in what is referred to the elaboration of the collected data, it is desired that there is a minimum intervention of the observer, if it cannot be eliminated totally, and the intrusion always being well determined.
- that the positioning of the antennas is automated, permitting as backup the manual control of the radio telescopes. As feedback signal the intensity of the solar radio emission is used.

- conserve and raise the possibilities of system operation that are to be substituted, trying to keep names, alias, measurement units, operation sequence and all that facilitates the acceptance and learning by the station personnel, of the new technology to be implanted.
- that the personnel required for the operation of the radio telescopes is minimal
- that the registry on paper is eliminated

In table 4-2 the necessary signals for the supervision and control of the radio telescopes are characterized. They are grouped by antenna and by commonly used signals. In each group the working frequency of each receiver, its wavelength, signal type, its name and its range in engineering units is specified.

It is important to indicate that all signals have been classified in inputs or outputs by reference to SCADA (Supervisory Control And Data Acquisition). That is, an analog input (AI) will be an output of the process and an input to the supervision system.

**Table 4-2 Signals used in the automation of the ERH.**

	<b>Freq.</b>	<b>Signal</b>	<b>Type<sup>1</sup></b>	<b>Range</b>
<b>RT2</b>	9.5 GHz	Intensity	AI	0-5 V
		Receiver Temperature	AI	0-5 V
		Limit of the East/West movement	DI	0 and 12V
		Rating of Attenuation for the Intensity	DO	0 and 9 V
		Compensation Generator	DO	0 and 9 V
		Modulation Generator	DO	0 and 9 V
		Motor Switched On East/West	DO	0 and 12V
		Direction East/West	DO	0 and 12V
		Double Velocity	DO	0 and 12V
		Rapid Movement	DO	0 and 12V
		Motor Switched On North/South	DO	0 and 12V
<b>RT3</b>	6.7 GHz	Intensity	AI	0-5 V
		Polarization	AI	0-5 V
		Receiver Temperature	AI	0-5 V
		Rating of Attenuation for the Intensity	DO	0 and 9 V
		Rating of Attenuation for the Polarization	DO	0 and 9 V
	15 GHz	Intensity	AI	0-5 V
		Polarization	AI	0-5 V
		Receiver Temperature	AI	0-5 V
	Both	Limit of the East/West movement	DI	0 and 12V
		Compensation Generator	DO	0 and 9 V
		Modulation Generator	DO	0 and 9 V
		Motor Switched On East/West	DO	0 y 12V
		Direction East/West	DO	0 y 12V
		Double Velocity	DO	0 and 12V
Rapid Movement	DO	0 and 12V		

		Motor Switched On North/South	DO	0 and 12V
<b>RTM</b>	230 MHz	Intensity	AI	0-5 V
		Rating of Attenuation for the Intensity	DO	0 and 9 V
	280 MHz	Intensity	AI	0-5 V
		Rating of Attenuation for the Intensity	DO	0 and 9 V
	Both	Receiver Temperature	AI	0-5 V
		Calibration Generator	DO	0 and 9 V
Connected Antenna		DO	0 and 9 V	
<b>Common</b>	Environment Temperature	AI	0-5 V	
	Luminosity of the Sky	AI	0-5 V	
	Attenuation Level	DO	0 and 9 V	
	Direction North/South	DO	0 and 12V	
<b>Total</b>	13 analog inputs, 2 digital inputs y 23 digital outputs			

<sup>1</sup> AI stands for analog input; DI for digital input and DO for digital output.

Grouping the signals with similar functions they can be described generally as followed:

***Total Radio Emission Intensity:*** Represents the magnitude of the total radio emission intensity that arrives at the receiver. It is an analog input and one of the variables that is being studied by the ERH. Habitually it is only called intensity. It is measured by the radio telescopes RT2 and RT3.

***Intensity of the linear polarized Radio Emission:*** Represents the intensity magnitude of the linearly polarized component of the radio emission. It is an analog input and another important variable for the investigators at the ERH. Habitually it is only called intensity. It is measured with the radio telescope RTM.

***Intensity of the circular polarized Radio Emission:*** Represents the intensity magnitude of the circular polarized component of the radio emission. It is an analog input and another important variable for the investigators of the ERH. Habitually it is only called polarization. It is measured with the radio telescope RT3.

***Receiver Temperature:*** It is an analog input that represents the temperature inside the receiver. Variations of the receiver temperature have a negative influence on the measurements; therefore it is very important to know and to keep its value stable. To achieve this, a temperature regulation circuit is implemented inside the receiver.

***Environment Temperature:*** It is an analog input that represents the environmental temperature in which the antennas are located (or being the temperature outside the receiver). It is a witness variable which permits to know the influence of the environment on the receivers.

***Luminosity of the Sky:*** It is the light emission level in the spectrum of visible frequencies in the area of the sky towards where the antennas are focused. It is an analogical input and a witness variable which permits the detection of clouds in the area of observation. Therefore it is also called Cloudiness.

**Level of Attenuation:** Digital output that defines the level of attenuation that the signal will suffer before it is recorded. The rise in amplitude of the radio emission intensity in moments of intense solar activity is several times its value. Therefore it is necessary to attenuate the signal so it will not exceed the range limit of the measurement device. On the other hand, if one would work with maximum attenuation in the state of normal activity, the variations of the measured signal would not be noticed.

**Setting of Attenuation:** Digital output that sets or activates the level of attenuation previously defined for a determined receiver.

**Compensation Generator:** Digital output that activates the compensation equipment. In the RT2 and the RT3 it eliminates the background emission and allows that only the variations of the object's emissions are recorded. It is also called noise generator. In the RTM it is employed for generating a calibration signal of known value equal to 400 K, thus called calibration generator.

**Modulation Generator:** Equipment that generates a synchronous signal that intervenes in the modulation and demodulation of the signals received by the antenna and transported to the receiver by the waveguides. Habitually it is only called modulation.

**Connected Antenna:** Digital output employed in the RTM to block the signal coming from the antenna towards the receiver to achieve the state of zero.

**Activated Motor:** Digital output that starts or stops the movement of the corresponding motor.

**Sense of Movement:** Digital output that defines the direction of the movement of the corresponding motor.

**Double Velocity:** Digital output that doubles the velocity of the movement of the corresponding motor. When inactive, the motor moves at the tracking speed. It is used to position the antenna with exactness.

**Rapid Movement:** Digital output that starts or stops the motor of rapid movement, which allows the antenna to move at a velocity several times faster than at the tracking speed. It is used to position the antenna at great speed and with little exactness.

**Limit:** Digital input which is activated when the antenna reaches the assigned position of one of the movement limits.

It is important to indicate that all of the before mentioned intensities are integrals since the antennas receive the Sun as a whole.

The study for the automation of the ERH resulted in the implementation of the SCADA Astrodata.

## **5. Astrodata**

### **Description of the SCADA (Supervisory Control And Data Acquisition)**

The Supervisory Control And Data Acquisition (SCADA) systems are especially designed to guarantee the functions that are indicated by its name.

The basic functions of a SCADA are:

- Data Acquisition
- Supervision
- Automatic Control

The SCADA Astrodata, which is installed in the Radio astronomical Station of Havana, is a system of specific aim. Figure 5-1 shows a block diagram which represents the general structure of the system.

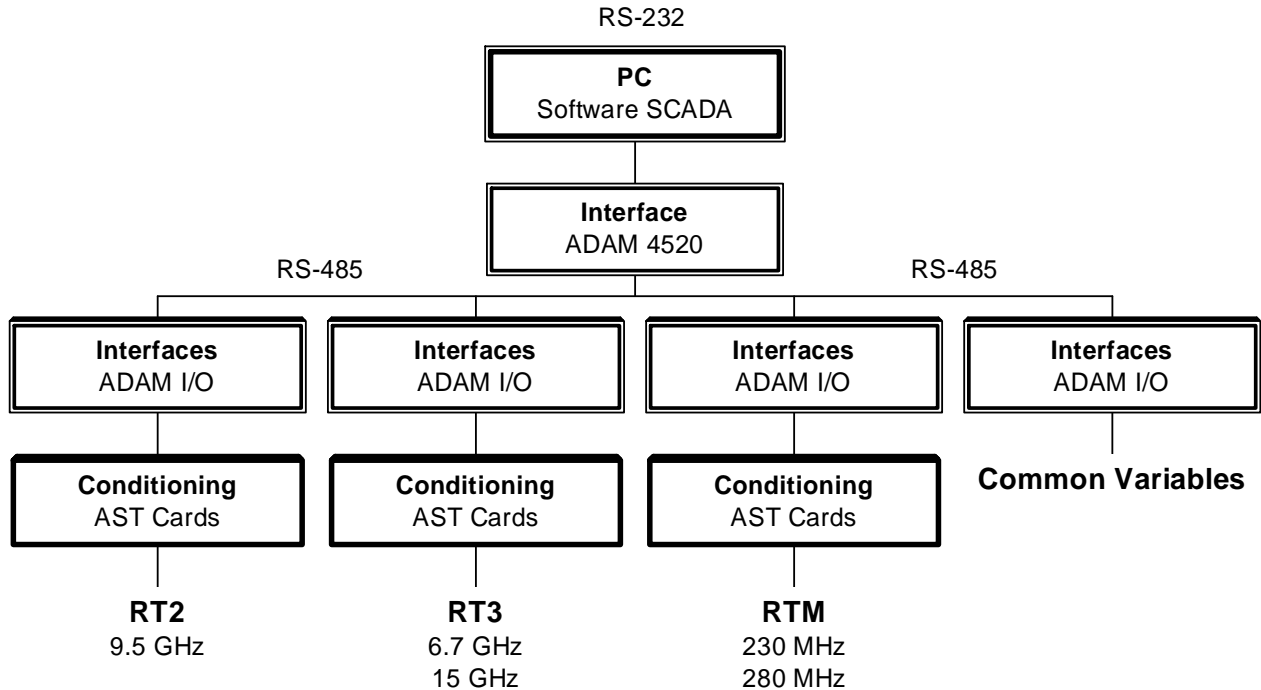


Figure 5-1 General diagram of the SCADA Astrodata

Following the technology and theory utilized in Astrodata will be described.

### **5.1 Hardware Components**

Like all SCADA, Astrodata counts four basic hardware components: the work platform, the interfaces, signals conditioning and the physical part of the net. On continuation each one is described.

### The work platform

A PC, Celeron 800 MHz, with 128MB RAM and a HDD of 20 GB is used. As well as 3.5" floppy drive, a CD-drive, a keyboard, a mouse PS/2, a communications port RS-232, two USB and one parallel. One monitor de 19" is used to show the graphical interface of the system.

### The interfaces

The implemented interfaces are Data Acquisition Modules of Advantech Co., Ltd (ADAM – Advantech Data Acquisition Modules) of the series 4000. Every one of the variables which are measured by sensors or manipulated by actuators, pass through the interfaces and the cards of signal conditioning.

The ADAMs are a collection of external modules for different types of signals and multinorma (various mA and V values), which permit the connection of the PC, the sensors and the actuators, through a distributed industrial net. They are based on a microprocessor controlled remotely in a communications net RS-485 by commands in the ASCII format. These modules administrate, after the model, conditioning of the signals, galvanic isolation, linearization, conversion A/D and D/A, digital input and output, local indication, data comparison, limit detection, alarms and functions of digital communication.

Some advantages of the use in modular architecture are:

- allow to acquire just the amount of I/O which is going to be implemented or a value very close to that
- the measuring and the conversion A/D or D/A is conducted very close to the sensors and actuators, thereby reducing the noise and information loss
- the length and the amount of conductors is minimized, since a major part of the data transmission is done by the RS-485 net
- the difference of potential is reduced between the extremes of the analog lines, provoked by the increase of the resistance in the conductors as a proportional function of its length
- makes it easy to detect and repair failures in the system
- decreases the cost of maintenance and repair

The implemented ADAMs are totally configurable by software, since they do not work with switches or configuration jumpers. This is done through the net and from the PC by sending new configuration commands, which will be activated immediately or (in some cases) when the module is reset.



**Figure 5-2: Two of the Astrodata interfaces, ADAM 4017 and ADAM 4050.**

### The conditioning of the signals

The system employs three types of signal conditioning cards that treat digital inputs and outputs. Its location inside the SCADA is shown in figure 5-1.

The cards AST01, AST02 and AST03 were totally designed and build at the ICIMAF; they used CMOS technology, fed by 12V to maintain the compatibility with the control process.

The cards AST02 and AST03 have duplicate entries, allowing manual or automatic control

The circuit of AST01 acts over the signal conditioning parts of the station. These parts guarantee that the signal coming from the receivers, enter the conditioning system of the station with an adequate level of tension. This way when the solar activity is normal or low, the signal is not attenuated, but when there is intense solar activity it is necessary to reduce the strength of the signal.

The card AST02 allows to control the velocity and the direction of rotation of the motor that moves the antenna in the east/west direction. It does as well the limit detection and gives information about that to the superior level, it reduces the energy consumption and the heating of the motor when it is stopped and guarantees the galvanic isolation with the potential step by optocouplers. It indicates the state of the inputs, the limits and every field of the motor.



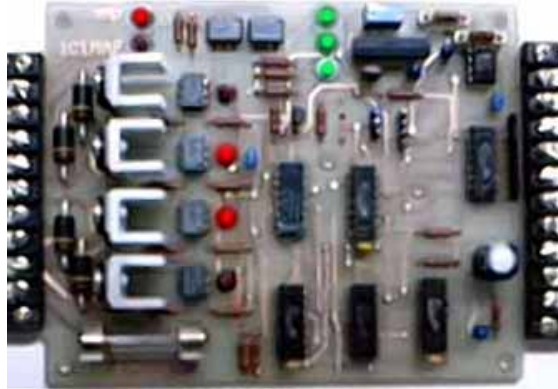


**Figure 5-3: AST02, signal conditioning card.**

It is of vital importance for the functioning of the station that the antennas stay focused on the Sun correctly. This is an element with constant movement that has to be followed. It is providing the intensity value of its radio emission as a response from the focus. Astrodata should correct the position of the antenna in case that the focus is lost, and for that by the card AST02, the velocity of movement of the antenna is varied until the correct position is reached.

The limit detection revises if the corresponding limit in the direction of antenna movement has been activated. In case the switch of the limit is activated at the end where the antenna is being moved, the motor is stopped independently of the state of the received inputs.

The card AST02 employs optocouplers to keep the power stage galvanically isolated. It guarantees as well the isolation of the input of the limit detection.

The AST03 cards allow the on-off control of a DC motor. They make the function of switching the motor on and off, and the change of its direction of rotation. They guarantee the galvanic isolation by relays with the step of potential. Two LEDs indicate the state of the outputs, one shows if the motor is energized and the other the polarity.

These cards are employed to control the functioning of the motors of the declination north/south and of the rapid movement east/west. In the latter they detect the activation of the limits (together with AST02) and they stop the motor, independently of the state of the send entries.

### The physical part of the net

To communicate with the different machines connected to the communication network, two net protocols are employed: RS-232 and RS-485. The RS-232 is employed to connect the PC with the bus to the RS-485 net. By the RS-485 the modules are connected among each other. To unite the two nets the conversion module ADAM4520 is used.

The ADAM-4520 is a converter module of the RS-232 protocol and RS-485 and vice versa. The PC which uses the RS-232 protocol is connected through the ADAM-4520 to the RS-485 network and communicated with the other interfaces.

In this case, the communication RS-232 is done by using three cables, one for transmission, another for reception and one as potential reference or ground (Gnd). No flux control signals are used. The communication speed used is 38.4 Kbps.

## **5.2 Software Components**

### The operating system

As operating system Windows 2000 Professional of Microsoft Corp. is used. This is an operating system of the Windows family, which presents a graphical work environment quite friendly and known to the majority of PC users. Its multitasking is not a real time operating system, but it is programmed to work in real time as can be seen further on.

### The real time system

The SCADA software Astrodata guarantees a soft real time environment in which all of the work is executed. It can be said that the system works in real time because it is programmed so that it fulfills the limitations in that it never surpasses the maximum period which can be allowed by the different operators of the system without the information being updated. This period is determined by the characteristics of the variables and the frequency of acquisition of the control data, and it is equal to 1 s.

### The programming language

The SCADA Astrodata was programmed with LabWindows CVI, a product of National Instruments that employs ANSI C as programming language and has many features grouped in libraries and classes, some specifically for the control of processes.

### The virtual instrumentation

In Astrodata every work window is a virtual instrument, designed by a programmer and an industrial designer, by the needs of the client. There they represent the data recorders, the alphanumerical indicators, the lights and sounds of the alarms, the start buttons and the adjustment of parameters.

Their similarity to the real instruments that exist in the station helps considerably with the training of the operators with the use of the SCADA.

In the figures 5-4, 5-9 and 5-10 some virtual instruments of Astrodata can be seen.

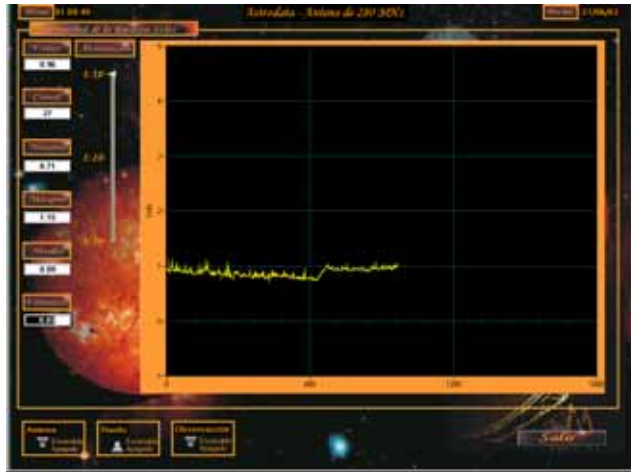


**Figure 5-4: Virtual Instrument for RTM 280 MHz.**

Astrodata has two work modes. The first one is as a simulator. The second one is as a real time system.

#### The simulator

Given the importance of a simulation tool to train the personnel, a working mode was included which does not need the processing and simulates all of the system functions.

The Astrodata simulator employs a random value generator for each variable of the process, or load real measurements previously saved in the database. This functionality allows the analysis of the data, too.

#### The analysis software

Although Astrodata does an online basic statistical analysis of the measurements, an external program for a more complete analysis should be used. With that goal any special software is applicable that is able to read files of text types like Excel and Statistica, among others. The statistical analysis online includes the calculation of the minimum, maximum, average and variance of each analog variable.

#### The communication protocols

As mentioned in paragraph 5.1, Astrodata works with two communication protocols: the RS-232 and the RS-485; and the protocol conversion module ADAM 4520 to pass them. Since the RS-232 and the RS-485 just define the physical part of the net, the manufacturer of the ADAM specifies the rest.

### **5.3 Structures and Functions of the Astrodata Software**

The structure of the Astrodata software can be divided into two main branches, one that includes the tasks that are executed offline and the other that contains all that is done online and in real time. The following diagram shows this classification.

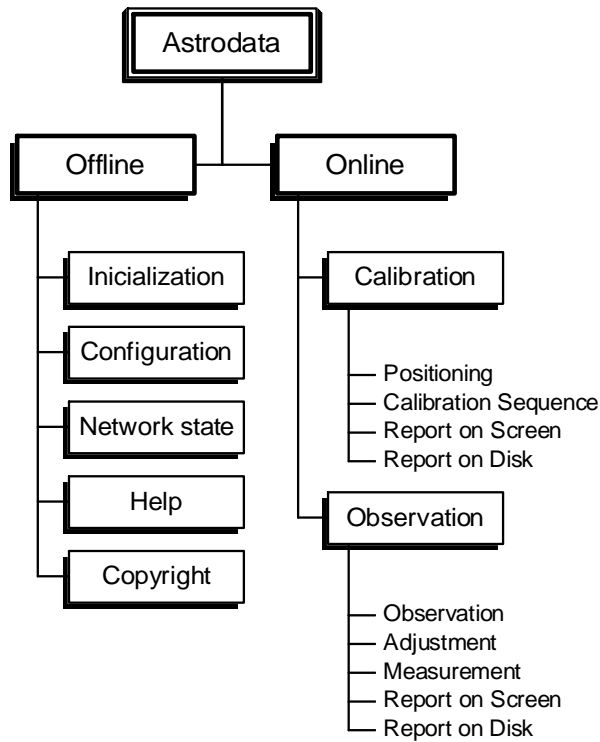


Figure 5-5: Structure of the real time system Astrodata.

At the beginning of the execution of Astrodata, the start window is shown as can be seen in the figure 5-6. It is connected by buttons to the blocks: initialization, configuration, state of the web, help, copyright, calibration and observation.

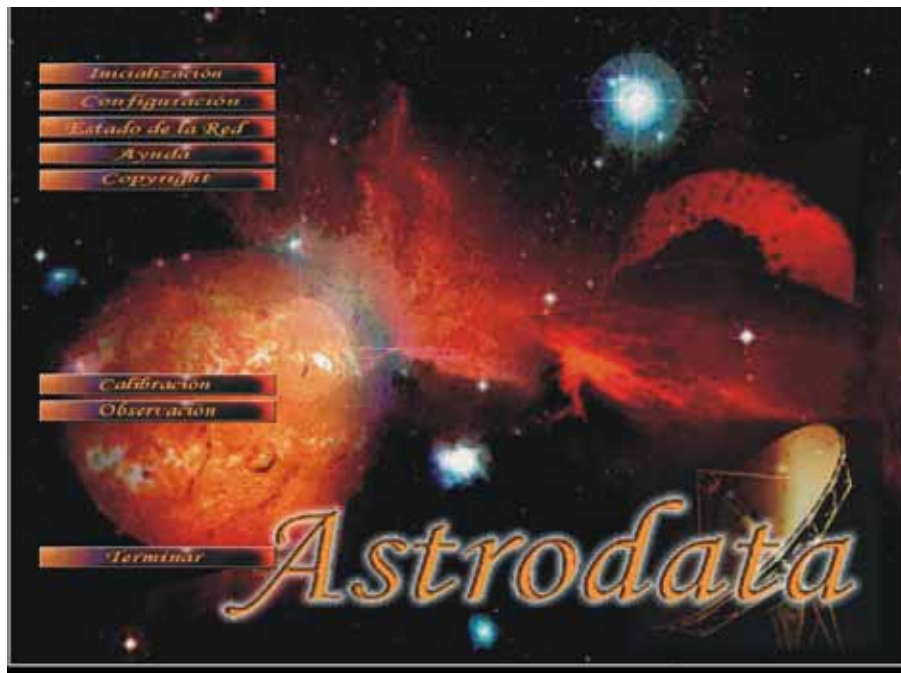


Figure 5-6: Start window of Astrodata.

### **Offline function blocks**

The offline functions are being executed in a non-periodic form and do not have any real time requirement. These include tasks of the definition of software parameters or of the processing, and information for the user. Following is a description of each one.

#### Initialization

Allows the assignation of values to the parameters of every process value, such as the name, the number of the used communication channel, the engineering unit in which the value is expressed, etc. This information is used in different reports.

#### Configuration

It commissions the assignation of values to the variables of SCADA. They define the state of the work (simulation or acquisition), the sample rate and the rate of saving to disc.



Figure 5-7: Virtual Instrument for the configuration of the system.

#### Network State

This block allows to disable the communication with one or various interfaces that can be connected or not to the communication net. It is very useful in failure situations and in those of repair or maintenance. Even if a module is broken or a part of the system has failed, the rest of the system can continue to function.



Figure 5-8: Virtual Instrument for the definition of the network state.

### Help

Provides online help necessary for the operation of the SACADA. It shows images of each virtual instrument indicating the functions of its components. It includes an index and links to the topics to find quickly the searched element.

### Copyright

Shows the legal rights of the author of the Astrodata software.

### Online function blocks

The functions that are executed online are all periodic; a real time environment is employed for them. Astrodata has two blocks of this type: calibration and observation. These have the related tasks implicated with data acquisition, supervision and the control of the process. Following each one of them is described.

### Calibration

This block is responsible for the calibration of the intensity and the polarization measurement for the antennas RT2 and RT3. This work is done every morning before the beginning of the observations, and in the afternoon while culminating the observations. In the antenna RTM this process is not done because it employs a calibration generator which is stable in time and provides a signal of 400 K.

In the calibration sequence of the intensity measurement one ought to receive the value of the compensation generator's temperature and therefore the following actions are performed:

- the intensity waveguide is placed
- the antenna is positioned at the meridian

- the level of the compensation generator is measured
- the sky level of the signal is being measured
- the zero level of the signal is being measured

In the calibration sequence of the polarization measurement one ought to receive the value of the temperature of the equivalent of the polarized emission and therefore the following actions must be taken:

- the waveguide of the polarization is placed
- the antenna is positioned at the meridian
- the sky level of the signal is being measured
- the zero level of the signal is being measured

To get the references as zero levels, as sky levels and as the compensation generator (see 4.3), a digital action sequence that controls the calibration is generated by software. Here the digital outputs of the modulation and compensation generator of the antenna to be calibrated are employed. Depending on the case analog inputs of the intensity, polarization, luminosity, receiver temperature and environment temperature take part in the measurement of each of the values of the levels.

The obtained measures are saved on disc, so that these values will be employed in the observation and the post processing of the data.

In both calibrations furthermore the tasks of post processing and report on the screen occur.

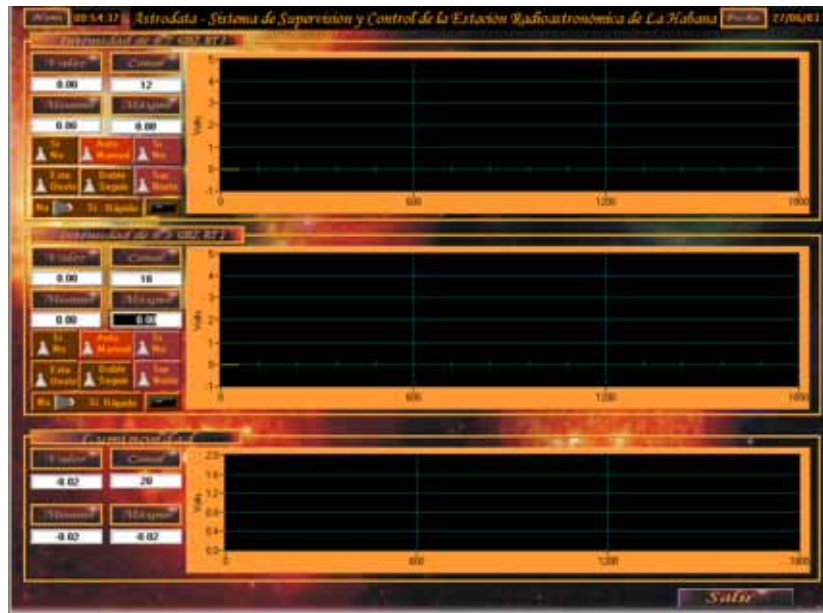


**Figure 5-9: Virtual Instrument for the positioning of the antennas.**



The digital signals of the rapid movement in the east/west direction of the antenna to be moved take part in the post processing task of the antennas.

With the SCADA Astrodata another type of calibration is done, which permits to correct the exactness of the measurement system. It is referred to the calibrations that are carried out using the patron radio sources Cas A and the moon, since these are normally done during the night. There is no task in Astrodata that is especially dedicated to this work, so that the same tasks of calibration and observation are used which are implemented during the day.

The moon is used for the calibration of the measurement system of the radio telescopes RT2 and RT3. This radio source emits like a black body with a temperature of 212 K. This value is not constant, because it varies with phase, which is expressed as a cosine function of the phase with an amplitude of 10 K. This method reaches a precision of about 90%.

The radio telescope RTM uses as calibration patron the radio source Cassiopeia A, this method reaches a precision of better than 90%. This radio source, as the moon, is worldwide considered a reference for the calibration of antennas in general.

### **Observation**

This is the most used block in the SCADA Astrodata. In it the tasks of observations, measurement, adjustment, screen report and disk report are being accomplished.

The tasks of automatic adjustment and automatic measurement are hourly works, with an interval that can be defined. The report on screen and the report to disk are done every sample rate so that they are periodic.

The task of adjustment is done before the task of measurement and has the function to direct the electrical axis of the antenna to the center of the Sun and obtain the best focus. This is necessary because of the Sun's own derivations in its trajectory and as correction to the mechanical system of the positioning of the antenna. For these automatic control methods are used which will be discussed in 5.4.

The task of measurement has the objective to supervise the variations in the amplification which present the instruments during the day. Having as information the value of the signal of the compensation generator (in RT2 and RT3) obtained in the calibration of the morning or the value of the signal of the calibration generator (in RTM), and comparing them with the value that is obtained here. Then it is possible to know the amplification factor of the receiving instruments, of the amplifiers of the high and low frequency, of the attenuators, etc. This procedure is done periodically to increase the exactness of the measurement.



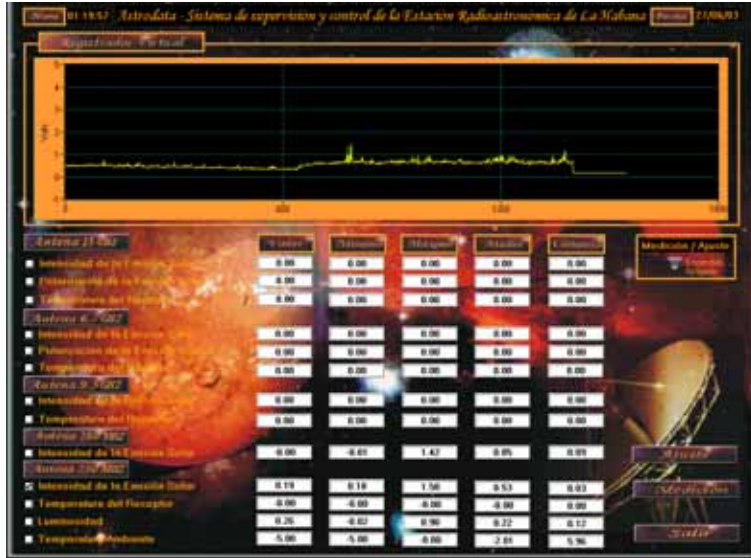


Figure 5-10: Virtual Instrument that shows the values of the analog input variables and a graphical registry of one of them (chosen by the operator).

Knowing the behavior of the amplification the necessary corrections can be done in the value of the measured signal. In addition, it allows as well the supervision of the instrument's functioning with the possibility to detect failures in them.

In the antennas RT2 and RT3 the task of measurement generates the following operation sequence:

- disconnecting the compensation generator for 2 minutes
- connecting the compensation generator for 2 minutes
- disconnect the modulation generator for 1 minute

In the antenna RTM the following operations sequence is generated:

- disconnecting the antenna and fixing the level of attenuation on 30 dB for 1 minute
- placing the level of attenuation to the level employed during the observation (level of operation) for 1 minute
- activate the calibration generator for 2 minutes

The obtained measurements are send to the database and will be used in the post processing of the data.

The database is in the ASCII format and presents the following structure: It has various fields, the first for the number of the sample and one for each variable. In each sample period the data recorders are added up with the values of the measured variables. It includes a header where some important data is put like the date and the time in which it was created, and the period of the sample. Having in mind the amount of variables, the

sample period and the duration of the daily work, it is calculated that approximately some 5.9 GB/year are saved.

During the observations the report on screen is presented as well to the operator by the virtual instruments. This report allows to keep the behavior of the Sun under supervision in every frequency. In case of a solar event the operator ought to start actions with the help of Astrodata which permits to obtain a good record of it.

Among other actions, before an event, the operator disables the tasks of automatic adjustment and automatic measurement to evade that these interfere with the observations.

A tool of this type has allowed the ERH to reach superior levels of quality in the information that they elaborate, contributing to increase their prestige and that of the country. In addition from the data base obtained by Astrodata the investigators of the IGA can broaden their studies.

## **5.4 The Theory of the Process Control in Astrodata**

In Astrodata various control schemes can be found in the different tasks that are executed in the online function block (see 5.3). Of interest are in this relation, in the block of calibration: the tasks of positioning and the calibration sequence. In the block of observation the tasks of observations, automatic adjustment and automatic measurement will be analyzed, from a suitable focus of the automatic control theory.

In continuation each one of these schemes will be analyzed.

### **Control schemes employed in the calibration**

#### **Positioning**

In the task of positioning of the antennas the virtual control on/off is used, which permits the rapid movement of the antenna in the manual or automatic mode.

The manipulated variables are the feed and the direction of rotation of the direct current motor that provokes the movement of the antenna, defined as rapid movement (see 4.5). And the controlled variable is the position of the antenna in regard to the ends of the route in the east/west axis.

The system comes with sensor elements of the end of route or limits, in both ends of the route. In addition, it possesses as well another sensor that indicates when the antenna is focused to the meridian.

The stop of the antenna in these extreme positions is done automatically by the regulation system. Equally this happens in the meridian when the corresponding switch is activated.

**Calibration sequence**

In the radio telescopes RT2 and RT3 the calibration of the measurement system (see 4.3) is carried out at the beginning and at the end of the observation phase. Therefore various sequences are executed where the sequential control, the batch control is used. The information that is obtained during the calibration is employed in the post processing of the measurements with the objective of increasing their precision.

The manipulated variables are the compensation generator and the modulation generator. The measured variables are the intensity in RT2 and the Intensity and the polarization in RT3.

In the radio telescope RT2 a sequence is used to calibrate the intensity channel. In the radio telescope RT3 two sequences are used, one to calibrate the channel of intensity and the other for the channel of polarization. The sequences of the channel of intensity pass through 3 stages and the polarization through 2. In total they execute each 2 sequences of the 3 stages and 1 sequence of 2 stages (see table 5-1 and 5-2).

**Table 5-1 Calibration sequence of the intensity channel.**

State		Compensation Generator	Modulation Generator	Time of Measurement
1	GR	ON	ON	2 min.
2	Sky	OFF	ON	2 min.
3	Zero	OFF	OFF	2 min.

**Table 5-2 Calibration sequence of the polarization channel.**

State		Compensation Generator	Modulation Generator	Time of Measurement
1	Sky	OFF	ON	2 min.
3	Zero	OFF	OFF	2 min.

**Observation task**

**- Control of the attenuation level**

In this scheme the manipulated variable is the level of attenuation, the final action element are the attenuators and the reference of the circuit is to keep the measurement of the signal in a range predefined presently between 1V and 4V. These extreme values are determined by the range of the input of the interfaces; to prevent the saturation of the components that form and keep its functioning inside of a lineal zone of its transfer characteristic.

For this an on/off multilevel regulator was programmed in closed loop, which controls the measurement of the intensity and the polarization, in the function manual and automatic. This regulator is taken because the elements of final action are of this type, that is there exist 5 attenuation levels in RT2 and RT3, and 3 levels in RTM. Each level corresponds to an attenuation coefficient by which it is possible to recover the real value of the measured variable.

The control strategy consists therein that if the measurement surpasses the earlier defined superior limit, the regulator increases the level of attenuation of this channel, provoking a decrease of the measured value. This will be done until the value of the measurement is smaller than the upper limit and the maximum level of attenuation is not reached.

On the contrary, if the measurement is getting smaller than the minimum level, the regulator decreases the attenuation level, provoking that the value of the measurement increases. This will be done until the value of the measurement will be higher than the lower limit, and minimum level of attenuation is not reached. This way the algorithm works in the form similar to a hysteresis cycle.

This control is programmed and executed in the SCADA software that runs on the PC. The system counts with 5 regulation circuits of this type.

#### **- Control of the tracking speed**

The speed with which the antennas move to keep their focus onto the Sun is a critical variable to obtain trustworthy measurements. The Sun moves in respect to the earth with an angular velocity of  $0.5^\circ/\text{min}$  from east to west, so that the antennas have to rotate in the corresponding axis at a similar velocity to maintain focused. Due to the narrow lineal zone that presents the response of the parabolic antennas (they are very directional) and with the wavelength of the signals they receive (a few centimeters), a precise focus of the antenna is necessary towards the zone of maximum solar intensity.

With this objective a control system with open loop was implemented using a proportional regulator that manipulates the rotation speed of the stepper motor that moves the antenna in the east/west direction. The controlled variable is the angular tracking velocity. The final action element is the stepper motor of each antenna.

The intelligent element of this regulation scheme is not found in the SCADA software but is supported by the hardware of the signal conditioning card AST02. The SCADA has 2 regulation circuits of this kind.

The regulator is formed by an oscillator and various logical hatches that, according to the position of the adjustment potentiometer, vary the frequency of the signal delivered to the stepper motor.

It has to be remarked that the regulation schemes of the attenuation level and of the tracking speed are discussed inside the task of observation because of their relevance and

fundamental role in it. They are employed as well in other tasks inside the block of observation as for example: the adjustment and the measurement.

### **Task of adjustment**

In the task of adjustment a regulation circuit is used where the controlled variable is the measurement of the intensity (its maximum), the manipulated variables are the alimentation and the sense of movement of the motors of the east/west and north/south axis, and the speed of the movement of the motor of the east/west axis, which makes this system a tracking problem with two degrees of freedom. This is tackled as a control problem with gradient techniques employing for it a sequential scheme.

The objective is to maximize the measurement of the intensity since with the gradient techniques one searches for a global or absolute extreme.

There exists a measurable external perturbation that is the luminosity, which can provoke that the searched extreme is not found. Therefore the search of the maximum is not for an absolute value but for a surrounding  $\varepsilon$  approximately the value.

For the search of the extreme an operation sequence is carried out, first in the east/west ( $\alpha$ ) axis and afterwards in the north/south ( $\delta$ ) axis, which are described in the following.

The system starts in the movement  $\alpha$ , without movement in  $\delta$  with a defined speed as tracking speed. Product of the mechanical system and the declination of the Sun in its trajectory is a misadjustment of the focus, with which the intensity of the solar radiation that is received by the measurement system does not have its maximum value. Therefore it is necessary to use a pursuit technique that allows to position the focus of the antenna in the desired maximum.

If the adjustment system is in the automatic mode, a displacement is initiated in the  $\alpha$ -axis, in the west direction and at double speed, and the value of the intensity is compared with its registered maximum value. If the difference increases the direction of the search for the maximum is changed by modifying the rotation direction of the motor so that the antenna is moved eastward until it reaches the maximum value or a value close to it. In this moment the motor is put to the tracking velocity in the west direction and one proceeds with the adjustment of the  $\delta$ -axis.

For this adjustment the direction of the motor of the  $\delta$ -axis is placed in the south direction and the motor stays alimented. If moving in this axis results in an increase in distance of the obtained maximum value, the direction of displacement is changed towards the north. The search is stopped when the intensity takes a value within a surrounding  $\varepsilon$  around the maximum value.

The system uses two regulation circuits of this type, one in RT2 and the other in RT3. In addition, there is as well the possibility of rapid movement described in the task of

positioning, which permits to run great distances between the position of the antenna and the Sun. This task has the possibility of manual control.

**Task of measurement**

For the correction of the measurements a calibration is necessary every two hours, which is done during the task of measurement, only if there is no presence of a solar event. The obtained information during the measurement sequences is employed to increase the precision of the data during the post processing.

In this regulation scheme the sequential control, the batch control, is used in a similar way in the task of calibration. It controls the measurement of the intensity and the polarization.

The manipulated variables in RT2 and RT3 are the compensation generator and the modulation generator. In the case of the RTM the variables Connected Antenna, Level of attenuation and calibration generator are manipulated. The measured variables are intensity and polarization in RT3 and intensity in RT2 and RTM.

For each telescope a sequence is done, resulting in total 3 sequences. The ones that are executed in RT2 and RT3 pass through 3 states. The one that is done for RTM has 4 states, which can be seen in table 5-3 and 5-4 respectively.

**Table 5-3 Measurement sequence in RT2 and RT3.**

	<b>State</b>	<b>Compensation Generator</b>	<b>Modulation Generator</b>	<b>Time of Measurement</b>
1	Sun	OFF	ON	2 min.
2	Sun + CG	ON	OFF	1 min.
4	Zero	OFF	OFF	2 min.

**Table 5-4 Measurement sequence in RTM.**

	<b>State</b>	<b>Connected Antenna</b>	<b>Attenuation Level</b>	<b>Calibration Generator</b>	<b>Time of Measurement</b>
1	Zero	OFF	1:30	OFF	1 min.
2	Sky	OFF	1:1	OFF	1 min.
3	Tube	OFF	1:1	ON	2 min.
4	Sun	ON	1:1	OFF	1 min.

**5.5 The Results**

Some events registered by Astrodata

The following two events are presented that were registered by the SCADA Astrodata. In the first, which is shown in Fig. 5-11, the image was captured, that was shown by the software for the registry of the solar event.

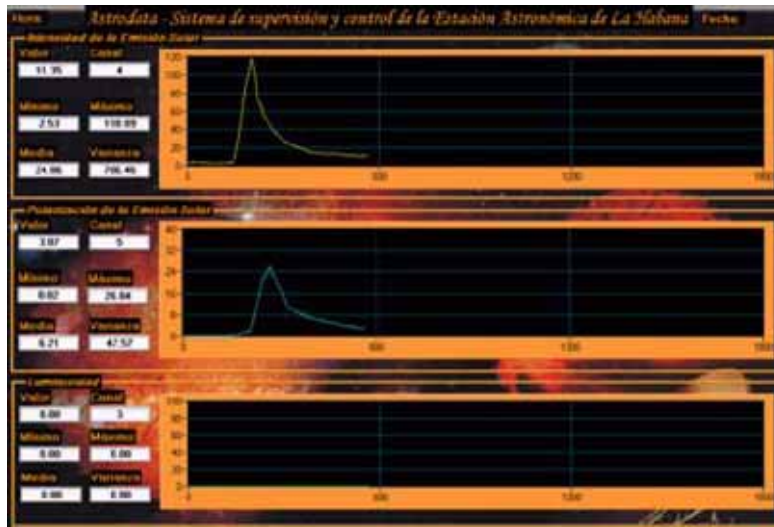


Figure 5-11: Measurements of the radio telescope RT3 obtained by Astrodata on August 24, 2001.

In the second event the measurements were taken of the database created by Astrodata and are represented by the graphical capabilities of Microsoft Excel. The values of attenuation of each signal serve to obtain the values without attenuation. The curves of the event can be seen in Fig. 5-12.

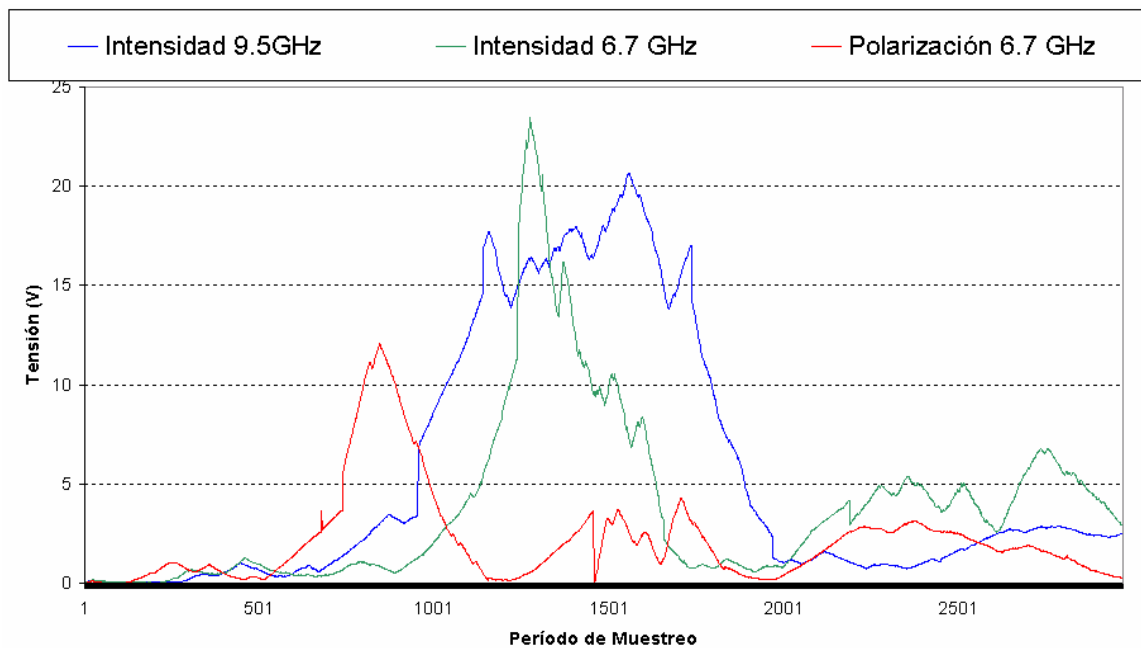


Figure 5-12: Measurements obtained by Astrodata April 15, 2001

### The advantages of the system

The greatest benefit obtained after the implementation of the SCADA Astrodata in the ERH is the considerable increment in the quality of the measurements by increasing the resolution of the measurement system and the amount of data per time unit.

One has to mention as well the following aspects:

- the disappearance of the errors as product of the wearing of the moving parts of the electromechanical indicators like the ones committed by the operator in the lecture of the values in these indicators.
- the loss of data as a product of the lack of paper or of other causes is reduced to zero. As the data is saved in digital format it is easier to obtain back copies
- the incorporation of an online statistical analysis of the data, which helps to improve the decision making during the operations
- the guarantee that the data, saved in text files in ASCII format, can be subjected to a more specific analysis later and spread with easiness to the groups of investigators.

From an economic point of view the following achievements are defined:

- by eliminating the data recorders, the investment of paper and ink is totally eliminated as well as spare parts for those.
- the costs and time of maintenance is reduced
- the space required to save and store the data collected by the station is reduced (earlier it were boxes of papers and now it is reduced to a few CDs).
- the distribution and the access to the data are made easier and less costly therefore the spreading and the post processing of them are more efficient.

The operators of the station benefit from the installation of the automatic system, so that:

- they do not need to interact with electromechanical equipment, change registry paper and refill the ink cartridges.
- the automatic system does not require continuous attention and permits them to manipulate the station at any time by the virtual instruments, guaranteeing the care of the data.
- the adjustment of position of the antennas is converted into an easier and more precise task, requiring fewer adjustments during the day.
- automatic adjustment capabilities of the position of the antennas were added as well so that the operator is freed from this task

The technicians in charge of the maintenance of the station are seeing their interests reflected by the change of the equipment of electromechanical data recorders already obsolete by a personal computer, so that:

- the maintenance is reduced to the maintenance of the computer and of the systems of conditioning the signals. For that they already have received an introduction.
- in case of a computer breakdown it is possible to immediately replace it with a very simple action: the disconnection of the RS-232 cable at the end of the broken down PC and the connection to a spare PC, which should have the corresponding



software installed. This is possible thanks to the employment of a serial port in the communication with the rest of the system.

The advantages in the work of the investigators are reflected as well in:

- obtaining the data in digital format and not in registry paper, which can include errors and information loss when digitalized.
- by having copies of the database saved in compact disks, these can be distributed among the interested or put in the web to allow the quick search and the analysis of the events of interest.
- The results of the investigations and the publication that they generate gain as well in quality and prestige.

## **6. Selection of the Solution**

### **6.1 The Low Frequency Blocks**

With the implementation of the Astrodata system the automation of the ERH (see 4.5) is not completely concluded. Astrodata can however be considered as part one of the process. To complete the automation of the ERH, further investigation needs to be done. The next step would be to eliminate the so-called low frequency blocks (see Fig. 6-1). They have this name because here the initial high frequency RF (Radio Frequency) signal has already been down converted to the much lower frequency IF (Intermediate Frequency). Furthermore the results are presented at an even lower frequency of 1 Hz.



**Figure 6-1: The low frequency blocks**

Their elimination would provide an important step in the automation of the station. First, since the signals would then be processed digitally a lot of potential error sources would be eliminated on the way. Secondly, a lot of space would be gained by removing the low frequency blocks from the station. Maintenance would be significantly reduced as well. In short, all the before mentioned advantages of a supervisory and control system would be accomplished.

The low frequency blocks are about the size of a refrigerator and consist of 25-year old soviet technology which performs a number of processes. These processes differ slightly from one telescope to another but generally they work in the same way. They consist of a number of electronical circuit boards which perform different tasks. Among these tasks are: attenuation, synchronous detection, square wave generator, alimentation of receiver components, paper registry and in the case of the RT2 the quadratic detector.

The signal coming from the receiver enters the low frequency block and is run through a quadratic detector (only RT2). The other telescopes have the quadratic detector integrated into their receiver. The quadratic detector is used to rectify the modulated signals after being converted to the intermediate frequency. The signal is then, if necessary, attenuated (that can be controlled manually or with the help of the Astrodata software) and what follows is a process called synchronous detection (RT2 and RT3), which is an important part of the Dicke type receiver. In this process the values of the intensity and the polarization (only RT3) are calculated from the modulated signal.

Due to another receiver type, the results for the RTM are calculated without the synchronous detection process. The other processing steps differ only slightly.

The intensities are measured with capacitors which have an integration time of one second. The result is send as a DC voltage to the integrated paper registry and is presented here in graphical form (all telescopes). Since the signals have a frequency of at least 170 Hz, the result on screen is the result of at least 170 measurements. The results are send through the Astrodata system as well to be displayed on screen and to be saved digitally. Then the results can be used by the investigators.

In addition to this, the low frequency blocks also contain the square wave generator. The square waves are send to the receiver where they are used to modulate the incoming signal. That is the modulation for the intensity (all telescopes) and the polarization (RT3). The low frequency block later uses the information of the time phase to process the signals.

When considering the automation of the low frequency blocks it is helpful to know that the quadratic detector as well as the square wave generator and the alimentionation for the receiver parts can still be operated when removed from the block. That means that even if it should not be possible to exchange all the equipment, the automation will still save a lot of space, and improve the quality of the data and its handling.

Since the major part of the automation is the task of signal processing, this is also the main objective in the task of eliminating the low frequency blocks. If considered as “black boxes” the problem is quite simple. There is a signal coming from the receiver of the telescope that enters the “black box “ and leaves it converted into information the investigators can work with.

To automate the low frequency blocks, obviously the incoming signals must be understood and well known.

## **6.2 The Signals**

To understand what the signal is like, one has to know how it is manipulated before entering the low frequency blocks. It may be helpful to recall the block diagrams of the telescopes in chapter 4 (Fig. 4-2, 4-3 and 4-4).

The processes inside the receivers of the RT2 and RT3 are quite similar. That is due to the fact that both have a Dicke-radiometer installed. Therefore the following process is valid for the RT2 and RT3 respectively.

The only difference between the two is the additional modulation for the polarization in the case of the RT3. This is done immediately after the signal has entered the receiver. A square wave generator, located within the low frequency block, sends a square wave, which has a frequency of 833 Hz to the receiver. The square wave is used to modulate the incoming signal. From here on the signal in RT2 and RT3 are subjected to the same procedures.

The signal is further put in contra phase with the signal coming from the compensation generator, which is located within the receiver. The compensation generator emits a signal that is equivalent to the temperature of the quiet Sun. The incoming signal is thereby reduced by the value of the quiet Sun, leaving only the difference, i.e. the solar activity (intensity).

After that, the signal is modulated with the help of another square wave. The square wave generator is located within the low frequency block and has a frequency of 168 Hz in case of the RT2 and 320 Hz for RT3 respectively. Basically the modulation generator is used to change the frequency of the RF signal to an IF range.

This signal then enters the quadratic detector, which, as earlier stated, is used to rectify the modulated signals after being converted to the intermediate frequency. Also stated earlier, in the case of the RT3 the quadratic detector is part of the receiver system and in case of the RT2, it is part of the low frequency block. The signals then enter the low frequency blocks.

Since the RTM telescopes are switch interferometers the procedure is somewhat different. The calibration generator which has a constant temperature of 400 K is injected into the incoming signals (Sun and sky). After that a square wave is sent by a generator which is located in the low frequency block to the receiver. The square wave which has a frequency of 2.2 kHz is used to modulate the signal. On continuation the signal enters the low frequency block.

Some signal characteristics are shared by all telescopes. All signals are being amplified and filtered in the receiver. This is done because the incoming signal is very weak in strength. Therefore it has to be amplified to be registered. The signals enter the low frequency blocks in the millivolts range.

The modulated square waves are symmetrical in the case of quiet Sun. The reference point or the line of zero is a function of the receiver temperature, which is stable in time. The square wave modulates around that value. The lower part of the wave has depending on the telescope the value of the reference level. At the RT2 and RT3 the value depends on the amount of current that the pin-diode lets pass as a minimum and at the RTM the value belongs to the signal from the sky. The upper part has the value of the signal

coming from the Sun. The intensity of the signal is calculated by taking the average values of adjacent upper and lower half-waves and subtracting them. The difference is the intensity. Obviously, in the case of the quiet Sun there is no difference and the square wave is symmetrical. During solar activity, however, the upper part shows variations of its value. Thus, creating an unsymmetrical wave and delivering the intensity values.

The square wave for the polarization, which is symmetrical for the quiet Sun as well, has its line of zero on top of the modulation for the intensity. It is floating above, thus its line of zero is not stable in time. It shows the same behavior during solar activity as the intensity modulated waves. Its value is calculated following the same procedure as for the intensity.

The following graphs (Figures 6-2 a-d) were taken with a digital oscillator in order to measure the characteristics of the signals. By that it was possible to determine some technical requirements (see 6.4). To learn more about the signals they were measured in all possible variations, e.g. the antenna in or out of focus, the compensation generator switched on or off, etc. Altogether 21 measurements were taken in addition to the calibration of the oscilloscope (see Appendix 2).

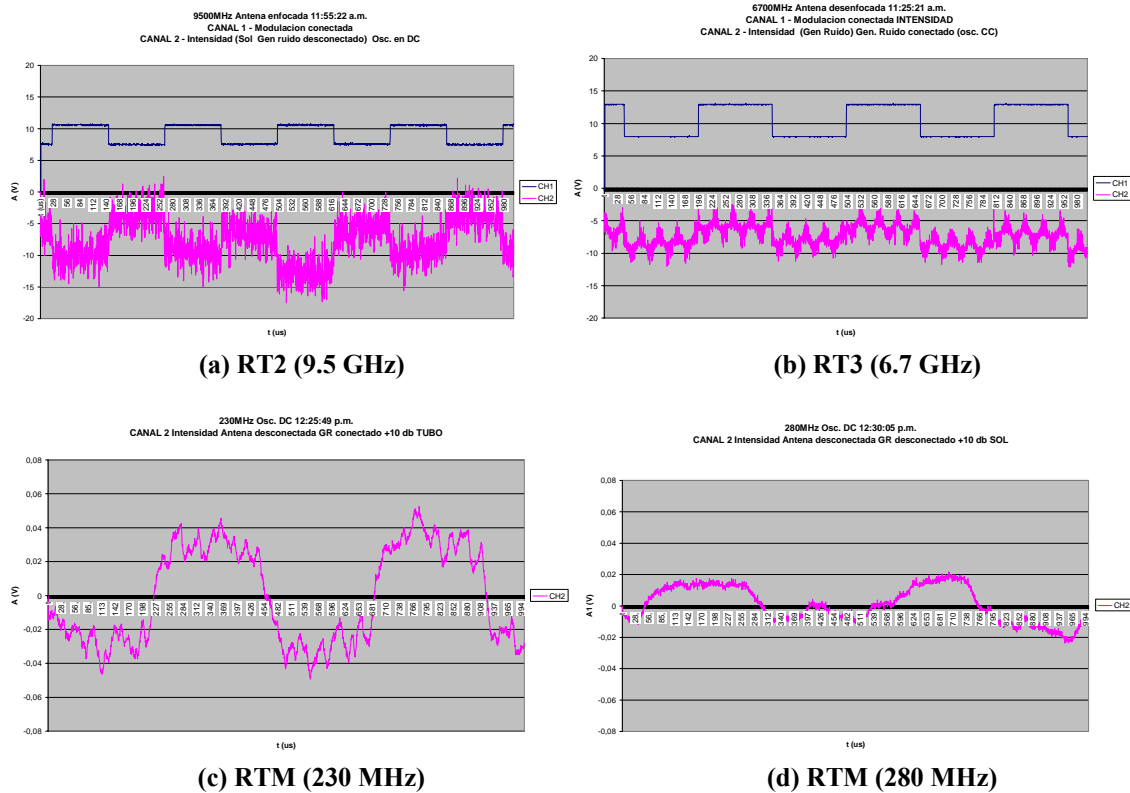


Figure 6-2 (a-d) Signals entering the low frequency blocks

The graphs show the signals as they would enter the low frequency blocks during the observation task. Although, for RT2 the compensation generator is not switched on, and for RT3 the antenna is not focusing the Sun.

The next step is to know how to convert these analog signals into digital ones.

### **6.3 Digital Signal Processing (DSP)**

The analog signals from the telescopes of the ERH are continuous and represent fluently the passage of the corresponding values. Analog to Digital Conversion (ADC) and Digital to Analog Conversion (DAC) are processes that allow digital computers to interact with these types of signals. Digital information is different from its continuous counterpart in two important respects: it is sampled, and it is quantized.

Both of these are the result of converting continuous signals into discrete ones. The resulting advantages are the potential to reduce the data and the possibility to process the values numerically. However, discretization can also be a source of additional errors.

Sampling converts the independent variable (time in this case) from continuous to discrete. That means that the values of the signal will be taken at determined points in time that are correlated with the sampling frequency. The values between these time points are either not known or not defined.

Quantization converts the dependent variable (voltage in this case) from continuous to discrete. Usually these values are displayed as multiples of fixed reference values. In general it is unavoidable but with a great number of small steps it can be pushed to a negligible value.

Digital data sampling systems use the binary system, in which a decimal number is displayed as  $2^m$ . The resolution, that is  $m$ , describes the number of steps at the quantization and is equal to the number of bits. Being as well the case at the ERH, measurement signals are usually in the  $\pm 10$  V region. If one chooses at the A/D-Conversion a quantization step of  $q = 2.44$  mV, the relative uncertainty in relation to the maximal value of 10 V, is  $0.244 \cdot 10^{-3}$ . This example is for a 12-bit value and is in general sufficient to neglect the quantization.

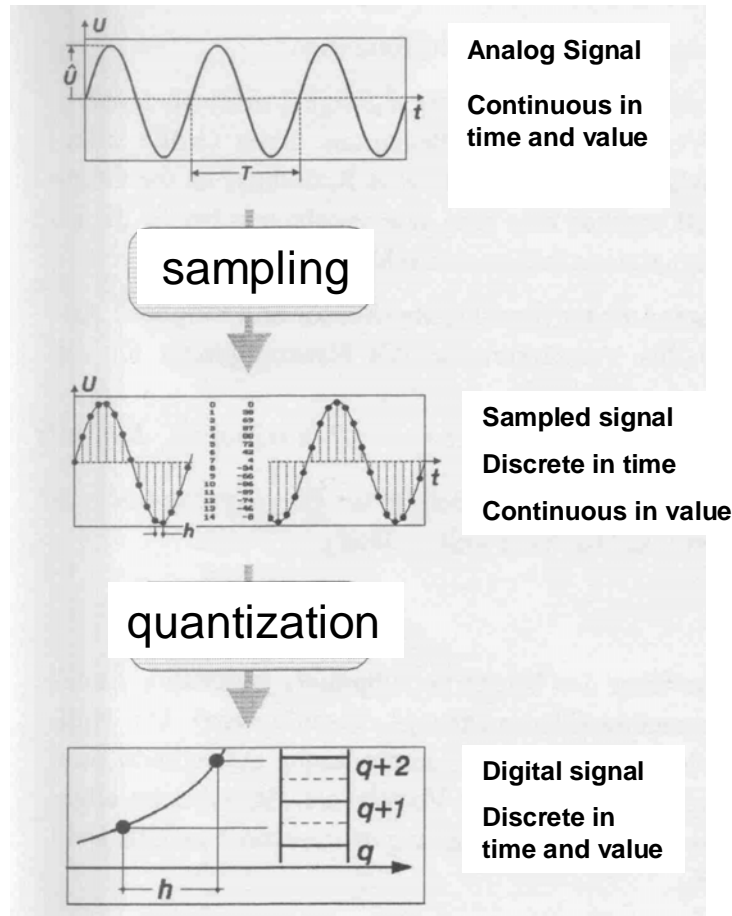


Figure 6-3: Digitization

The definition of proper sampling is quite simple. If the analog signal can be exactly reconstructed from the samples of a continuous signal, the sampling was done properly. If the main objective of a measurement is to investigate the oscillations, the sampling has to be done following determined rules to prevent the so-called Aliasing, where the sinusoid changes the frequency during sampling.

The sampling theorem states that a signal can be reconstructed if the maximal signal frequency is smaller than half the sampling frequency.

The sampling theorem indicates that a continuous signal can be properly sampled, only if it does not contain frequency components  $f_g$  above one-half of the sampling rate  $f_a$ :

$$\text{Shannon's sampling theorem } f_g < f_a/2 \qquad h < 1 / 2f_g,$$

with  $h$  being the sample interval. The expression “Nyquist frequency” is commonly used for the half of the sampling frequency, which is the highest measurable frequency with the sample interval  $h$ .

$$\text{Number of values to sample } N = T/h \geq 2f_g T$$

In case that the signal contains higher frequencies as the Nyquist frequency, these will be displayed on the frequency region of  $f < f_a/2$ , so that the original signal cannot be reconstructed completely from the sampling values.

To evade this systematical error there are two independent measures that can be taken:

1. The use of a sampling frequency that fulfills Shannon's theorem
2. The use of an antialiasing filter. With this filter all frequencies greater than the Nyquist frequency will be filtered out of the signal before it is sampled, so that all remaining frequencies fulfill the sample theorem.

## **6.4 Technical and Scientific Requirements**

In addition to the basic need to sample the incoming signals, there is something else that has to be considered. It is the scientific objective that the investigators at the ERH want to see fulfilled as well.

Among the scientific requirements is the request from the investigators that the signal is being measured with a high degree of stability that is not affected by fluctuations. Therefore they proposed to take twenty measurements of every half-wave from which to calculate its average. The obtained intensity value is independent of fluctuations in the signal strength within a half-wave, thereby reducing the probability for errors in the measurement.

With the RTM having the highest signal frequency, this value has to be taken as reference for the sample rate. The frequency is at about 2.2 kHz. With the requirement of measuring 20 times the intensity in a half-wave, which has a frequency of about 4.4 kHz, leads to a sample rate of about 88 kHz, which is well above the Nyquist theorem for sampling. To have some room for fluctuations and because it is easier to find on the market a sample rate of 100ksps (kilo-samples per second) was chosen.

Furthermore, the signal has to be sampled with a determined degree of resolution. The modulated signal has a voltage of 5 Volts which is equivalent to two times the temperature of the Sun. The Sun's temperature is to be considered  $T_{\text{Sun}} \sim 2000 \text{ K}$ . The investigators need at least a resolution that shows changes in the Sun's temperature, (and by that changes of the intensity) of 1% of the Sun's temperature which was 2000 K, that is 20 K or 0.025 V. Taking this volume as a unit. High solar activity can lead to signal intensities of up to 25 Volts, which is 1000 times more than the required measurement exactness. To be able to record these intensities a resolution of at least 10 bit is necessary.  $2^{10} = 1024$ .

The required resolution for the polarization is yet to be determined but it is very probable that the chosen resolution will be sufficient for the polarization as well.



During solar activity the signal strength (intensity) can reach up to 2.5 Volts. Since the signal is modulated, the solution must have a bipolar input of at least  $\pm 2.5$  Volts or with the use of the offset voltage an unipolar input of 0-5 Volts.

If possible the polarization should be divided into the two rotation directions (right and left). How this could be done is still being analyzed.

The low frequency blocks do not only deliver the information from the signal, but are also doing other tasks (see 6.1). It has to be considered if and how these tasks could be exchanged. These include attenuators, square wave generators and RT2's quadratic detector. It would be possible to continue using some of these parts if no solution can be found for them.

Furthermore, the solution has to be compatible with the already employed technology at the ERH. There is one PC connected through a serial RS-485 network with the Astrodata modules. This has to be included in the considerations.

In addition to the scientific and technical requirements, the cost of the solution has to be considered as well. Due to the economic circumstances in Cuba the solution has to be reasonably economic. Furthermore, it should be possible to obtain the solution within a reasonable time frame which might be problematic due to the embargo.

There are three possible solution approaches. The first would be to outfit the computer with a multi-channel ADC-card, in which the signals are introduced. This would not take the Astrodata network into account and the PC would be used for the calculations. However, this does not look like the best solution since there would be no smooth implementation into the Astrodata network and the PC's CPU might be blocked for other tasks.

The next solution would be to construct one or more external modules, which could be connected to the Astrodata network and that take care of the signal processing. Another solution is to buy such an external module, which has already proven its usefulness in practice. This solution, appearing as the best approach, was therefore chosen.

## **6.5 Shopping**

After an extensive search in the internet for an economic solution in modular form, the TERN AE86-P (detailed information in Appendix 1) was finally found. It is an external module that fulfills the requirements. Its sample rate with 300 ksp/s is well above the desired specification. It has eight analog input channels, which is enough for all the signals that have to be sampled. It also has four digital output channels which might be used to send the modulation signal to the receivers. It is also equipped with an RS-485 port which enables it to be connected to the Astrodata network. In addition to that the price was with \$ 200 reasonably low.

However, some technical questions were still open, like can the module communicate with the C routine already installed and working at the ERH. After contacting Singapore to clear up some of the technical questions, it turned out that the communication was conducted through the TERN software, which would have been delivered with the module in a development kit. Unfortunately it was too expensive. 800 dollars for software that can be programmed at the ICIMAF is just too much. Unfortunately the necessary information to program the hardware was not available.

Resuming the search for a similar product that would not require programming or at least one that could be programmed by the client was resumed. It was discovered that almost all modular solutions were constructed in more or less the same way. A circuit board with a small microprocessor, ADC, memory, RS-485 port and many for the solution unneeded characteristics. Apparently every solution on the market was over dimensioned for the ERH solution. In addition to that all the modules had to be programmed.

The initial idea, that there might be products out there, which not only sample the incoming signal, but provide as well the results of the sampled data, therefore not requiring the use of extra software, was abandoned.

Analyzing the situation, it was decided to build the module in the institute as was already done with the AST Astrodata modules. That way, the module can be manufactured ideally for the needs and requirements of the ERH. Furthermore, the installed communication routine can be kept without changes. Saving time and reducing the possibility of errors.

Another internet search was initialized, this time with the objective of finding CMOS, ICs (chips) that fulfill the technical requirements and of course the most economic solution. Therefore not only the products had to be found, by studying the datasheets to see if the product was indeed suitable for the solution by meeting the specification requirements. Furthermore the prices of the products were investigated and compared.

Among these products were Analog-Digital-Converters (ADCs), Programmable Gain Amplifiers (PGAs) that can be used to exchange the attenuators in the low frequency blocks, microprocessors of the PIC type, DC-DC voltage converters, to galvanically isolate the computer system from the receiver end, and many more. The complete list can be found in Appendix 6.

Instead of building one module for all incoming signals, it was decided to build a module for each telescope (signal). By doing so a real modular solution was taken. That way, even in the case of the failure of a module it would be possible to exchange the module with that from another telescope. This might prove very useful if the failure happened during a solar event and the failure module being the one belonging to the telescope with its receiver frequency in the events maximum. Thus, reducing the loss of data and assuring the working condition of the ERH as well as allowing the investigators to continue their work.

Now the ERH has the blueprints (see Appendix 6) available for a modular solution that fulfills the technical and scientific requirements to exchange the analog low frequency blocks with a modern digital solution.

## **7. Implementation of the Solution**

As soon as a sponsor is found and a way to get the parts needed into the country, work will start on building the modules. The implementation into the ERH will follow when this task is done successfully. That way finishing the supervisory and control system for Havana Radio Astronomical Station.

## **8. High-Tech Sensors & ERH, IGA, ICIMAF**

An extensive database was created with information about state of the art sensors used in space missions. The database contains information about the instrument of the mission, in which region of the spectrum it is used and for which science. The implemented search function allows the investigators to search for specific mission parameters, like instrument type, frequency or spectral region. As results the instruments are listed, that belong to the search category. A part of this database can be seen in Appendix 4. With this information the investigators at the ERH have now the possibility to study possible upgrades to their station in connection with sensor technology.

Furthermore the relationship between various studies, e.g. the atmosphere and the effects of the Sun can be observed. By knowing the effects of the Sun on other celestial bodies or their atmospheres it is possible in the future to develop a better understanding of the effects of the Sun here on Earth.

In addition, by having a reference of highly specialized instruments it is now possible to establish contact to foreign institutes that have already worked on a possibly similar subject. This results in a possible exchange of ideas, information and specialists, thereby creating the international cooperation between the IGA, ICIMAF and other institutes. This thesis can be considered as the possible initiation between Cuban and German institutes and universities.

## **9. Summary**

The task to exchange the analog low frequency blocks with a digital solution was carried out by studying the processes that take place within the low frequency blocks (LFB). The signal coming from the receiver enters the LFB and what goes out of the LFB is the information about the intensity and polarization that the investigators can use. The signal coming from the receiver was studied in great detail to be able to perform the calculations. With consideration of the scientific and technological requirements of the ERH an Internet search for an appropriate solution was initiated.

The initially found modules turned out to be over dimensioned, incompatible with the existing communications routine and too expensive. Thus, it was decided to build a suitable solution at the ICIMAF. This was at the end the most economic and technologically best suited/tailored solution. Another Internet search was initiated with the goal to find appropriate hardware that not only fulfills the technological requirements but also offers the lowest price. With all the necessary components found the blueprint is now available and ready to be build, as soon as the parts arrive at the station.

With the implementation the supervisory and control system of the ERH would be finished. In the future further improvement might be achieved by learning from sensor technology used at other observatories or on satellites. Thereby continuing to keep the station up to date and forming international cooperations, improving the knowledge of the Sun and the Sun-Earth relationship.

## **References**

- [1] G. Evans, C.W. McLeish  
ISBN: 0-89006-055-X  
RF Radiometer Handbook  
Artech House
- [2] Victor F. Veley  
ISBN: 0-13-595414-2  
Modern Microwave Technology  
Prentice Hall
- [3] F. Ulaby, R. Moore, A. Fung  
ISBN: 0-89006-190-4  
Microwave Remote Sensing Volume I  
Addison Wesley
- [4] G.D. Roth  
ISBN: 0-387-06503-2  
Astronomy A Handbook  
Springer
- [5] K. Scaifers, G. Traving  
ISBN: 3-411-00940-3  
Meyers Handbuch über das Weltall  
Meyers Lexikonverlag
- [6] J. Mitton  
ISBN: 3-440-07007-7  
Astronomie von A-Z  
Franckh-Kosmos
- [7] S. Smith  
ISBN : 0-9660176-3-3  
The Scientist and Engineer's Guide to Digital  
Signal Processing, California Technical Publishing
- [8] G. Alvarez Bestard  
Astrodata. Sistema de Supervisión y Control  
de la ERH
- [9] Dale E. Gary  
Physics 728, Radio Astronomy,  
(<http://physics.njit.edu/~dgary/202>)
- [10] Jürgen Morawietz  
Radiostrahlungsarten der Sonne  
(<http://privat.eure.de/mora/strahlg.htm>)
- [11] White, Kassim, Erickson  
Solar radioastronomy with the LOFAR  
(Low Frequency Array) radio telescope  
([http://ovsa.njit.edu/fasr/02\\_spie\\_lofar.pdf](http://ovsa.njit.edu/fasr/02_spie_lofar.pdf))

## **List of Figures**

<b><u>Figure</u></b>	<b><u>Title</u></b>	<b><u>Page</u></b>
2-1	The electromagnetic spectrum (Credit: Prof. Dale E. Gary – Introduction to Astronomy Lecture 5 – Light, <a href="http://physics.njit.edu/~dgary/202/Lecture5.html">http://physics.njit.edu/~dgary/202/Lecture5.html</a> )	6
2-2	(a) Peak condition for the electric and magnetic fields of a vertically polarized TEM wave, (b) vector diagram of a vertically polarized wave, (c) electric and magnetic fields in the TEM wave (Image taken from “Modern Microwave Technology”)	7
2-3	Polarized light (image taken from “Meyers Handbuch über das Weltall”)	9
2-4	Absorption in the atmosphere (Credit: NASA/IPAC)	11
2-5	(a) Half-wave dipole aerial, and (b) 13-element Yagi aerial with its directional polar diagram. (Image taken from “Astronomy A Handbook”)	14
2-6	A broadside array of 16 dipoles and its horizontal directional pattern. (Image taken from “Astronomy A Handbook”)	15
2-7	Green Bank Telescope (GBT): The largest fully steerable single dish in the world, 100 x 110 m (c) National Radio Astronomy Observatory / Associated Universities, Inc. / National Science Foundation	16
2-8	Aerial view of VLA in its most compact configuration. (c) National Radio Astronomy Observatory / Associated Universities, Inc. / National Science Foundation	17
2-9	Radio H-R diagram (from <a href="http://physics.njit.edu/~dgary/202/Lecture12.html">http://physics.njit.edu/~dgary/202/Lecture12.html</a> )	21
2-10	Schematic of a pulsar (from <a href="http://physics.njit.edu/~dgary/202/Lecture12.html">http://physics.njit.edu/~dgary/202/Lecture12.html</a> )	22
2-11	Quasar 3C175, Image courtesy of NRAO/AUI	23
3-1	A schematic view of solar structure ( <a href="http://physics.njit.edu/~dgary/202/Lecture10.html">http://physics.njit.edu/~dgary/202/Lecture10.html</a> )	24
3-2	Radio images of the chromospheric network structure and sources of magnetic elements. ( <a href="http://physics.njit.edu/~dgary/202/Lecture10.html">http://physics.njit.edu/~dgary/202/Lecture10.html</a> )	27
3-3	A schematic view of a solar flare ( <a href="http://physics.njit.edu/~dgary/202/Lecture11.html">http://physics.njit.edu/~dgary/202/Lecture11.html</a> )	30
3-4	Schematic diagram of metric bursts types ( <a href="http://physics.njit.edu/~dgary/202/Lecture11.html">http://physics.njit.edu/~dgary/202/Lecture11.html</a> )	31
4-1	Radio telescopes of the ERH: The RT2 (a), the RT3 (b) and the RTM (c)	36
4-2	Block diagram of RT2	37
4-3	Block diagram of RT3	37
4-4	Block diagram of RTM	38
4-5	Block diagram of a Dicke-Receiver	39
4-6	Post processing of the measurements of a day of observation (a). Data recorder (b).	42
5-1	General diagram of the SCADA Astrodata	46
5-2	Two of the Astrodata interfaces, ADAM 4017 and ADAM 4050.	48
5-3	AST02, signal conditioning card.	49
5-4	Virtual Instrument for RTM 280 MHz.	51
5-5	Structure of the real time system Astrodata.	52
5-6	Start window of Astrodata.	52
5-7	Virtual Instrument for the configuration of the system.	53
5-8	Virtual Instrument for the definition of the network state.	54
5-9	Virtual Instrument for the positioning of the antennas.	55
5-10	Virtual Instrument that shows the values of the analog input variables and a graphical registry of one of them (chosen by the operator).	57
5-11	Measurements of the radio telescope RT3 obtained by Astrodata on August 24, 2001.	63
5-12	Measurements obtained by Astrodata April 15, 2001	63
6-1	The low frequency blocks	66
6-2(a-d)	Signals entering the low frequency blocks	69
6-3	Digitization (image taken from MRT-handout)	71

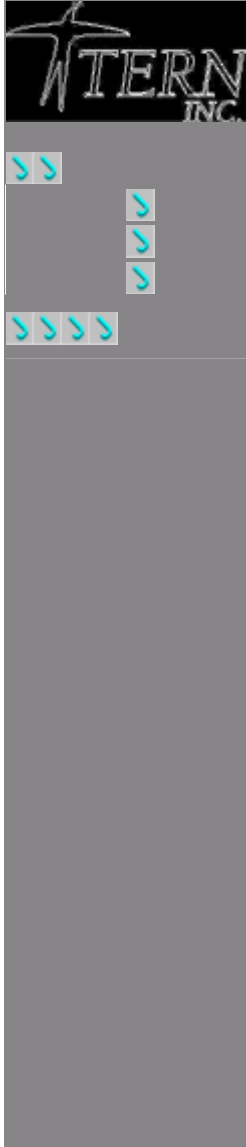


## **List of Tables**

<b><u>Table</u></b>	<b><u>Title</u></b>	<b><u>Page</u></b>
4-1	Values of the intensity in different frequencies and during a period of normal solar activity (without events).	38
4-2	Signals used in the automation of the ERH.	43/44
5-1	Calibration sequence of the intensity channel.	59
5-2	Calibration sequence of the polarization channel.	59
5-3	Measurement sequence in RT2 and RT3.	62
5-4	Measurement sequence in RTM.	62

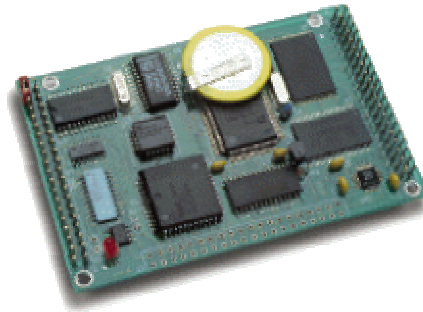
## Appendix

### Appendix 1 – The TERN A-Engine-86



#### A-Engine-86 / A-Engine-86-P / A-Engine-86-D

16-bit external data bus microprocessor module, 300 KHz ADC/DAC, 256KW 16-bit Flash, 16-bit SRAM



AE86



Download the [manual](#).  
Download printable [AE86](#) catalog page.  
Download printable [AE86-D/P](#) page.

#### A-Engine-86 Specs:

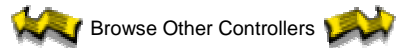
- \* Measures 3.6x2.3x0.3 inches
- \* 16-bit CPU (186), x86 compatible
- \* 40 MHz system clock
- \* Power consumption: 190 mA at 5V
- \* Power saving mode: 30 mA at 5V
- \* Temperature (sample): -40 to 80 C
- \* Up to 512 KB Flash
- \* Up to 512 KB battery-backed SRAM
- \* 2 high-speed PWM outputs, PWD
- \* 24 I/O lines from PPI
- \* 32 I/O lines from CPU
- \* 512 bytes serial EEPROM
- \* 8 external interrupt inputs
- \* 3 16-bit timers/counters
- \* Up to 3 serial ports
- \* 8 12-bit ADC (300 kHz sample rate)
- \* 4 ch. 12-bit DAC(200 kHz)
- \* Real time clock, battery, watchdog
- \* Interface for LCD, keypad

#### A-Engine-86-P Adds:

- \* Measures 3.6x2.9x0.3 inches
- \* RS232/RS485 drivers for serial port
- \* Switching regulator

#### A-Engine-86-D Adds:

- \* Measures 3.6x3.2x0.3 inches
- \* RS422 drivers for one port (SER1)
- \* 4 additional chs. high-speed DAC
- \* 4 external 16-bit counters



#### Ordering Information (Qty 1/100/1K/5K+)

**AE-86** (40 MHz) \$189/\$151/\$113/\$66  
**AE-86-P** (40 MHz) \$199/\$161/\$120/\$71  
**AE-86-D** (40 MHz) \$199/\$161/\$120/\$71

Includes Am186ES with 64 KW (128 KB) SRAM, 32 I/Os, 2 UARTs, 3 timers, 82C55 with 24 I/O lines, watchdog timer, 512 byte EE, and 512KB 16-bit Flash. Does **not** include add-on options. OEM option discounts available.

Measuring 3.6 x 2.3 x 0.3 inches, the **A-Engine86™** (AE86) is a C/C++ programmable microprocessor module based on a 40 MHz, 16-bit CPU (Am186ES, AMD). The AE86 is ideal for industrial process control and high-speed data acquisition.

In addition to offering a 16-bit external data bus, the **AE86** supports on-board 512 KB 16-bit Flash and up to 512 KB 16-bit battery-backed SRAM. All chips are surface-mounted. The on-board Flash can be easily programmed in the field via serial link using the **ACTE** kit. With its 16-bit external data bus, it can normally achieve performance that is almost

**Add-on Options:**

<b>1) 16-bit SRAM: 512KB</b>	\$40
<b>2) Real-time clock and battery</b>	\$20
<b>3) UART (SCC2691) + RS232/RS485 for AE-86-P/-D</b>	\$20 + \$10
<b>4) 4 ch. 12-bit DAC. 200 KHz (2 chips for AE86-D)</b>	\$60
<b>5) 2 ch. 12-bit DAC (LT1446)</b>	\$40
<b>6) 8 ch. 12-bit ADC, 300 KHz</b>	\$40
<b>7) 11 ch. 12-bit ADC, (P2543)</b>	\$30
<b>8) <a href="#">VE232</a> interface board (For AE-86)</b>	\$69
<b>8) RS485/422 driver for SER1 (For AE-86-D)</b>	\$10/\$20
<b>9) Sockets for expansion: two 20x2, one 25x2</b>	\$9
<b>10) On-board switching regulator for AE-86-P</b>	\$30

twice as good as those of the other A-Engine variants based on the Am188ES microprocessor.

A real-time clock (RTC72423) provides information on the year, month, date, hour, minute, second, and 1/64 second. A 512-byte serial EEPROM is on-board. Two DMA-driven serial ports support communication up to 115,200 baud. A third UART SCC2691 may be installed.

A **high-speed**, 300K samples per second, 8-channel, 12-bit parallel ADC (AD7852) can be installed. This ADC includes sample-and-hold and precision internal reference, and has an input range of 0-5 V. The **AE86** also supports a 4-channel, 5 ms settling time, 200 KHz parallel DAC (DA7625, 0-2.5V).

On-board 16-bit programmable timers/counters can be used to count external events or to generate PWM outputs. Pulse Width Demodulation (PWD) can be used to measure the width of a signal in both its high and low phases.

The AE86 provides 32 multifunctional I/O pins from the CPU, plus 24 bi-directional I/O lines from a PPI (82C55). Schmitt-trigger inverters are provided to increase noise immunity for external interrupt inputs. A supervisor chip (691) provides power failure detection and a watchdog timer.

A serial 12-bit ADC (P2543) may also be installed, offering 11 single-ended 0-5V inputs with a 10 KHz sample rate. A 2-channel 12-bit serial DAC (LT1446) provides 0-4.095 V analog voltage outputs capable of sinking or sourcing 5 mA. The 82C55 PPI can interface to an LCD and keypad.

The *A-Engine-86* shares many similar features with the [A-Engine](#), as well as a similar pin-out and physical dimensions with the [i386-Engine](#) and [V25-Engine-LM](#).

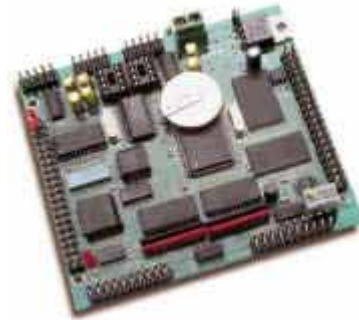


**AE86-P**

The slightly larger **A-Engine-86-P** (AE86-P) provides the same basic features as the AE-86 and provides a few other integrated functional units. The AE86-P provides an on-board switching regulator that allows the controller to accept a wider range of input voltages. It also has on-board RS232/RS485 drivers for the serial ports.

The standard AE86 requires the use of an expansion board such as the

[VE232](#) for standard operation (unless your OEM board can provide a 5V regulated voltage supply and RS232 voltage-level drivers). The AE86-P provides that functionality on-board.



**AE86-D**

Another variant of this family of boards is the **A-Engine-86-D** (AE86-D). Similar to the AE86-P, the AE86-D is an integrated controller with on-board voltage regulators and serial port drivers. In addition, the primary feature of the AE86-D is that it offers three external 16-bit **counters**. These counters are ideal for specialized applications that deal with high-frequency external events... such as the output of flow meters.

The AE86-D is also designed for other flexible applications. It offers another DA7625, providing 4 more channels of high-speed parallel DAC. The AE86-D can also be optionally configured with a RS422/RS485 driver for SER1, instead of the usual RS232 design.

#### **OTHER CONTROLLERS**

On the spectrum of performance power for TERN controllers, the AE86 boards would probably be placed right in the middle. On the fewer feature/lower-performance (and lower-cost) side, there are products such as the [A-Engine](#), [FlashCore-B](#), and [R-Engine](#). If you're looking for more processing power in a similar small profile, check out the [i386-Engine](#) and [586-Engine](#).

*Similar controllers:* [A-Engine](#), [A-Core-86](#), [i386-Engine](#), [R-Engine](#), [586-Engine](#)  
*Expansion boards:* [Kpad](#), [MemCard](#), [MotionC](#), [P300](#), [FlashCore-B](#), [PowerDrive](#).

## **Appendix 2 – Oscilloscope Measurements of the Signals**

Calibracion del Osciloscopio (exp0)

### **RT2**

Modulacion conectada, Intensidad (Sol) Gen. Ruido desconectado (exp2)

Modulacion conectada, Intensidad (Sol) Gen. Ruido desconectado (exp 3)

Modulacion conectada, Intensidad (Sol + Gen R) Gen. Ruido conectado (exp4)

Modulacion conectada, Intensidad (Sol + Gen R) Gen. Ruido conectado (exp5)

Modulacion desconectada, Intensidad (cero) Gen. Ruido desconectado (exp6)

Antena desenfocada, Modulaci3n desconectada, Intensidad (Gen Ruido) Gen. Ruido conectado (exp7)

Antena enfocada, Modulacion conectada, Intensidad (Sol Gen. Ruido desconectado) Osc. en DC (exp13)

Antena enfocada, Modulacion conectada, Intensidad (Sol + Gen Ruido conectado) Osc. en DC (exp14)

Supervisory and Control System for Havana Radio Astronomical Station

Antena enfocada, Modulación desconectado (cero), Intensidad (Gen Ruido conectado) Osc. en DC (exp15)

**RT3**

Antena desenfocada, modulación conectada, Intensidad (Gen Ruido) Gen. Ruido conectado (exp8)  
 Antena desenfocada Nivel de Referencia, Modulación conectada, Intensidad (Gen Ruido) Gen. Ruido conectado (exp9)  
 Antena desenfocada, Modulación conectada INTENSIDAD, Intensidad (Gen Ruido) Gen. Ruido conectado (Osc. CC) (exp10)  
 Antena desenfocada, Modulación conectada POLARIZACION, Intensidad (Gen Ruido) Gen. Ruido conectado (Osc. CC) (exp11)  
 Antena desenfocada, Modulación conectada POLARIZACION, Modulación Intensidad (exp12)

**RTM**

230 MHz, Osc. DC, Intensidad Antena conectada GR desconectado (exp00)  
 230 MHz, Osc. DC, Intensidad Antena desconectada GR desconectado EQUIVALENTE (exp01)  
 230 MHz, Osc. DC, Intensidad Antena desconectada GR desconectado +30 dB CERO (exp02)  
 230 MHz, Osc. DC, Intensidad Antena desconectado GR conectado +10 dB TUBO (exp03)  
 280 MHz, Osc. DC, Intensidad Antena desconectado GR conectado +10 dB TUBO (exp04)  
 280 MHz, Osc. DC, Intensidad Antena desconectada GR desconectado +30 dB CERO (exp05)  
 280 MHz, Osc. DC, Intensidad Antena desconectada GR desconectado +10 dB Sol (exp06)

**Appendix 3 – Price Comparison List**

<b>ADC</b>	<b>Price Break</b>	<b>Unit Price (USD)</b>
AD677KD	6	66.73500
AD977AAN	9	45.88556
AD7853LARS	59	9.73508
AD7870JN	1	29.22000
AD7876BN	1	30.90000
AD7891AP-1	54	24.50000
AD7891AS-1	1	26.25000
AD7891BS-1	12	29.40000
AD7895AN-10	50	8.77500
AD7895AN-3	50	8.77500
AD7896AN	50	11.92500
ADC12130CIN	1	7.18000
ADS7808P	1	16.31000
ADS7809P	Call	Call
LTC1400CS8	1	10.00000
TC500ACPE	1	5.00000
AD1674	1	21.83 - 106.94
ADS787	1	8.30
ADS7871	1	8.33
LTC1603	111	15.65
LTC1603	1000	9.95
LTC1604	1	44.50 - 63.13
LTC1604	1000	20.50
LTC1605	1	36.13 - 51.00
LTC1605	1000	17.00
LTC1605-2	1	36.88
LTC1605-2	1000	17.00

Supervisory and Control System for Havana Radio Astronomical Station

LTC1606	47	35.94
LTC1606	1000	19.50
LTC1608	1	35.00 - 49.13
LTC1608	1000	16.50
LTC1609	1	31.75 - 35.00
LTC1609	1000	14.95
ADS7811	1000	36.15
ADS7864	1000	6.65 - 7.65
ADS8323	1000	7.10 - 8.90
ADS8364	1000	18.10

PGA

PGA 202	1	12.91000
---------	---	----------

DC-DC

NMH0512S	1	14.04000
NTA1212M	1	8.78000

MCP 41010	1	1.68000
MCP 41050	1	1.68000
MCP 41100	1	1.68000

**Appendix 4 – Space Missions Database (Fragment)**

Instrument Name	Instrument Type	Spectrum	Unit	PI	Mission	Launch Date	PDF	Organization
ASCAT	scatterometer	microwave	5.255 GHz	Astrium GmbH, Germany	MetOp	2005		ESA/NASA
AVHRR	imaging radiometer	VIS - IR	0.58 - 12.5 microns	NASA and ITT, USA	MetOp	2005		ESA/NASA
GOME-2	spectrometer	UV - VIS	249 - 790 nm	Galileo Avionica, Italy	MetOp	2005		ESA/NASA

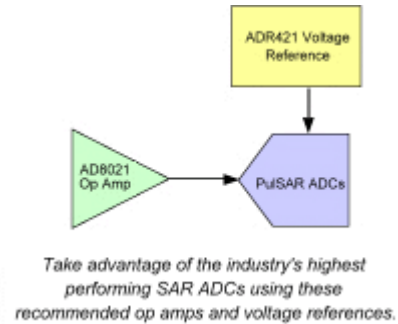
## Appendix 5 – Data Sheets

### AD7680

#### 100 kSPS, 16-Bit PuISAR® ADC in 6 Lead SOT-23

##### Features

- Fast Throughput Rate: 100 kSPS
- Specified for VDD of 2.5 V to 5.25 V
- Low Power: 4 mW typ at 100 kSPS with 3 V  
Supplies 17 mW typ at 100 kSPS with 5 V Supplies
- Wide Input Bandwidth: 86 dB SNR at 10 kHz Input Frequency
- Flexible Power/Serial Clock Speed Management
- No Pipeline Delays
- High Speed Serial Interface SPI/QSPI/ $\mu$ Wire/DSP Compatible
- Standby Mode: 0.5  $\mu$ A max
- 6-Lead SOT-23 Package



##### Applications

- Battery-Powered Systems Personal Digital Assistants Medical Instruments
- Mobile Communications
- Instrumentation and Control Systems
- Remote Data Acquisition Systems

##### General Description

The AD7680 is a 16-bit, fast, low power, successive-approximation ADC. The part operates from a single 2.5 V to 5.25 V power supply and features throughput rates up to 100 kSPS. The part contains a low-noise, wide bandwidth track/hold amplifier, which can handle input frequencies in excess of 100 kHz.

The conversion process and data acquisition are controlled using CS and the serial clock, allowing the devices to interface with microprocessors or DSPs. The input signal is sampled on the falling edge of CS and the conversion is also initiated at this point. There are no pipelined delays associated with the part.

The AD7680 uses advanced design techniques to achieve very low-power dissipation at fast throughput rates. The reference for the part is taken internally from VDD. This allows the widest dynamic input range to the ADC. Thus the analog input range for the part is 0 to VDD. The conversion rate is determined by the SCLK frequency.

## **Appendix 6 –Module Blueprints and Component List**

### List of Material for Down Converter

Used	Part Type	Designator	Description
4	.1u	C15 C19 C20 C21	CAPACITOR
4	.33u	C13 C16 C17 C18	CAPACITOR
10	1K	R8 R16 R17 R18 R19 R20 R21 R22 R23 R24	RESISTOR 1/8W
1	1u/16V	C1	Capacitor
8	10K	R6 R9 R10 R11 R12 R13 R14 R15	RESISTOR 1/8W
2	10u/16V	C2 C14	Capacitor
1	22pF	C10	Capacitor
1	22pF	C11	Capacitor
1	50K	R1	Potentiometer
1	520	R4	
1	AD7680	U5	
1	AN78L05	U11	REGULADOR DE TENSION
1	AN78L12	U12	REGULADOR DE TENSION
1	AN79L12	U13	REGULADOR DE TENSION
1	BNC 413194-1	P1	BNC Connector

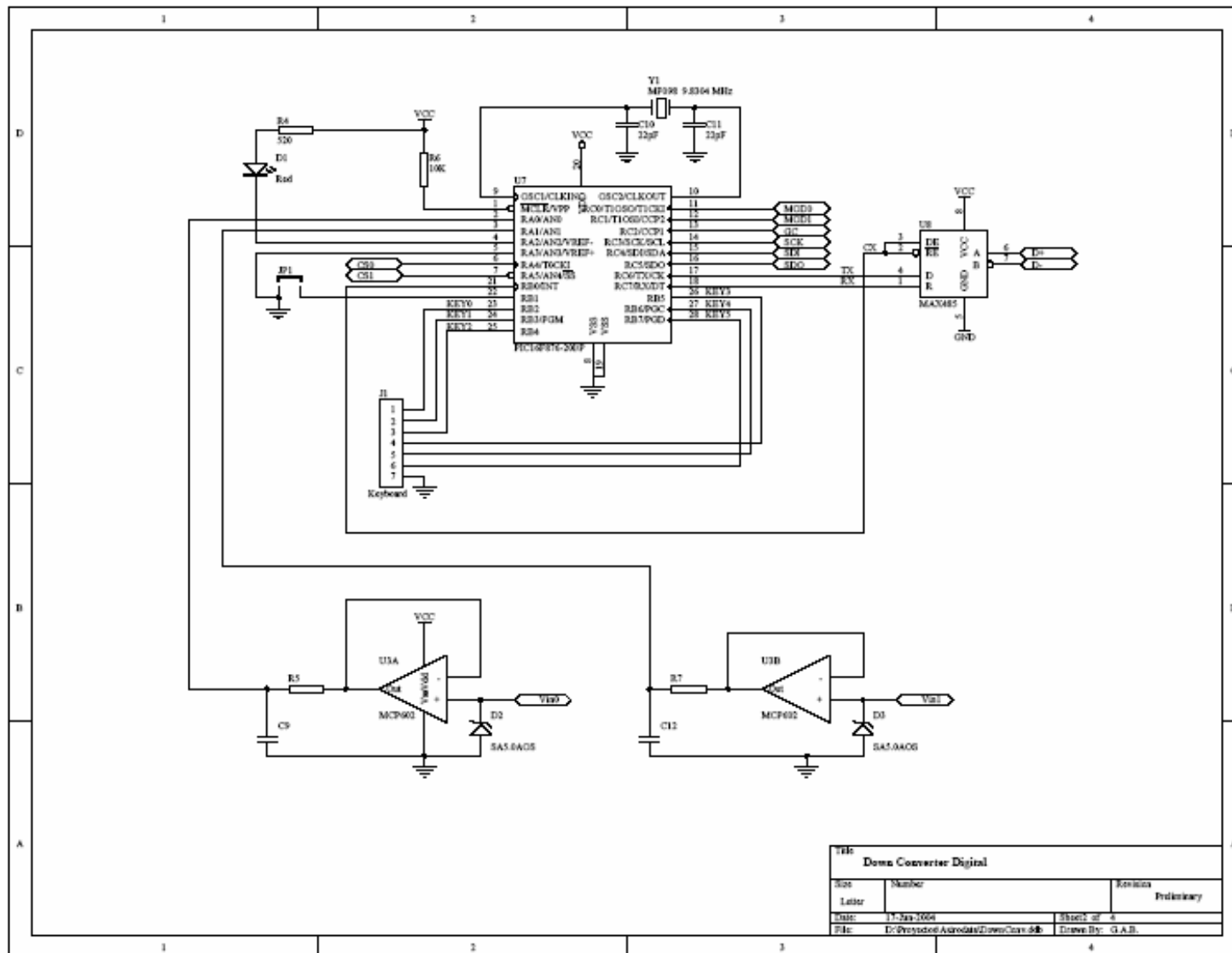


Supervisory and Control System for Havana Radio Astronomical Station

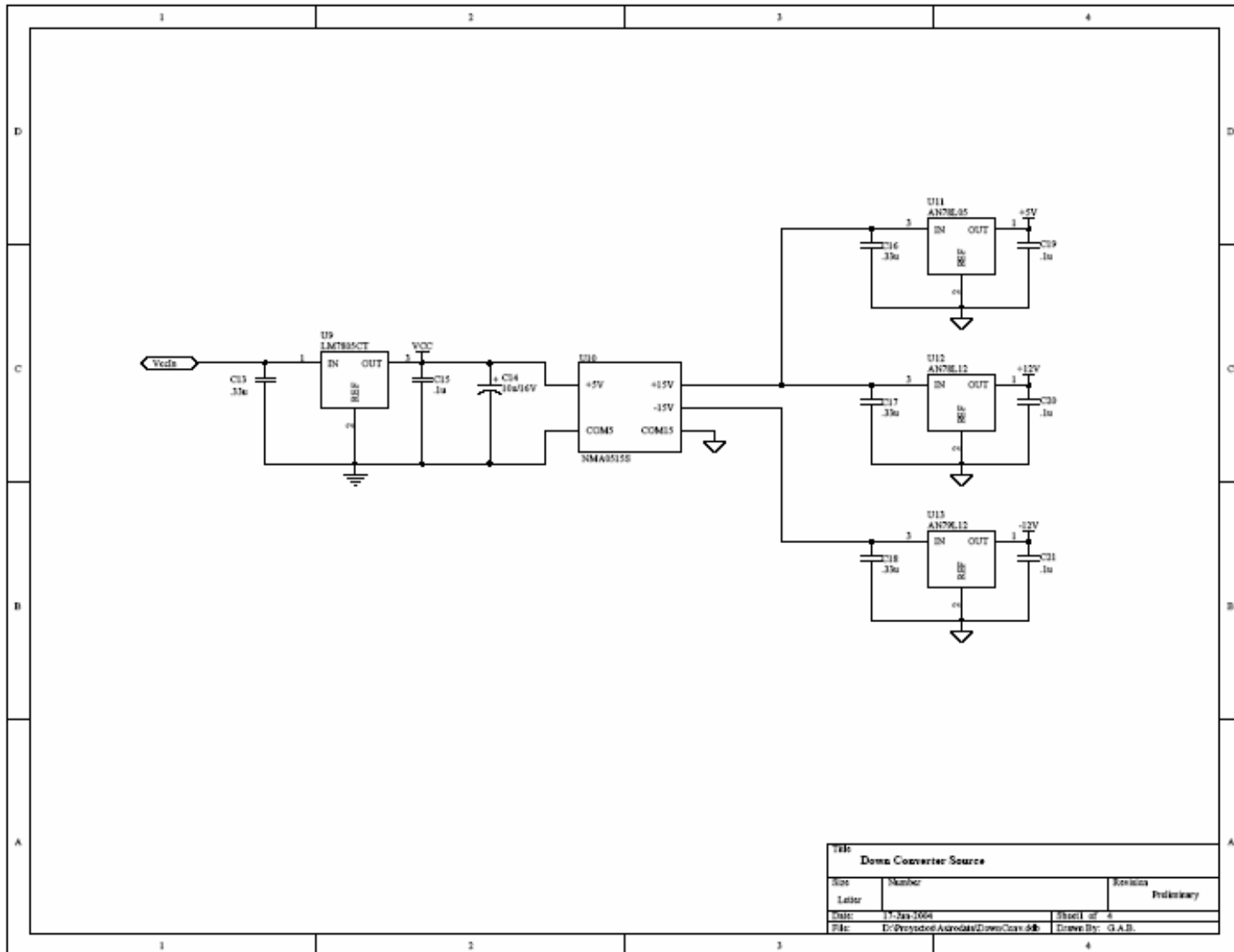
1	EDSTL950/10	J2	Connector
1	Keyboard	J1	Connector
1	LM7805CT	U9	REGULADOR DE TENSION
1	MAX485	U8	DIFFERENTIAL BUS TRANSCEIVERS
10	MB10414	U14 U15 U16 U17 U18 U19 U20 U21 U22 U23	Optoisolator
1	MCP41XXX	U6	POTENCIOMETRO DIGITAL SPI
2	MCP602	U2 U3	AMP OP
1	MCP1541	U1	VOLTAGE REFERENC
1	MP098 9.8304 MHz	Y1	Crystal
1	NMA0515S	U10	
1	PGA203	U4	Digitally-Controlled Programmable Gain Instrumentation Amplifier
1	PIC16F876-20I/P	U7	8-Bit CMOS Microcontrollers With A/D Converter
1	Red	D1	LED
2	SA5.0AOS	D2 D3	Zener Diode



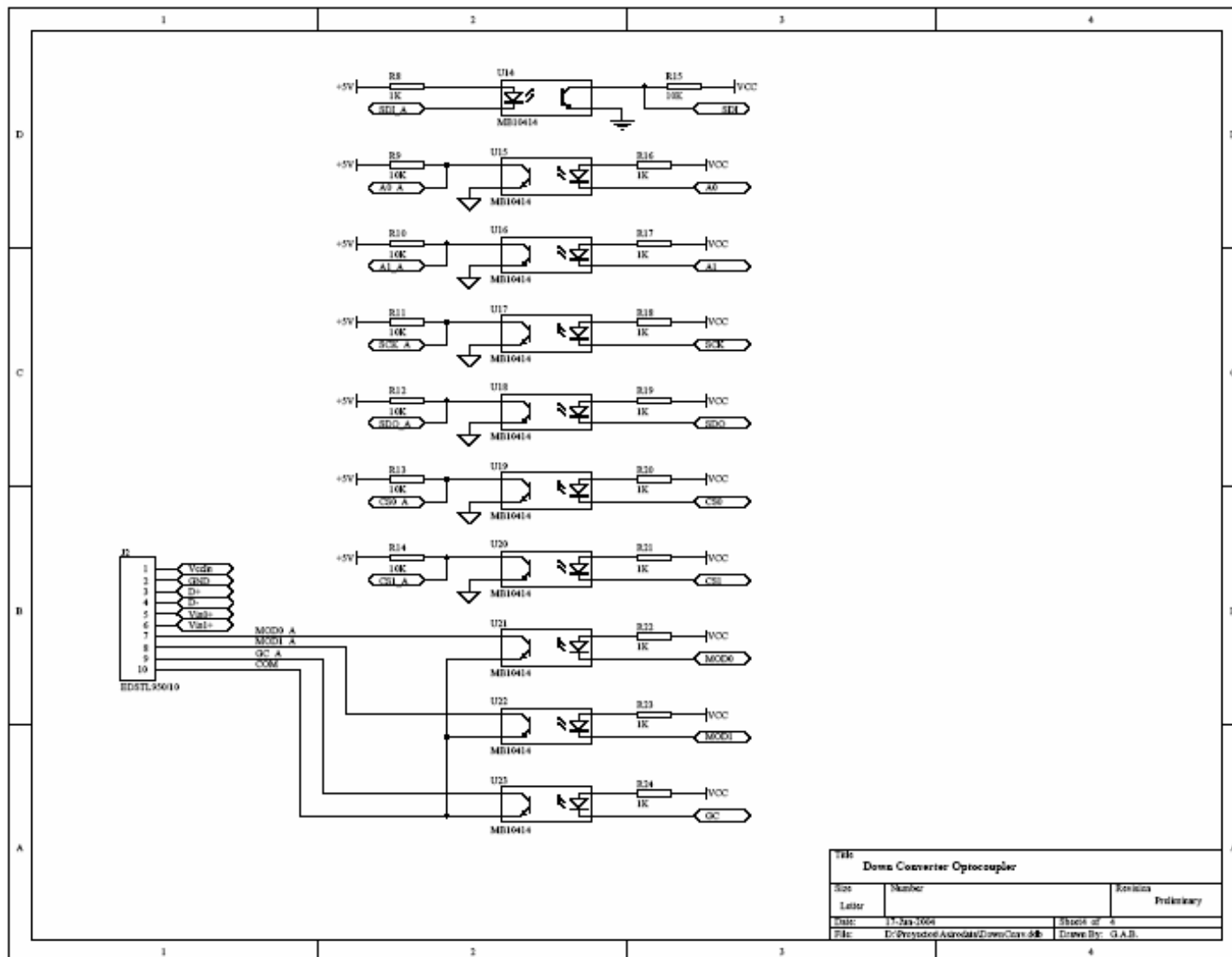
# Supervisory and Control System for Havana Radio Astronomical Station



Supervisory and Control System for Havana Radio Astronomical Station



Supervisory and Control System for Havana Radio Astronomical Station



Supervisory and Control System for Havana Radio Astronomical Station

Product	Description	Fabricant	Distributor	Distributor Code	Quantity	Price	Sum
NMA0515S	DC/DC CONVERTER, 1W +/-15V; Depth, external: 6mm; Length / Height, external: 10mm; Power rating: 1W; Width, external: 19.5mm; Case style: SIL; Density, power: 0.85W/cm <sup>3</sup> ; Efficiency: > 80%; Flammability rating: UL94V-__	NEWPORT COMPONENTS	FARNELL	330760	1	£ 5,43	\$ 9,63
AD7680BRJ-R2 or AD7680BRJ	IC ADC 16BIT LP UNIPOLAR 6-SOT23	Analog Devices Inc	Digi-Key		1		
AD7680ARM	IC ADC 16BIT LP UNIPOLAR 8-MSOP						
AD7680BRM				AD7680BRM-ND		\$ 11,06	\$ 11,06
AN78L05	VOLTAGE REG POS 5V 100MA TO-92, Built-In Overcurrent Limit & Thermal Overload Protection Circuit	Panasonic - SSG	Digi-Key	AN78L05-ND	1	\$ 0,53	\$ 0,53
AN78L12	VOLTAGE REG POS 12V 100MA TO-92, Built-In Overcurrent Limit & Thermal Overload Protection Circuit	Panasonic - SSG	Digi-Key	AN78L12-ND	1	\$ 0,53	\$ 0,53
AN79L12	VOLTAGE REG NEG 12V 100MA TO-92, Built-In Overcurrent Limit & Thermal Overload Protection Circuit	Panasonic - SSG	Digi-Key	AN79L12-ND	1	\$ 0,52	\$ 0,52
ED950/10	10 pins, 5mm Lead Spacing — Plugs, Rated Voltage: 300V • Rated Current: 15A • Temperature: -30°C/+105°C • Flame Class: UL 94 V-0 • Color: Green	On-Shore Technology	Digi-Key	ED1709-ND	1	\$ 4,00	\$ 4,00
EDSTL950/10	10 pins, 5mm Lead Spacing — Horiz. Headers, Rated Voltage: 300V • Rated Current: 15A • Temperature: -30°C/+105°C • Flame Class: UL 94 V-0 • Color: Green	On-Shore Technology	Digi-Key	ED1809-ND	1	\$ 1,71	\$ 1,71
LM7805CT	IC REG 1A POS 0-125DEG C TO-220, Short-Circuit & Thermal Protection	Fairchild Semiconductor	Digi-Key	LM7805CT-ND	1	\$ 0,57	\$ 0,57
MAX485CPA	IC TXRX RS485/RS422 LOWPWR 8-DIP	Maxim	Digi-Key	MAX485CPA-ND	1	\$ 2,76	\$ 2,76
MCP1541-I/TO	IC VOLTAGE REFRNCE 4.096V TO92-3	Microchip Technology	Digi-Key	MCP1541-I/TO-ND	1	\$ 0,50	\$ 0,50

Supervisory and Control System for Havana Radio Astronomical Station

MCP41010-I/P	IC POT DIGITAL 10K 1CH SPI 8-DIP	Microchip Technology	Digi-Key	MCP41010-I/P-ND	1	\$ 1,68	\$ 1,68
MCP602-I/P	IC DUAL OPAMP SNGL SUPPLY R-R 8DIP, Single Supply, Rail-to-Rail	Microchip Technology	Digi-Key	MCP602-I/P-ND	2	\$ 0,88	\$ 1,76
MP098	CRYSTAL B2MHZ HC-49 SERIES $\pm$ .005% (50PPM) 0°C to +70°C, HC-49/U Case, 20pFLoad Capacity, 45 Max. ESR	CTS-Frequency Controls	Digi-Key	CTX084-ND	1	\$ 0,94	\$ 0,94
PGA203KP	IC PROG GAIN INSTR AMP 14 DIP	BUR-BROWN	Digi-Key	PGA203KP-ND	1	\$ 12,91	\$ 12,91
PIC16F876A-I/SP	IC MCU FLASH 8KX14 EE 28DIP, 22 I/O (5 Ch. 10-Bit A/D)	Microchip Technology	Digi-Key	PIC16F876A-I/SP-ND	1	\$ 7,05	\$ 7,05
413194-1	BNC PC Board/Panel Mount Jack Connectors 75 Ohm Right Angle, VALOX, White	AMP	Digi-Key	A24600-ND	1	\$ 5,43	\$ 5,43
SA5.0AOS	Transient Voltage Suppressors 500 Watts	ON Semiconductor	Digi-Key	SA5.0AOS-ND	2	\$ 0,55	\$ 1,10
							<b>\$ 62,68</b>